Universities Press
Educational Monographs

Jawaharlal Nehru Centre for
Advanced Scientific Research

DETERMINISTIC CHAOS

Complex Chance Out Of Simple Necessity

N KUMAR

DETERMINISTIC CHAOS

Complex Chance Out of Simple Necessity

The Educational Monographs published by Universities Press in collaboration with JNCASR address the needs of students and the teaching and research community.

Published

Elements of Cosmology : Jayant V. Narlikar

Forthcoming

Dynamic Himalaya : K.S. Valdiya

Cooperation and Conflict in Animal Societies : Raghavendra Gadagkar

Electrostatics of Atoms and Molecules : S.R. Gadre

Titles published earlier by Wiley Eastern

Superconductivity Today : T.V. Ramakrishnan and C.N.R. Rao

Supercomputers : V. Rajaraman

The World of Bohr and Dirac: Images of 20th Century Physics : N. Mukunda

Educational Monographs

DETERMINISTIC CHAOS

Complex Chance Out of Simple Necessity

N Kumar
Raman Research Institute
Bangalore 560 080, India

Jawaharlal Nehru Centre
for Advanced Scientific Research

Universities Press

First published 1996
ISBN 81 7371 042 2

Distributed by
Orient Longman Limited

Registered Office
3-6-272, Himayatnagar, Hyderabad 500 029 (A.P.), India

Other Offices
17, Chittaranjan Avenue, Calcutta 700 072
160, Anna Salai, Madras 600 002
Kamani Marg, Ballard Estate, Mumbai 400 001
1/24, Asaf Ali Road, New Delhi 110 002
80/1, Mahatma Gandhi Road, Bangalore 560 001
365, Shahid Nagar, Bhubaneshwar 751 007
41/316 'Gour Mohan', Ambady Lane,Chittoor Road, Ernakulam 682 011
S.C.Goswami Road, Panbazar, Guwahati 781 001
3-6-272, Himayatnagar, Hyderabad 500 029
28/31, 15 Ashok Marg, Lucknow 226 001
City Centre Ashok, Govind Mitra Road, Patna 800 004

Typeset by
Access Center, Secunderabad 500 003

Printed in India at
Navya Printers, Hyderabad, 500 482

Published by
Universities Press (India) Limited
3-5-820, Hyderguda, Hyderabad 500 029

To

Ann, Revati and Rohini

Contents

Foreword
Preface

1. Introduction 1
   1.1 What is deterministic chaos? 1
   1.2 Deterministic reductionism 2
   1.3 Sensitive dependence on initial conditions: the butterfly effect 3
   1.4 Nonlinearity 5
   1.5 Small can be chaotic 8
   1.6 Examples of deterministic chaos 9
      1.6.1 Leaking faucet 9
      1.6.2 Turbulence in pipe flow 10
      1.6.3 Rayleigh–Bénard convection 12

2. The tools and language of chaos 16
   2.1 Phase space and phase flow 16
   2.2 Attractors 18
   2.3 Poincaré section 21
   2.4 Dissipative and conservative flows in phase space 23

3. Simple models of chaos 25
   3.1 Logistic map 25
      3.1.1 Universality 29
      3.1.2 More on the logistic map: Tangent- and period-doubling bifurcations, intermittency 31
   3.2 Circle map 33
   3.3 Routes to deterministic chaos 39

4. Strange attractors 41

5. Chaos without dissipation: Hamiltonian chaos 47
   5.1 Hamiltonian dynamics 49
   5.2 Integrable and non-integrable systems 51
   5.3 Invariant tori: resonant and non-resonant cases 53
   5.4 KAM theorem 55
   5.5 Twist map 56

5.6 Destruction of resonant tori and soft chaos 57
5.7 Standard map 60
5.8 Driven pendulum 60

6. Fractals, multifractals and reconstruction of strange attractors 64
6.1 Fractal dimension 65
6.2 Examples of fractals: Cantor dust, Koch snow flake 66
6.3 Correlation and information dimensions 68
6.4 Multifractals and the spectrum of singularities of local density of points: the $f(\alpha) - \alpha$ plot 69
6.5 Reconstruction of strange attractors 72

7. Concluding remarks 76

Appendix A 80
Lyapunov exponent 80

Appendix B 82
Randomness of deterministic sequences: Bernoulli shift, Baker transformation and the Smale horseshoe 82
B.1 Baker transformation 84
B.2 Smale horseshoe 85

Appendix C 87
Linear stability analysis 87

Appendix D 90
Saddle point and homoclinic point: Generator of Disorder (GOD) 90

Suggested further reading 93

Index 95

Foreword

The Jawaharlal Nehru Centre for Advanced Scientific Research was established by the Government of India in 1989 as part of the centenary celebrations of Pandit Jawaharlal Nehru. Located in Bangalore, it functions in close academic collaboration with the Indian Institute of Science.

The Centre functions as an autonomous institution devoted to advanced scientific research. It promotes programmes in chosen frontier areas of science and engineering and supports workshops and symposia in these areas. It also has programmes to encourage young talent.

In addition to the above activities, the Centre has undertaken a programme of publishing high quality Educational Monographs written by leading scientists and engineers in the country. These *are short accounts of interesting areas in science and engineering* addressed to students at the graduate and postgraduate levels, and the general research community.

This monograph is one of the series being brought out as part of the publication activities of the Centre. The Centre pays due attention to the choice of authors and subjects and style of presentation, to make these monographs attractive, interesting and useful to students as well as teachers. It is our hope that these publications will be received well both within and outside India.

C.N.R. Rao
President

Preface

This book is about *Deterministic Chaos*. That is, how simple physical laws, such as Newton's laws of motion, acting on simple physical systems, such as a pendulum, can turn out an irregular and seemingly random motion that is too complex to predict or compute to any given degree of accuracy in the long run. *Chaos* is the science of complexity of change — Nature's apparent madness in method.

There are compelling reasons why one ought to be mindful of chaos. First, chaos exists and it is common. It is obviously there in the turbulence of a fluid in flow — through pipes, past obstacles, in rotation, or in convection when heated from below, beyond certain thresholds of velocity, temperature gradient, etc. It also lurks in the dripping of a leaking faucet as the flow rate is gradually turned on. It underlies the long-term unpredictability of weather and it seems to be implicated in the fluctuations of share prices in stock markets. The erratic reversals of the polarity of earth's magnetic field, of which we have had at least sixteen in the past four million years, are suspected to hide an erratic geomagnetic dynamo. So is possibly the case with the occurrence of earthquakes. Indeed, researchers have detected chaos at work in the most unexpected places, often masquerading as noise, e.g., in ecology (rise and fall of the population of certain moths, fishes, and of other competing species in a given region), epidemiology (recurrence pattern of epidemic infections like measles as different from small pox), economics (fluctuation of commodity and stock prices), dynamical diseases like apnea (a temporary cessation of breathing) and disturbed chemical and biological clocks (the circadian rhythms of mosquitoes). Chaos-informed analysis of the erratic signals from the schizophrenic brain (EEG) and the arrhythmic heart (ECG) are opening up new directions in brain research and cardiology. Thus, chaos is the rule rather than the exception, or a mere oddity. In fact, all motions in physics and reactions in chemistry turn chaotic for some initial conditions when driven hard enough, far from equilibrium, to the nonlinear regime — when more becomes different.

Second, chaos provides a novel, non-Newtonian world-view where chance emerges out of the very necessity of the deterministic laws. It provides a powerful and controlled way of thinking meaningfully about many an old as well as new phenomenon, such as turbulence, that otherwise appears a maelstrom of confusion. Here chaos has a philosophical flavour that one cannot resist.

Third, while chaos is definitely all about complexity, it itself is rather easy to get acquainted with. And what is more, here one can go a long way without much formal training beyond the level of pre-university science. Most encouraging! This is so because some of the most powerful methods developed for the study of chaos are also mostly qualitative in nature and are best visualized through pictures — a kind of visual mathematics you might say (see the Visual Mathematics Library (Vismath) publication *Dynamics: The Geometry of Behaviour* by Ralph H. Abraham and Christopher D. Shaw, Aerial Press, Santa Cruz (1981), for a delightful exposition). Thus, one typically asks what happens to a geometrical form when it is alternately and repeatedly stretched out and folded back. In fact, repeated application (or iteration) of a simple recursive rule is the standard tool for producing and analysing chaotic motions. After all, more and more iterations can eventually lead to something that either stays put (constant), or keeps on repeating itself (periodic), or keeps changing without ever repeating itself (aperiodic). The last one signifies chaos. There is no other alternative! Further, chaos, because of the inherent *sensitive dependence on initial conditions*, can be put to practical use — chaotic mixing by advection in fluid flows for example. This is much faster than molecular-level diffusion and much less energy consuming than vigorous stirring. This has obvious relevance to pollutant dispersal and industrial mixing. As we will see later, chaos has within it barriers to mixing that must be fully appreciated.

And finally, studying chaos can be great fun, especially if you own a programmable calculator, or better still a personal computer. With simple programmes you can generate complex patterns that evolve creatively as if possessing a free will of their own. One cannot ignore the eudemonic aspect of chaos study.

Our knowledge of chaos is of recent origin. It all began in the early 1960's with the MIT meteorologist Edward Lorenz trying out his convective toy model simulating weather on his computer and finding it impossible to get reproducible outputs. Rounding off errors of the digitized computation were obviously getting amplified uncontrollably. Chaos was, of course, detected even earlier but dismissed as mere noise as by Balthasar van der Pol, who complained of intermittent noise while tuning the capacitor in a neon-bulb R–C

relaxation oscillator driven by a sinusoidal voltage. But scientific interest in chaos has really mushroomed in the last two decades or so, and has become a growth industry by now.

In order to see chaos in the proper perspective consider the following. The first half of the twentieth century had witnessed the revolutionary development of three of the greatest scientific conceptions of the human mind. The first two are *quantum mechanics* and *special relativity* that together dominate the realm of the small — molecules, atoms and so on down to the smallest constituents of matter and the fundamental forces that hold them together. The third is *general relativity* (gravitation) that dominates the realm of the very large. These are the great framework theories to which all happenings in the physical world must be justified. The second half of this century, at its turn now has, however, witnessed the development of yet another scientific conception — the idea of *deterministic chaos*, that some believe is as revolutionary in that it represents a new paradigm — of uncertainty consistent with determinism. Quantum mechanics and relativity have shown that the classical Newtonian laws of physics are at best approximate and have a limited domain of validity: Nature does not obey the laws of classical physics exactly. But deterministic chaos goes differently: Chaos obeys the letter of the law that be, but not the spirit of it! What could be simpler than a damped, rigid pendulum driven by a periodic force off resonance? And yet, beyond a threshold condition the motion becomes erratic after just a cycle or two and as unpredictable as the successive outcomes of a tossed coin. How can this unpredictable 'chance' emerge from the very necessity of the deterministic law? The answer lies in the *sensitive dependence on the initial conditions*. The latter blows out of proportion an 'ever so-small-a-swerve of an atom'. And this there must always be. This is the basis of the new world-view that deterministic chaos has offered: *Chance out of necessity*!

Scientific literature on chaos in the form of original research papers in journals and monographs has simply exploded. It goes by the forbidding name 'Nonlinear Dynamical Systems'. But all this is for experts. There are also several popular books on chaos, e.g. the 1987 bestseller by James Gleick addressed to the general public.

In this book, however, I have addressed the curious lot among students of Science and Engineering at all stages of their undergraduate studies. I also have in mind college teachers who may want to enliven their lectures, on mechanics in particular, with some current topics. Much of the book is, however, accessible to anyone with a pre-university science background.

The book is organized as follows. Chapter 1 is a general introduction to deterministic chaos. Most basic concepts have been introduced here. It is essentially complete in itself. I strongly urge the reader not to skip it. It is intentionally written in a discursive style. Chapter 2 introduces some simple geometric tools such as phase-space flows, maps, attractors, Lyapunov exponents, etc., mostly through pictures. Chapter 3 treats the period-doubling route to chaos through the celebrated examples of the *logistic map* and the *circle map*. Other routes to chaos are also briefly mentioned. Chapter 4 discusses the *strange attractor* — the heart of chaos. Chapter 5 introduces chaos in non-dissipative dynamical systems — *Hamiltonian chaos*. It presupposes some knowledge of Hamiltonian mechanics, and acquaints the reader with the celebrated *KAM theorem*. Chapter 6 offers a lightning course in fractals that underlie the strange geometric structure of strange attractors. Chapter 7 concludes with general remarks on other aspects of chaos not discussed in the book, and some open questions. There is a set of four Appendices that help the reader with technical matters like linear stability, Lyapunov exponents, saddle points, separatrices, homoclinic orbits, etc. Finally, for the highly motivated reader I have suggested a selection of books and articles. In particular, the book *Chaos and Nonlinear Dynamics: An Introduction for Scientists and Engineers* by Robert C. Hilborn (Oxford University Press, Oxford, 1994), with its list of annotated references, should be of much help.

I would like to express my gratitude to Prof. N. Mukunda for carefully scrutinising the manuscript and making valuable suggestions. The organization of matter for this book was also much facilitated by reference to the chapter on chaos in the book *Invitation to Contemporary Physics* (World Scientific, Singapore, 1990) that I had co-authored with Dr. Ho-Kim Quang and Dr. C. S. Lam. I have also benefited much from reading *Chaotic Dynamics: An Introduction* by G. L. Baker and J. P. Gollub (Cambridge University Press, Cambridge, 1990), and *Exploring Complexity* by G. Nicolis and I. Prigogine (W. H. Freeman, San Francisco, 1989). Finally, I would also like to thank my long-time friend Mr. R. Ashiya of ISRO Satellite Centre (ISAC), Bangalore, for his keen interest in this project and for bringing several references to my attention.

Prof. P. W. Anderson of Princeton University has spoken of the study of complexity as 'the leading edge of Science' and 'exhilarating'. And chaos, after all, is all about the complexity of change. So, read on — with attention!

N. Kumar
Bangalore, 1996

1 *Introduction*

1.1 What is deterministic chaos?

By chaos we mean an irregular, seemingly random change in time or motion which is too complex to predict in detail or rather compute with any given precision in the long run. We say *seemingly* random because the physical laws and the forces that govern the motion are all perfectly deterministic and given — Newton's laws of motion, springs and friction for example. Hence the more appropriate term *deterministic chaos* is used in order to distinguish it from what is merely a stochastic noise that results from the unreckoned and uncontrolled forces that may be acting on the system from the outside. A textbook example of the latter is the Brownian motion of a speck of pollen moving zigzag in water under the influence of countless impulses from the unobserved water molecules (the unpredictability here results from the statistical complexity of the system — the large number of molecular degrees of freedom involved that defy all attempts at book-keeping). Deterministic chaos is, however, different. Even a small system, that is one consisting of a small number of sub-units (or degrees of freedom) can become chaotic. Thus, a system of just two coupled oscillators can act up and show chaos if excited beyond an energy threshold. It is this complex and seemingly unpredictable behaviour of relatively simple systems that deterministic chaos is all about. Such systems are computationally irreducible, in the sense that watching their own evolution continuously is the shortest and the most efficient procedure for determining their future course.

Let us get acquainted with chaos through some common real-life examples. Think of a game of chance of your choice. It may involve a mere tossing of coins, or the shuffling of a pack of cards, or the spinning of a wheel of fortune, or doing just about any such thing that people often do for fun and occasional profit. You may have watched the erratic movements of the kinetic toys that are found in expensive gift shops. Or, if you are given to serious thought, you may have wondered at the everchanging pattern of daily weather and the hopeless task of forecasting it in the long term. You may have also been fascinated by the smooth streamlines of water flowing past an

obstacle and growing into a roaring turbulence with its bottomless pit of novelty eddying downstream. Or perhaps the rising column of cigarette smoke, breaking abruptly into whorls on attaining a certain height above the lighted tip. You may have often listened to the monotonous dripping of a leaking faucet developing into a never repeating pattern, like the beats of an infinitely inventive drummer, as the flow is gradually turned on. Or you could perhaps experiment now with numbers if you own a programmable calculator, or a PC. You could generate a sequence of numbers by the repeated application (that is, iteration) of a set of simple arithmetic operations, such as choosing an arbitrary input number, between 0 and 1, multiplying it by 2 and retaining just the fractional part of the product as the output which then serves as input for the next round of iteration. You will be surprised to find that the sequence of numbers so generated through the strictest (mathematical!) determinism turns out to be as random as the outcomes of the tossing of a coin. Indeed, it is by some such device that computers generate their store of random (or rather pseudo-random) numbers. The list of examples is endless. Now ask yourself what is the common element in all these examples. The answer that leaps to the mind is, of course, unpredictability. It is there in the tossing of the coin and understandably so; but strangely enough it is also there in the rising column of the cigarette smoke and in the little arithmetic game that we had devised, despite their simplicity and the strictly deterministic laws that govern them. Let us sharpen this observation further.

1.2 Deterministic reductionism

The laws of classical (that is Newtonian) physics are deterministic. Given a complete knowledge of the initial conditions, namely the initial positions and velocities of all the particles, the entire future course of events is determined uniquely. This is the Newtonian world-view that has served us so well. Just think of the accuracy with which astronomers can calculate the positions of planets and comets and the times of eclipses years in advance; or contemplate the unthinkable precision of the calculations that bring beams of electrons and positrons together in a head-on collision at LEP (the Large Electron–Positron collider at CERN in Geneva). Similar triumphs of deterministic dynamics led Pierre Simon Marquis de Laplace to pronounce an extreme reductionism that viewed the whole universe as a mere outworking of the deterministic laws that do not permit 'ever-so-slight-a-swerve' of even an atom from its determined trajectory, calculable in principle. All we need is the complete set of initial conditions (and perhaps a Laplacean

demon to do the reckonings). The necessity of the deterministic laws leaves no room for the play of chance. Randomness and probability emerge as mere convenient measures of the missing information about the initial conditions. These derived concepts are useful when the information is partially, contaminated or priced, but otherwise of no fundamental significance. In principle, the universe is as predictable and calculable as the motion of the cue ball on the billiards table, or of a simple pendulum — only much more complex. This reassuring 'billiards-ball' world-view of Laplace, with its razor-edge exactness in principle, was, however, suspected of missing the point, or of being irrelevant, by James Clerk Maxwell; it was questioned more critically later by the great French mathematician Henri Poincaré at the end of the 19th century. It is now known to be in *serious error, in a well-defined sense*, as demonstrated by the recognition of deterministic chaos. Poincaré spoke of the *sensitive dependence on initial conditions* that could square up ideal determinism with real chaos that prevails. Let us examine how.

1.3 Sensitive dependence on initial conditions: The butterfly effect

The strict determinism of classical physics is, of course, not in doubt. What is really in question is the insistence on the complete and exact specification of the initial conditions — the numerical values of positions and velocities of all the particles composing the system. Now specifying any such initial data involves physical measurements and all such measurements are necessarily approximate due to finite instrumental accuracy. For example, every vernier has a least count. The relevant question then is whether these approximately known initial conditions permit quantitative predictions which are approximate roughly in the same numerical proportion. In fact it is in this, and this practical sense only, that predictability acquires meaning operationally. The errors due to the rounding off of the numerical initial data must remain bounded, or at worst grow linearly with time. The system must be error tolerant and robust. But, what if the initial errors grow exponentially with time? Then no matter how small but finite initially, the errors get amplified catastrophically, and much too quickly at that. Such an error will not go away merely by increasing the numerical accuracy with which the initial conditions are known. All that the latter can do is to delay the catastrophe slightly (logarithmically). Such is the tyranny of exponentials! Such a runaway propagation and growth of errors blurs the correlation between the final output and the initial input (data) after a sufficient lapse of time which, in practice, turns out to be rather

short. This loss of memory of the initial conditions is what makes the long-range prediction all but impossible while the evolution is still strictly deterministic. We say that the system has become chaotic!

This idea is best illustrated graphically through a 'phase space' picture as in Fig.1.1(a). The abscissa (X) and the ordinate (Y) represent, respectively, the position and the velocity of a 'particle', and thus specify its instantaneous state and, therefore, determine its future trajectory completely and uniquely inasmuch as the laws of motion are strictly deterministic. We can see now that the two trajectories that started off initially at two closely spaced points diverge out far apart. The exponential divergence with time may be written as $e^{\lambda t}$ and $\lambda > 0$ is then called the *Lyapunov exponent* (see Appendix A). It measures how fast the divergence develops. This is reminiscent of the instabilities we know from common experience, e.g. of objects critically poised on a pinnacle — a needle standing vertically on its point, or a marble resting atop a convex vessel. The slightest disturbance, as if a mere 'thinking at it', will produce effects totally out of proportion to the cause, namely the needle falling off to the left or to the right, say. For a chaotic system of course, *every point* on its trajectory has this instability. An 'ever-so-slight-a-swerve' will lead to an entirely different destination. Reminds one of the 'clinamen' of Lucretius who argued that such minimal swerves of atoms give the plurality of the observed universe. This point is further driven home by the following example taken again from billiards. It has been claimed that an initial miscue of the cue ball (positional uncertainty) of the order of the diameter of a nucleus (about 10^{-13}cm), or even much less, can get amplified to the size of the billiard table after just about 15 collisions with other balls and with the edges of the table! Or better still, the gravitational force due to an electron at the edge of the universe can alter the cue ball course qualitatively in just about *one minute*! Imperceptibly small differences at the points of contact of the convex curved surface of the ball with other surfaces get amplified exponentially. See Fig.1.1(b). This remarkable sensitivity is referred to figuratively as the *butterfly effect* [1] — the flap of a butterfly's wings in Brazil sets off a tornado in Texas! For a chaotic system, the underlying strict determinism manifests at a scale which is too fine grained to be sensible to our coarse-grained sensors that necessarily have finite resolution.

The above discussion merely hints at a possible scenario that seems odd enough. The question now is: what can possibly cause

[1]This figurative statement dramatizes the unpredictability of weather because of the extreme sensitivity of the atmosphere to perturbations. It first appeared in an address by E.N. Lorenz at the annual meeting of the American Association for the Advancement of Science, in Washington on 29 Dec. 1979. It epitomizes chaos now.

this hypersensitivity to initial conditions? Do we, for instance, have to fine tune parameters? The answer is no, we do not have to. What is needed is nonlinearity — the single most creative principle at work in Nature.

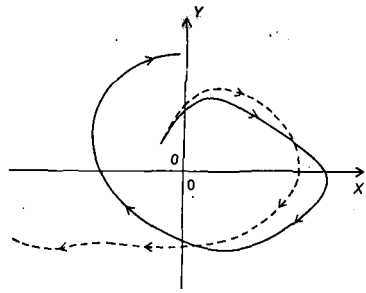

(a)

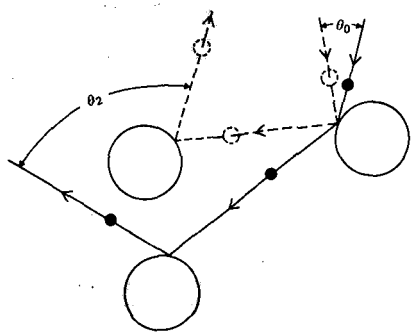

(b)

Fig.1.1(a) Sensitivity to initial conditions (SIC). Divergence of two initially neighbouring trajectories. **(b)** Defocusing of trajectories by the convexity of scattering surfaces giving sensitivity to initial conditions.

1.4 Nonlinearity

Nonlinearity is Nature's way of ensuring that *more may be different.* It is something like changing the rules of the game depending on the current status (or stage) of the game, thus generating surprises. By

contrast, linearity is nothing but *more of the same*. Thus, $X_{n+1} = 2X_n$ is a linear recursion relation that generates X_{n+1} from X_n by just doubling it. Here the previous nth output X_n acts as input for the next $(n+1)$th output X_{n+1}, and the process is to be repeated, or iterated. A change in X_n produces a proportional change in X_{n+1}. The constancy of the multiplier 2 is the constancy of the rule of the game of multiplication. We get an entirely predictable and readily calculable growth. The effort involved in computing the output at the end of n iterations, starting with a given seed, or initial value X_0, is more or less independent of n no matter how large n is. Now let us introduce a nonlinear feedback. Let $X_{n+1} = 2X_n \pmod 1$. We have mentioned this example earlier. It is called the *Bernoulli shift* (see Appendix B). In plain English it reads thus — choose any input number X_0 between zero and one, multiply it by two, discard the integer part of the resulting number and retain the fractional part as the output, X_1. The last operation is abbreviated as (mod 1) above. Repeat, or iterate this operation any number (n) of times and get the sequence $X_0, X_1, X_2, \ldots, X_n$. It should be obvious that the X's will all be between 0 and 1 by the rule of construction. This may be likened to a dynamical system but with discrete time n. You can imagine X_n to be the population of a community at the end of the nth year. Or, your savings bank balance n years after the initial deposit. (For an amusing example, let X_0 be your initial deposit with the bank and X_n its compounded value at the end of n years, expressed as a fraction of some maximum 'ceiling' fixed by the bank. The bank has an unbelievably high interest rate that would double your balance every year, but for the unfortunate proviso that should at any stage your balance exceed the ceiling, that is unity, you will be left only with the fractional part of it — a kind of Sisyphean bank account if you like.) Doubling at each iteration is a linear amplification that would make X_n eventually exceed 1, but the proviso (mod 1) is a nonlinear feedback that folds it back into the unit interval. We will see now how this combination makes the system evolve in a most unpredictable manner, making it chaotic despite its deterministic simplicity. It shows *sensitivity to initial conditions* (or SIC for short).

Let us start with the initial value, or seed, $X_0 = 0.1249$, say. Successive iterations give $X_1 = 0.2498$, $X_2 = 0.4996$, $X_3 = 0.9992$, and so on. Now we start again with a slightly different seed $X_0' = 0.1251$, say, that differs from the earlier seed X_0 by just 0.0002 (the 'error', if you like). Successive iterations now give $X_1' = 0.2502$, $X_2' = 0.5004$, $X_3' = 0.0008$, and so on. Now compare $X_3 = 0.9992$ and $X_3' = 0.0008$ and you should get the point. The two sequences, or trajectories (the unprimed and the primed), that started with

a mere difference of 0.0002, have already diverged drastically. In fact it can be demonstrated that for large enough n, the points X_n jump erratically on the unit interval, covering it almost uniformly, but randomly with constant probability density. This can be made more transparent by writing the numbers in the binary system, i.e. as sequences of zeros and ones. Written this way, the values X_n will resemble the outcomes of the tossing of a true coin, with the heads and the tails representing ones and zeros respectively. What we have here is a random number generator, or *generator of disorder* (GOD for short). We will return to this curious example of what is technically known as the *Bernoulli shift.* Note that when multiplied by 2, the binary sequence shifts one place to the left (see Appendix B). The reason for all this is quite clear. It is just the stretching (multiplication by 2) and the folding-back (mod 1) that accompany every round of iteration. The stretching-out doubles the initial separation, while the folding-back confines them by re-injection into the unit interval and, in doing so, sends them out to different destinations, amplifying the separation catastrophically. We see here the snowballing of the initial error. A synthetic chaos, if you like.

The stretching-out and folding-back described above is essential to the mixed-upness that goes with chaos. A striking illustration of this mixing is the routine kneading of dough by the baker for rolled, multilayered pastries, or by the taffy candy puller. After about twenty stages of rolling-out and folding-back, the dough would have been elongated a millionfold and reduced to molecular thickness, leading to an intricate texture of multilayers! Add a blob of food colouring and what you get is an apparently uniformly coloured mass. But a closer examination will reveal a highly ramified fine-grained structure of alternating white and coloured layers — the initially neighbouring points ending up far apart. This repeated operation of stretching-out and folding-back is known as the *baker's transformation* and is shown schematically in Fig.1.2 (see also Appendix B).

We emphasize again that the evolution law described by the stretching-out and folding-back, such as $X_{n+1} = 2X_n \pmod 1$, is strictly deterministic. Yet there is no way we can explicitly write down the outcome X_n as a function of n that is computable with a short computer programme, whose length is more or less independent of (or weakly dependent on) n. We have to run through the entire course of n iterations in full. There is no short cut, no compression of information possible. It is this kind of computational complexity, called the algorithmic complexity, that characterises chaos (Appendix B). In the final analysis, the *simple* can be equated with the *periodic*, and the *complex* with the *aperiodic.*

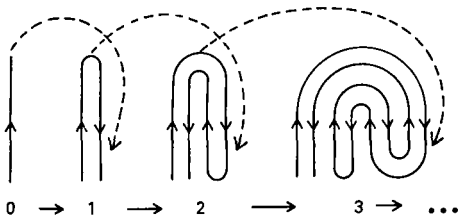

Fig.1.2 Successive stages of stretching and folding-back. Baker's transformation (schematic).

1.5 Small can be chaotic

A small system is one that consists of a small number of interacting sub-units (dynamical degrees of freedom). A well-known example would be the pendulum that Galileo had studied some 400 years ago. The interesting and surprising thing about deterministic chaos is that even a small system, with a small number of degrees of freedom, can become unpredictable. Thus a damped pendulum driven by an external sinusoidal force can become chaotic if driven hard enough. So can the system of two nonlinearly-coupled oscillators when sufficiently excited. Indeed, it would hardly be surprising if a system with a large number of degrees of freedom behaved chaotically. The web of effects caused by interactions among the multitude of degrees of freedom can get all too quickly entangled beyond our power to resolve it. The complexity here would be that of information handling and processing. The complexity of a truly chaotic system, on the other hand, is algorithmic as discussed before.

One could try to create a semblance of chaos through incommensuration. Consider a system of a large number of pendulums oscillating independently at frequencies which are incommensurate, i.e., the ratios of frequencies are irrational numbers. It is clear that such a dynamical system as a whole will be aperiodic — the state of the system (the set of all positions and velocities) will almost but never quite repeat itself. This quasi-periodicity is, however, not chaos. There is no mixed-upness here. It is not robust. That is, and this is important, a small nonlinear coupling, as may be provided by the common support for the two pendulums, can

lead to frequency entrainment. The incommensurate frequencies can get phase-locked into the nearest commensurate values. This makes the system periodic again. Such frequency entrainment was first observed by Christiaan Huygens in the 17th century when he noticed that two clocks hanging on the same wall ran in precise synchronism. Here the coupling, though weak, is provided through the common suspension or support.

But how small can this small be? As we will see later, there is a minimum number of degrees of freedom needed for chaos. Thus, for a system evolving continuously in time through differential equations, the state space must be at least three dimensional. Two dimensions turn out to be a straitjacket. For chaotic behaviour there must be an escape into the third dimension. For a discrete time evolution through difference equations such as $X_{n+1} = 2X_n \pmod 1$, which are not invertible, there is no such minimum.

1.6 Examples of deterministic chaos

We conclude this chapter with some common examples of chaos taken from real life.

1.6.1 Leaking faucet

A leaking faucet with its monotonous drip-drip-drip ... is not an uncommon sight or sound. The regularity of its dripping pattern makes it a water-clock. The dripping pattern, however, changes as the flow rate (the control parameter) is gradually turned on. First, at a low enough flow rate, we have the drip-drip-drip ... with the drops falling at equal time intervals, say T_0. Thus, the repeat unit consists of a single interval T_0, i.e. a single drop. Beyond a threshold of the control parameter, however, the pattern changes abruptly to pitter-patter-pitter-patter ... The repeat pattern now consists of one short and one long interval, T_1 and T_2, say. We say that the period has doubled. By doubling what we mean here is that the repeat unit now consists of two successive drops — the twosomeness of it — and not the actual length of the time interval (which, if anything, must have diminished). This new pattern with period two, persists till the control parameter hits yet another higher threshold. Then the pattern again changes — the repeat unit now consists of four successive drops with unequal intervals T_3, T_4, T_5, T_6, say. Thus the period has doubled again. What has happened is that each of the two periods has bifurcated into one short and one long period as is shown schematically in Fig.1.3. And so on, at successive thresholds. Thus at the kth threshold, we have the

kth bifurcation, giving period $\sim 2^k$. However, the successive control-parameter thresholds come closer and closer and eventually, at a critical flow rate, converge to a point of accumulation as k tends to infinity. There the period becomes 2^∞, that is, infinite. The dripping pattern never repeats itself! It becomes aperiodic, as if dripping to the tune of an infinitely inventive drummer. This is chaos.

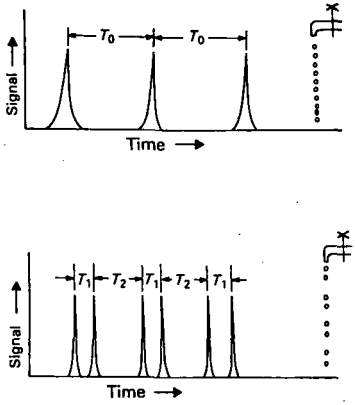

Fig.1.3 Period doubling in a leaking faucet. From 2^0-cycle (period T_0) to 2^1-cycle (periods T_1, T_2).

It is important to note that the actual lengths of time intervals and the threshold values of the flow rate may depend on all sorts of details — the surface tension of the liquid, its density and viscosity, the diameter of the faucet, etc. But the period-doubling bifurcation pattern is, however, robust and universal. You may, for example, replace water with alcohol and still have the same scenario. It is called the period-doubling route to chaos and there is more about this later.

1.6.2 Turbulence in pipe flow

This example is taken from fluid dynamical turbulence — the last unsolved problem of classical physics. The simple experiment described is essentially the original experiment of Osborne Reynolds, who pioneered research on turbulence in the late 19th century. A long glass tube is connected to a reservoir of water and the flow

is made visible by injecting a 'thread' of dye into the mouth of the tube along its axis (Fig.1.4(a)). Initially, at low flow velocity the thread remains parallel to the axis of the tube, indicating a laminar (streamline) flow. As the velocity is gradually increased (by increasing the pressure head) beyond a critical threshold, the thread of dye abruptly begins to oscillate wildly and within a short distance from the point of entrance, the dye spreads uniformly throughout the tube. The control parameter here is the dimensionless number called Reynolds number $R_e = VL\rho/\mu$, where V is the flow velocity in the tube, L the tube diameter, ρ the fluid density and μ the fluid viscosity. Thus R_e is the ratio of the transverse length scale of the macroscopic flow to the characteristic length scale on which the velocity tends to vary. It is also the inertial-to-dissipative force ratio as one can learn from the Navier–Stokes flow equation. It really measures the nonlinear effects. At large R_e, the flow is dominated by inertia while at small R_e, it is dominated by viscosity. Wide range of R_e is encountered in Nature, from 10^{-6} for a bacterium to 10^6 for a human swimmer to 10^9 for a submarine. For swimming, at low Reynolds number (< 1), one uses viscosity (ciliary propulsion). For higher Reynolds number (> 1), one chooses inertial propulsion (flagellation). The critical threshold condition for the transition from laminar-to-irregular (turbulent) flow is $R_e = R_c$, with R_c about 2000 (but it is sensitive to pipe roughness and can be as high as 10^5 if the pipe is very smooth and the flow is increased very slowly. On the other hand, the critical Reynolds number for the reverse, irregular-to-laminar flow transition is about 2300 and is much less sensitive to these conditions). What seems to happen is that as R_e exceeds R_c, the flow goes through a bifurcation sequence of self-limiting instabilities, cascading into fully developed turbulence all too quickly. By self-limiting we mean that the initial exponential growth of a linearly unstable amplitude settles down to a finite value due to nonlinear effects. Turbulence is also encountered downstream, in the flow of a fluid past obstacles, such as a cylinder (Fig.1.4(b)), i.e., in the wake with an open boundary. In the gradual transition between the onset of the first instability and the fully developed turbulence, we have patterns of vortices and their shedding, the so-called *Karman vortex street* (for an excellent visualization, see *An Album of Fluid Motion*, Milton D.van Dyke, Parabolic Press, Stanford, 1982). The wild fluctuations of the fluid velocity in turbulence can be probed very accurately by the *Doppler velocimetry method*, i.e. by the shift in the frequency of a laser beam scattered by the fluid in motion, to 1 part in 10^{12}! It confirms the unpredictability of the chaotic motion. Similar vortex instabilities occur in the *circular Couette flow* of a fluid confined between two

cylinders when the angular velocity of the inner cylinder exceeds a critical Reynolds number. This Taylor vortex flow turns turbulent at a higher Reynolds number in a manner which is not fully understood.

Turbulence in pipe flow, and in open wakes, are still incompletely understood phenomena. In any case, the two appear to be quite different. They are obviously governed by the deterministic Navier–Stokes equations (these nonlinear equations are essentially Newton's equations of motion adapted to fluid flow). However, the route to chaos (from laminar flow to turbulence) is far from clear. The original idea of the great Russian physicist L.D. Landau that turbulence results from the incommensuration of frequencies of the modes appearing one at a time as a result of instabilities, is not tenable.

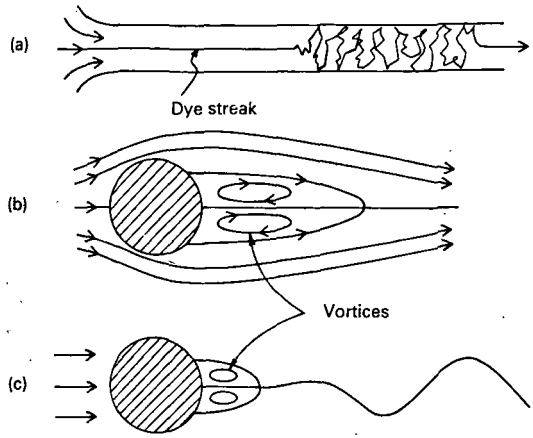

Fig.1.4 (a) Laminar to turbulent transition in closed (pipe) flow beyond critical Reynolds number. Abrupt onset downstream; (b) steady streamlines of open wake flow past cylinder; (c) onset of first instability downstream beyond critical Reynolds number. Higher flow rates give vortex shedding and finally turbulence.

1.6.3 Rayleigh–Bénard convection

This is yet another example of chaos in a fluid set in convective

motion controlled by a vertical temperature gradient. Confine a fluid between two horizontal, parallel, thermally conducting plates, with the lower plate warmer than the upper one. For a sufficiently small temperature difference δT, heat is simply conducted away from the hotter bottom to the cooler top plate without any mass motion. But beyond a threshold value of δT_{c1}, the steady state becomes unstable and convective rolls set in. This happens when the buoyancy forces exceed the frictional forces. The heated and hence the lighter fluid at the bottom plate rises to the cooler top plate, loses the excess heat and then moves out and down, forming a spatially organized pattern that resembles rotating parallel cylinders (Fig.1.5) (similar convection gives rise to the 'Mackerel Sky'

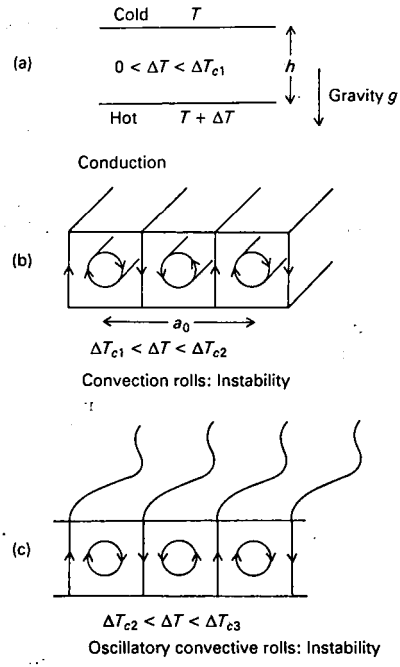

Fig.1.5 (**a**) Thermal diffusion without convective flow; (**b**) Rayleigh–Bénard convective rolls instability; (**c**) oscillatory convective rolls instability. Period-doubling bifurcations cascade to turbulent mixing eventually as Rayleigh number is increased.

on a hot summer day visualized by condensation. Other convection patterns such as the hexagonal Bénard cells are easily demonstrated in the laboratory. Indeed, they are easily made on the surface of coffee prepared by pouring boiling water into a cup containing instant coffee and then quickly adding the cream). At a still higher temperature difference beyond the threshold δT_{c2}, the cylinders begin to wobble transversely. More complex patterns develop at successive thresholds and finally the sequence of instabilities (bifurcations) cascades into a fully chaotic motion beyond the critical threshold $\delta T_{c\infty}$. In fact the route to chaos turns out to be precisely the period-doubling bifurcation discussed above in the case of the leaking faucet (the control parameter for the Rayleigh–Bénard system is the dimensionless Rayleigh number $R_a = g\rho\alpha h^3 \delta T/\nu a$, where g is the acceleration due to gravity, ρ is the density, α is the thermal expansion coefficient, h is the height of the cell, ν is the kinematic viscosity (dynamic shear viscosity divided by density) and a is the thermal diffusivity (thermal conductivity divided by specific heat)).

It was precisely this convective system that Edward Lorenz had reduced to a three-dimensional state-space to model weather in the 1960s, and discovered chaos. A highly sophisticated and controlled version of this experiment was done by Albert Libchaber in 1977 using 'helium-in-a-box'. It confirmed the period-doubling route to chaos. The low viscosity of liquid helium scaled down the cell size to millimeters and the temperature difference to millidegrees and allowed very precise and controlled experimentation at R_a as high as 10^{15} or more.

Above, we have described briefly a few of the commonly occurring fluid dynamical systems that are all well described by the deterministic Navier–Stokes' equation (Newton's laws of motion in disguise) and yet show complex, unpredictable behaviour, that is deterministic chaos. But examples abound. There are also chemical reactions that show periodic-to-chaotic transition, in which concentrations of reactants fluctuate in time and space. The most celebrated example is that of the Belousov–Zhabotinski (BZ) reaction that has been known to chemists for about half a century now. The typical preparation consists of cerium sulphate ($Ce_2(SO_4)_3$), potassium bromate ($KBrO_3$) and malonic acid ($CH_2(COOH)_2$) — all dissolved in sulphuric acid (H_2SO_4). The state space has three dimensions corresponding to the concentrations of $HBrO_2$, Br^- and Ce^{4+}. Under the condition of stirred flow, the concentration of Ce^{4+}/Ce^{3+} can fluctuate chaotically beyond a critical threshold of flow rate. The high flow rate ensures reduced residence time of the reactants in the open reactor. This is essential to avoid equilibration. These fluctuations can be made visible by adding a

colouring reagent, ferroin. The resulting chaotic alternations of red and blue on time scales of a fraction of a minute are visible to the naked eye. The conceptual relevance of this chemical chaos to biological clocks is obvious, e.g. the beating of the heart and various circadian (daily) rhythms.

It has become clear now that most systems maintained far from equilibrium organize themselves in space and time. And chaos is an essential aspect of this self-organization beyond certain thresholds.

2 *The Tools and Language of Chaos*

We have observed earlier that while chaos itself is all about complexity, some of the most powerful tools used for studying chaos are rather graphical in Nature and, therefore, simple to appreciate. They give a qualitative, global understanding of chaos. This chapter is meant to introduce briefly some of these pictorial-geometrical tools. One can, as a matter of fact, go a long way towards describing chaos just through these pictures. Some of these methods were developed by the great French mathematician, Henri Poincaré at the end of the 19th century. When we speak of geometrical forms here, the exact shapes and sizes are often not quite relevant. Two forms are taken to be the same if they can be continuously deformed into each other. We say that they are topologically the same. Thus a sphere and an ellipsoid are topologically the same, but a torus (doughnut) is quite different. Surprisingly this is something that a four-year old learns even before he or she can tell a circle from a square. This greatly helps bring out the intrinsic commonality of otherwise dissimilar dynamical systems.

2.1 Phase space and phase flow

This is a straightforward generalization of the commonly used idea of Cartesian coordinates, the three numbers (X_1, X_2, X_3) needed to position a particle in the familiar three-dimensional Euclidean space, much the same way as we need to know the latitude, the longitude and the altitude of an aircraft to pinpoint its location. We say that the particle has three degrees of freedom. In order to specify completely the state of motion of the particle, however, we need not only the three coordinates but also the corresponding three components of velocity (or momentum), making up six numbers in all. Thus, for N particles, the same reasoning would require $6N$ numbers. We can now imagine a space of $6N$ dimensions. A single point in this hypothetical space represents completely the state of motion of all the $6N$ particles at any instant of time. We call it the *phase space.*

As the N-particle system evolves in time according to the laws of motion, the representative point describes a trajectory or an orbit in

the phase space. Now the laws of motion being deterministic second order differential equations, there must be a unique trajectory passing through any given phase point inasmuch as the phase point gives the positions and velocities of all the $6N$ particles at the given instant of time. It follows then that these phase trajectories cannot intersect or self-intersect. They can, however, close on themselves. *This avoided crossing is the essence of the deterministic dynamics.* (It should be noted here that sometimes, for ease of visualization, we look at the projection of the trajectory on one of the many planes, the $X_1 - X_2$ plane say, much the same way as we may look at the shadow of a kite on the ground. This projected figure of the trajectory on the plane can, of course, cross itself, simply because we have 'flattened' the orbit.) One more generalization is called for. In the study of chaos we may talk about non-mechanical systems where $X_1, X_2, X_3, \ldots$ at any given instant of time determine the entire course of evolution in time. The phase space now becomes a *state space* with $X_1, X_2, X_3, \ldots$ as the axes. Figure 2.1 shows some typical trajectories in the phase space of a harmonic oscillator, damped as well as undamped, having one degree of freedom. The phase space in this case is two-dimensional — it is a phase plane. Hereafter we use the terms state space and phase space interchangeably.

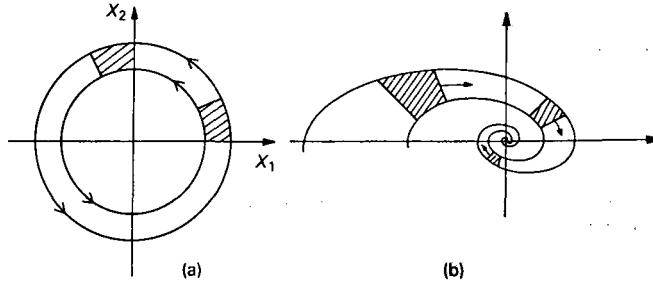

Fig.2.1 (a) Phase flow incompressible for undamped oscillator; (b) phase flow compressible for damped oscillator (schematic).

Next, consider a dust of phase points occupying a region of the phase space at some initial time. This would represent an ensemble of identical systems prepared with different initial conditions. With the passage of time, as each phase point moves deterministically, the cloud of phase points will sweep through the phase space and occupy a new region at a later time. Something like the flow of a fluid — a phase fluid if you like. We may now ask if the volume

of the phase fluid has changed. It is a simple fact that for motion without 'dissipation' (or friction), the volume remains constant — the phase fluid is incompressible — as in the case of an undamped oscillator (Fig.2.1). On the other hand, for a dissipative system (i.e. one with friction) the phase volume contracts with the passage of time as in the case of a damped oscillator. Non-dissipative dynamical systems are said to be conservative (or Hamiltonian systems). In our study of chaos, we will be mainly concerned with dissipative systems. Friction is ubiquitous!

Next, what about the shape of the phase-dust cloud? Well, it changes in all cases. But for systems showing chaos, it becomes rather weird. It thins out and begins to cover a region of space sparsely (Fig. 2.2). But more of this later.

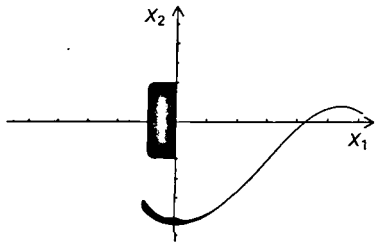

Fig.2.2 Thinning out of phase fluid for dissipative flow (schematic).

Incidentally, all that has been said so far refers to motion in continuous time — it is a phase-flow. If, on the other hand, there is a discrete time (n) evolution as in $X_{n+1} = 2X_n \pmod 1$, it is referred to as a *map* rather than a *flow*. (In this case the phase space is two-dimensional, the two axes being X_{n+1} and X_n, the successive iterates.)

2.2 Attractors

The question naturally arises: what happens to a trajectory if we wait long enough? Let us assume that the trajectory remains confined to a finite volume of the phase-space as is expected of a dissipative motion anyway. The simplest possibility is that it eventually (asymptotically) settles down to a point and stays put there. We refer to it as being *asymptotically stable* — a point of stable equilibrium at which all motion becomes dead beat. We call it a stable *fixed point* (Fig.2.3). Thus, for a damped harmonic oscillator the origin is the fixed point. The fixed point is stable because if the particle is

displaced slightly away from it, it returns to it, in fact spirals into it. The stable fixed point is an *attractor* — it attracts trajectories in its neighbourhood, which is its domain of attraction. For the damped harmonic oscillator, the entire phase space is its domain of attraction. We can obviously also have an unstable fixed point or a saddle point (Fig.2.3). A simple example will suffice. Consider the discrete evolution $X_{n+1} = X_n^2$. You start with an initial value X_0 and keep squaring it (iteratively) to get the successive X's. Now it is clear that for X_0 lying between -1 and $+1$, the successive values get progressively smaller and converge to 0. Clearly, $X = 0$ is a stable *fixed point*, an *attractor*. The domain of attraction is the open interval -1 to $+1$. On the other hand, for any X_0 lying outside this interval, the successive values iterate away to infinity. So there is an attractor at infinity, with the domain of attraction outside the above interval. But what about $X_0 = 1$? Clearly it stays put on squaring (i.e., $1^2 = 1$) and hence it too is a fixed point, but an unstable fixed point. Slightly displaced, the values iterate to zero or to infinity. It is actually a repeller.

Next in the hierarchy of attractors is another geometrical object, a *limit cycle*. Here the trajectory closes on itself, that is to say that the system settles down to a stable periodic oscillation (Fig.2.3). It is *asymptotically stable*. It becomes a clock. In a two-dimensional state space, the limit cycle is the only attractor other than the fixed point. Some thought will convince you that this is a direct consequence of the fact that a phase trajectory cannot cross itself (it can, however, close on itself). In order to have a more complicated attractor, the phase trajectory must escape in the third dimension. A remarkable, rather amusing, example of a fixed point or a limit cycle is provided by the iteration procedure called *Robinsonization*. Consider the following statement: "In this sentence the number of occurrences of 0 is —, 1 is —, 2 is —, 3 is —, 4 is —, 5 is —, 6 is —, 7 is —, 8 is —, 9 is —, ". Now try to fill in the blanks (—) faithfully. The ten entries in the ten blank spaces constitute the vector with ten components. Start off with a seed vector $X_0 =$ (0, 1, 2, 3, 4, 5, 6, 7, 8, 9), say. Now look at these entries while reading the sentence and update them faithfully. You should get the vector $X_1 = (2, 2, 2, 2, 2, 2, 2, 2, 2, 2)$. Now repeat this process to get the vectors X_2, X_3, X_4 and so on. You will soon find out that $X_5 = X_6 = \ldots = X^* = (1, 11, 2, 1, 1, 1, 1, 1, 1, 1)$. You have clearly hit a fixed point X^*. This fixed point has a domain of attraction in the space of ten-dimensional vectors noted above. Indeed, there is one more such fixed point. There is also a two-state loop (i.e. a period-2 attractor). For an interesting discussion of Robinsonization, see *Metamagical Themas: Questing for the Essence*

of Mind and Pattern by Douglas R. Hofstadter, Page 390, Bantam Books, New York, (1985).

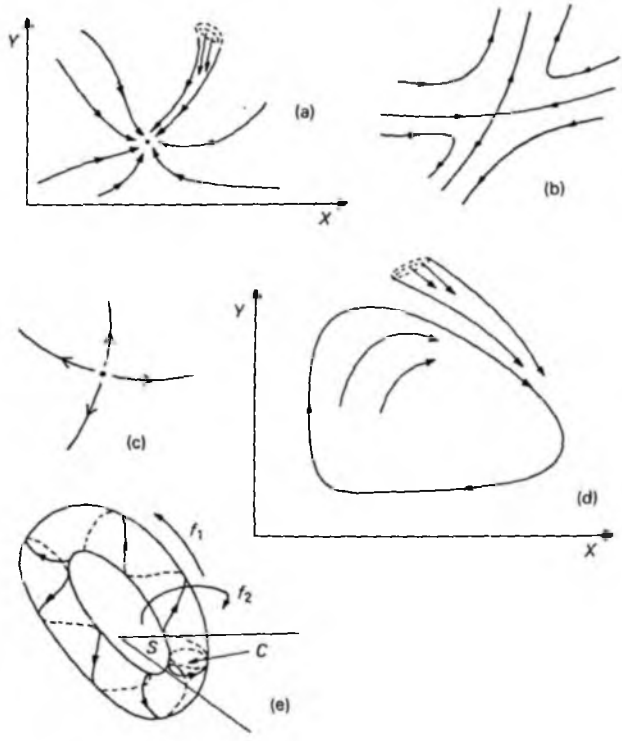

Fig.2.3 (**a**) Stable fixed point; (**b**) saddle point; (**c**) unstable fixed point; (**d**) limit cycle; (**e**) biperiodic torus.

Next to the limit cycle representing a singly-periodic motion, one has a biperiodic torus (Fig.2.3(e)) — a doughnut-shaped attractor in a state space which is at least three-dimensional. Here the trajectory winds round in the latitudinal as well as in the longitudinal direction of the torus with frequencies f_1 and f_2, say (hence the name biperiodic). Clearly, if the ratio f_1/f_2 is rational (equal to ratio of two integers), we have a periodic motion and the trajectory eventually closes on itself. If f_1/f_2 is an irrational number, we have a quasi-periodic motion — the trajectory comes arbitrarily close

to closing on itself but never quite does so. One can have higher-dimensional tori (multiple period motions) in higher dimensions.

The attractors mentioned above all correspond to regular motions. Is there an attractor that corresponds to deterministic chaos? The answer is in the affirmative. It is called the *strange attractor.* It is perhaps the most profound discovery in the theory of deterministic chaos. It is an enigmatic, geometrical object of fractional dimension. We will return to this later.

Thus, attractors are geometrical objects in the phase space to which the trajectories are attracted and on which they eventually lie. They have domains, or 'basins' of attraction. In general there may be several attractors in the phase space with their domains of attraction separated by separatrices — like valleys separated by ridges. Together they form a landscape called the *phase portrait* — the geography of the phase space. One may wonder about the points on the boundaries of the *basins of attraction.* It is like sitting on the fence. Well, this set of points (the basin-of-attraction boundary) can be a bizarre object, called the *Julia set.* As a small example, for the complex map $z_{n+1} = (z_n)^2$, the unit circle $|z| = 1$ is one such set. But in the general case of $z_{n+1} = (z_n)^2 - \mu$, the Julia set is a fractal object.

2.3 Poincaré section

A trajectory in a higher than two-dimensional phase space is often hard to visualize. One resorts to looking at its projection on a plane. It is like following the shadow of a kite on the ground. Indeed, one can reconstruct the actual trajectory from its projections on several planes. There is, however, a much more powerful approach based on the idea of *Poincaré section* which is more like *snapshots* of the phase-space motion taken at regular time intervals. The idea is simplicity itself.

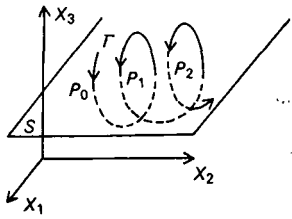

Fig.2.4 Poincaré section for three-dimensional phase flow. S denotes surface of section.

Consider a three-dimensional state space (X_1, X_2, X_3). Choose a *section plane*, X_1–X_2, say. For higher dimensions it will be a *surface of section*. Now mark the points at which the trajectory crosses this plane successively in the same sense, downward along the negative X_3-axis, say (Fig.2.4). We thus get a set of snapshot points P_0, P_1, P_2, ... This set constitutes the *Poincaré section*. Inasmuch as the motion is deterministic, there must be a rule (a mapping) relating the successive points, i.e. $P_{n+1} = f(P_n)$, which really expresses the coordinates of the point P_{n+1} in terms of those of the previous point P_n through the function f. This is known as the Poincaré map (or the first return map). The time periods elapsed between successive returns need not necessarily be equal. What is achieved here is the reduction of the three-dimensional continuous flow to a lower, two-dimensional discrete map. In exceptional cases the points P's may lie on a smooth curve, giving strong dimensional reduction. The nonlinear three-dimensional *differential* equations are replaced by nonlinear algebraic two-dimensional *difference* equations that are much easier to handle. (Thus, we could have the famous Hénon map $X_{n+1} = 1 + Y_n - aX_n^2$, $Y_{n+1} = bX_n$. You could amuse yourself by plotting this two-dimensional map with $a = 1.4$ and $b = 0.3$. You will get the *Hénon attractor*.) And yet, the essential qualitative features of the phase flow are fully retained. If the flow was periodic following a limit cycle attractor, the successive points P_0, P_1, P_2, ... of the Poincaré section will collapse to a single point. If, on the other hand, the flow trajectory lived on a biperiodic torus, the Poincaré section will be a finite set of points or a quasi-continuous curve, depending on whether the two frequencies of the biperiodic motion are mutually commensurate (have a ratio which is rational) or incommensurate (have a ratio which is irrational). And finally, if the dynamics is chaotic, the Poincaré section will be a splatter of points covering an area — successive points of intersection jumping erratically all over the area. Also, for dissipative flows, the Poincaré section will generate a discrete map that will contract areas in the plane too.

The idea of the Poincaré section has a natural generalization to higher than three-dimensional flows. In general, for an n-dimensional flow, we take a section with an $(n-1)$ dimensional hypersurface, locally transverse to the flow. Thus, we reduce the dimension by one which is a great simplification.

There is yet another way of dimensional reduction involving the idea of the *first return map*. One constructs the *Poincaré surface of section* and records the successive intersections of the orbit with the surface as before, and then considers the sequence for just one variable, (X_n) say, so generated (one could also measure X values

at some regular time intervals, or every time X has some local extremal value or crosses a prescribed level). From this sequence, for a single variable, one can obtain an amplitude plot of X_{n+1} against X_n — the first return map. As we will see later it is possible to essentially reconstruct the underlying attractor from such a map. Thus, for instance, if this plot generates to a good approximation a curve with a single hump and a smooth maximum, the system is expected to have the universal features of the logistic map, which will be discussed later.

2.4 Dissipative and conservative flows in phase space

Every point in the phase space or state space describes a unique trajectory governed by the deterministic laws of motion. We can thus imagine the phase space to be filled with a fluid — a phase fluid — that flows. For a system without dissipation (i.e. a *conservative system*) the volume of any element of the fluid is a constant of motion, as in the case of an undamped harmonic oscillator. On the other hand, for a dissipative (non-conservative) flow, the volume diminishes with time. To know whether a phase flow is dissipative or not is quite simple. Consider the case of a damped harmonic oscillator along x-axis. Let X_1 be the coordinate and $X_2 \equiv \dot{X}_1$ its velocity (the overhead dot denotes rate of change of velocity with time, that is it is a time derivative). Then the motion of the oscillator is given by $\dot{X}_1 = X_2$, $\dot{X}_2 = -\omega_0^2 X_1 - \eta X_2$, where ω_0 is the natural circular frequency and η the friction coefficient. These two first-order differential equations are completely equivalent to the usual single second-order differential equation. Thus the phase space is two-dimensional (X_1, X_2) and the phase velocity of any point at (X_1, X_2) is uniquely determined by the coordinates X_1, X_2 (because the right-hand side is fixed by X_1 and X_2). This is exactly how it should be for a phase-space description. Now, to check if the motion is dissipative (i.e. phase volume contracts), all we have to do is to find the divergence of the velocity field $\dot{\mathbf{X}}$. Then $Div\, \dot{\mathbf{X}} = -\eta$, which is negative, thereby verifying contraction and hence dissipation.

For the dissipative motion the phase volume must eventually tend to zero, that is, it must converge to an attractor of a dimension lower than that of the phase space. For example, for a two-dimensional phase space, the trajectory may tend to a fixed point (dimensionality 0) or to a limit cycle (dimension 1), both being less than 2, the dimension of the phase space. Similarly, for a three-dimensional phase space, the attractor may be a torus (two-dimensional surface).

But, in general, in three and higher dimensions there are other possibilities — the attractor may have fractional dimension (to be discussed later).

One last point. For an n-dimensional phase space, the coordinates X_1, X_2, X_3, ... all evolve according to equations such as $X_1 = f_1\ (X_1, X_2, X_3, \ldots)$, $X_2 = f_2\ (X_1, X_2, X_3, \ldots)$ and so on. Such systems are said to be autonomous. Time does not occur explicitly in the functions f_1, f_2, f_3, ... A point in the phase space completely determines the trajectory passing through that point. Even systems which are not autonomous can be made so by augmenting the phase space. Just consider time as the additional variable, $X_{n+1} = t$ so that $\dot{X}_{n+1} = 1$. We now have an $(n + 1)$ dimensional phase space. This is how a damped oscillator driven by a sinusoidally varying time-dependent force is reduced to the usual phase-space description.

3 *Simple Models of Chaos*

3.1 Logistic map

We will now introduce and discuss in some detail one of the simplest models of chaos, the *logistic map*. This has become something of a poor man's laboratory to gain hands-on experience with chaos. Despite its simplicity and seemingly contrived form, it shows a gamut of behaviour that is common to a whole class of real dynamical systems if viewed properly. Indeed, it is this universality of behaviour that makes the study of this simple model really worthwhile.

The logistic map is a difference equation of the form

$$X_{n+1} = \lambda X_n(1 - X_n) \equiv f(X_n) \tag{3.1}$$

giving the evolution of a variable X as function 'f' of discretized time 'n'. Here λ is a parameter (control parameter) which is tunable. You start with an initial condition X_0 (seed value X_n for $n = 0$), put it in the right-hand side (RHS) and get X_1 as the output. You can now repeat (iterate) this process by treating X_1 as your new input on the RHS and get X_2 as the output and so on. This is the kind of repeated operation (iteration) that computers are really good at. The logistic map is the discrete version of the corresponding continuous (differential) equation introduced by P.F. Verhulst in 1845 to model population growth subject to limited resources (or logistics). Hence the qualifier *logistic*. The discrete version was subsequently studied extensively, notably by the physicist turned ecologist-biologist Robert May in 1976. Here X_n denotes the population in the nth year expressed as a fraction of its maximum possible value. Clearly, when the population is small it multiplies happily (boom) unmindful of the resource limitation. But when it grows too large, the resource crunch is felt and this may lead to a decline of the population (bust). However, it may also lead to oscillations, or even chaotic fluctuations depending on the logistics. The control parameter λ in this case, is called the *boom and bust* parameter. Of course, as we have seen, such a one-dimensional discrete map (the first return map) can arise naturally as a Poincaré

section of trajectories in a three-dimensional phase space. It may turn up unexpectedly therefore. It is trivially verified that any quadratic map 'f' can be reduced to the logistic form by proper scaling and translation such as $X' = aX + b$.

Some general features of this one-dimensional nonlinear difference equation strike us at once. All through we maintain λ positive and less than four. First, note that if we start off with an initial value of X between zero and one, the future values also lie in the same unit interval. So the phase space (to be introduced shortly) is a finite one, a unit square in fact. Further, since X_{n+1} is obtained from the previous value X_n by multiplying it by $\lambda(1-X_n)$, it is clear that for $\lambda(1-X_n)$ greater than 1, the successive values will grow bigger and bigger — that is, a change in X_n will get amplified. This is the 'stretching-out' we had referred to earlier. But, of course, X_n cannot increase indefinitely. Somewhere $\lambda(1-X_n)$ will become smaller than 1 and then the subsequent values must diminish. This is the 'folding-back' that we had referred to earlier. This 'stretching-out and folding-back' is essential to chaotic behaviour.

We will now study the evolution of X_n with n by iterating the logistic difference equation. This is done best graphically by plotting X_{n+1} (output) as the ordinate against X_n (input) as the abscissa. Thus we have a two-dimensional phase space (or rather phase plane) which is a unit square in this case. Now we plot the function $f(X)$ against X which is a parabola standing on the horizontal axis, giving you the ordinate X_{n+1} for the abscissa X_n. Finally, we draw the diagonal joining (0, 0) to (1, 1). We are now all set to study the evolution graphically.

Let us fix the control parameter (λ) that determines the steepness of the parabola to be less than 1. Then the parabola is readily seen to lie entirely below the diagonal. Start off with any initial value (input) X_0. To get X_1, we go up vertically to meet the parabola and then move horizontally till we meet the diagonal at P_1, say. The abscissa of P_1 is then our output, X_1. Similarly, to get the next point X_2, we move vertically up from P_1 till we meet the parabola and then horizontally till we meet the diagonal at P_2, say. The abscissa of P_2 is then our next output, X_2 and so on. It is clear that for λ less than unity, we zigzag down to the origin (0, 0) as $n \to \infty$, and stay put there (Fig.3.1). This is so no matter what the initial value X_0 is. The origin is a stable fixed point, an attractor with the entire unit interval as its basin of attraction. We denote it by a starred value, $X_0^* = 0$.

This situation persists for λ less than unity (i.e., till the diagonal becomes tangent to the parabola at the origin). For λ greater than 1, however, it changes qualitatively. It is readily seen that starting with

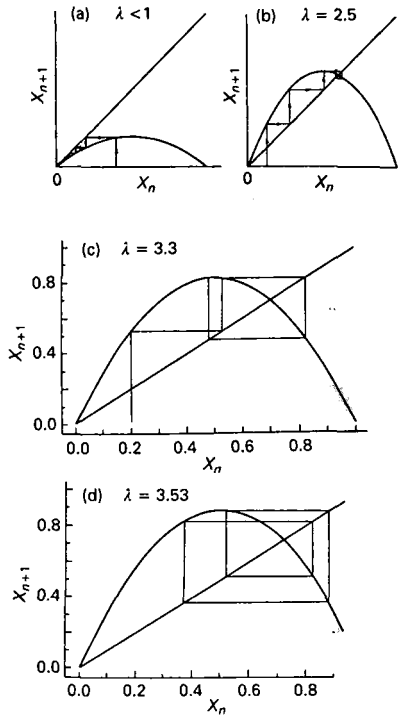

Fig.3.1 Stable fixed point (**a**) at origin; (**b**) away from origin; (**c**) period-2; (**d**) period-4 (schematic).

any initial value X_0, we now zigzag up to a different fixed point X_1^*, say (Fig.3.1). The earlier fixed point X_0^* has become unstable now. A little algebra will help us find these two fixed points. By definition, a fixed point X^* must get mapped onto itself on iteration. Thus, in the case of the logistic map, $X^* = \lambda X^*(1 - X^*)$. This gives two roots, $X_0^* = 0$ and $X_1^* = 1 - 1/\lambda$. A look at stability will show that X_0^* is stable for λ less than 1 while X_1^* is stable for λ greater than 1. For stability all we require is that $|df/dx| < 1$ at the fixed

point (see Appendix C). The stability criterion turns out to be just that the slope of the parabola at the point of its intersection with the diagonal be less than unity in absolute magnitude. (A student of electrical engineering would readily see the connection with the self-excitability of a d.c. shunt generator.) Physically, the fixed point X_1^* implies a periodic oscillation of period 1 (single iteration step). Just think in terms of the Poincaré section of a limit cycle. We call it a period-one orbit, a 1-cycle, or a 2^0-cycle for uniformity of notation later.

Things become curiouser and curiouser as λ is tuned to larger values. Thus, for λ greater than a threshold $\lambda_1 = 3$, both X_0^* and X_1^* become unstable. There are no stable fixed points any more. Instead, the map settles down to alternating between a pair of values, (Y_1^*, Y_2^*) say, which together constitute a stable attractor set now (Fig.3.1). Thus, as we iterate the map, after some transients we converge to a two-step square dance, $Y_1^* \to Y_2^* \to Y_1^* \to Y_2^* \to \ldots$ Hence we call it a period-2 orbit, or a 2^1-cycle, and say that there has been a *period-doubling bifurcation*. You can now guess what happens next. As the control parameter crosses the next threshold $\lambda_2 = 3.44\ldots$, we have a new attractor consisting of a set of $4(=2^2)$ points, $Z_1^* \to Z_2^* \to Z_3^* \to Z_4^* \to Z_1^* \to Z_2^* \to \ldots$ We have a 2^2-cycle. In general, at the nth threshold λ_n, we have the nth period-doubling bifurcation to period-2^n orbit, or a 2^n-cycle. Where does all this lead us to? Well, it turns out that the successive thresholds come on closer and closer, and as $n \to \infty$ they accumulate at the critical value $\lambda_\infty \equiv \lambda_c = 3.5699\ldots$, where the period becomes infinite. The motion has now become aperiodic. It never quite repeats itself. This is the onset of chaos! The phase point X^* jumps all over the unit interval, covering a set which is fractal (see Chapter 6).

This period-doubling bifurcation route to chaos is best illustrated through a scheme called the bifurcation diagram, in which we plot the attractor set against the control parameter (Fig.3.2(a)). One clearly sees the 'pitchfork' bifurcations cascading into chaos at λ_c.

What happens beyond λ_c ? Well, this calls for a much more detailed analysis. Broadly speaking, one has periodic windows in λ interrupting chaos. We call it *intermittency*. The limiting value $\lambda = 4$, however, calls for special attention. A simple substitution, $X_n = \sin^2\theta_n$, gives an equivalent recursion relation $\theta_{n+1} = 2\theta_n$ (mod 2π). This is precisely the example we had encountered earlier except for the minor change from mod 1 to mod 2π. It, therefore, shows the stretching-out and the folding-back so very characteristic of chaos.

3.1.1 Universality

It comes as a pleasant surprise that the beautiful bifurcation phenomenon described above is common to most maps '$f(X)$' that have a single hump, or convexity, of tunable steepness. The details of the precise form, whether a parabola or a semicircle etc., turn out to be irrelevant. All one requires is a quadratic map, with a non-vanishing second derivative at its maximum. This has been called *structural universality*. By contrast, in general maps such as $f(X) = 1 - a|X|^n$, and in particular the 'tent' map $f(X) = 1 - |2X - 1|$ for $0 \leq X \leq 1$ are qualitatively different.

The idea of universality manifests itself more strongly at yet another quantitative level. As we have noted earlier, the successive thresholds (λ_n) get closer and closer as $n \to \infty$. One can quantify this by asking for the ratio of the successive spacings, $(\lambda_n - \lambda_{n-1})/(\lambda_{n+1} - \lambda_n)$. It turns out that this ratio tends to a number $\delta = 4.6692 \ldots$ as $n \to \infty$. What is again a pleasant surprise is that this number is universal — it is the same for most single-hump maps. The feature that determines this universality class is the quadratic Nature of the map at its maximum. Parabolas and most other single hump maps '$f(X)$' have such a quadratic maximum. It is the Nature of the map in the infinitesimal neighbourhood of its maximum that controls the long-time (large n or asymptotic) behaviour of the orbit (X_n). The universal number δ is the celebrated *Feigenbaum number*, named after its discoverer Mitchell Feigenbaum who zeroed in on it on his hand-held calculator, an HP-65! There is yet another universal number associated with the ratio of spacings of the points of successive attractors, (Y_1^*, Y_2^*), $(Z_1^*, Z_2^*, Z_3^*, Z_4^*)$ say, at the successive thresholds λ_n as $n \to \infty$. With reference to the pitchfork bifurcation, it is really the ratio of the openings of the successive generations of forks (Figs.3.2(b) and (c)). The spacings get smaller and smaller and the ratio converges to a universal number $\alpha = 2.5029 \ldots$ rather rapidly. This kind of numerical universality is called the *metric universality*. The idea is quite reminiscent of the universality of critical exponents at second-order phase transitions, like the paramagnetic to ferromagnetic transition at the Curie temperature. It is precisely this universality that makes the study of the logistic map worthwhile. Otherwise, it would have remained just another amusing oddity.

There are several cousins of the one-dimensional logistic map. One has, for example, the complex logistic map $z_{n+1} = z_n^2 - \mu$, which has some of the properties of a two-dimensional logistic map. An interesting aspect of this map is the set of all complex numbers μ such that the seed $z = 0$ does *not* iterate away to infinity. The set

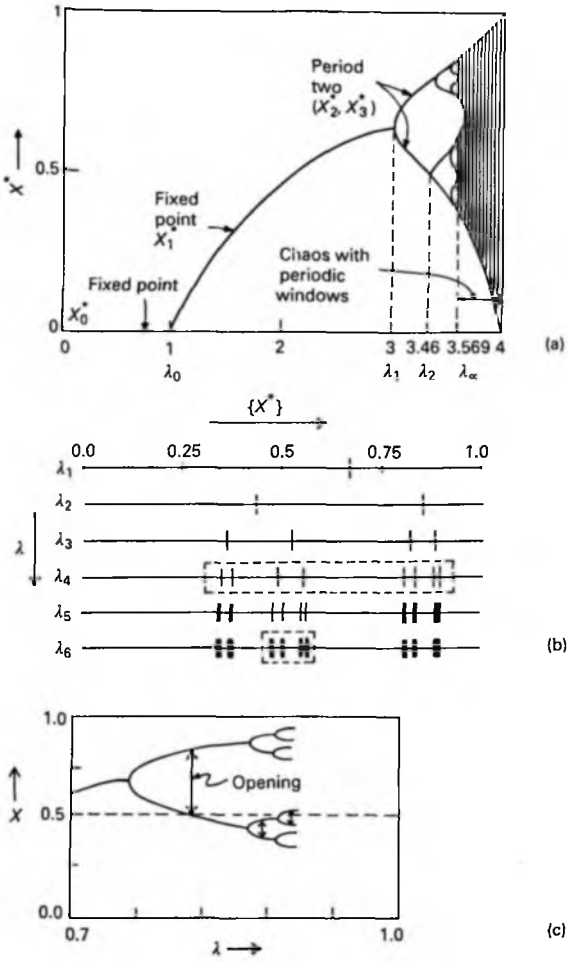

Fig.3.2(a) Bifurcation diagram for period-doubling route to chaos (schematic); **(b)** logistic map attractor sets $\{X^*\}$ at successive period-doubling bifurcations $\{\lambda_i\}$. Spacing at λ_6 is α^2 times that at λ_4, hence self-similar, shown within dotted boxes (schematic); **(c)** logistic map. Bifurcation diagram showing openings of successive forks measured from $X = 0$. The asymptotic ratio defines α as $\lambda \rightarrow \lambda_\infty$.

of all such numbers in the complex μ plane defines a strange cactus-like figure called the *Mandelbrot set.* One could also think of coupled logistic maps, indeed a lattice of coupled logistic maps, that may simulate spatially extended chaotic systems.

3.1.2 More on the logistic map: Tangent- and period-doubling bifurcations, intermittency

As we have discussed before, a period-N orbit by definition returns to the initial point after N iterations. Each point (X^*) of the associated attractor set is, therefore, a fixed point of the modified Nth-return map $g \equiv f^N$, that is $X^* = f^N(X^*) \equiv f(f(f \ldots (f(X^*) \ldots))) \equiv g(X^*)$, with the map '$f$' acting iteratively N times on X^*. This is formally no different from the prototypical period-1 orbit case $X^* = f(X^*)$ except for the replacement of f by g. Again, stability demands $-1 \leq g'(X^*) \leq 1$. A little thought should convince us that the limiting value $g'(X^*) = 1$ corresponds to the condition that $g(X)$ be tangent to the diagonal $X_{n+N} = X_n$ line at X^*. The resulting bifurcation is said to be the *tangent bifurcation.* Thus, at $\lambda = 1$ there is a tangent bifurcation at which the attractor $X_0^* = 0$ becomes a repeller while X_1^* becomes an attractor. The other limiting value $g(X^*) = -1$ similarly corresponds to the condition that $g(X)$ be perpendicular to the diagonal $X_{n+N} = X_n$ line. This is the *period-doubling bifurcation.* It is clear that as λ increases, the slope $g'(X^*)$ starts with the value $+1$ (corresponding to tangent bifurcation) where the orbit first appears and ends with a value -1 (corresponding to period doubling bifurcation) and the orbit bifurcates with a doubling of the period.

Let us illustrate this with the simple example of period-2 orbit (i.e. 2^1-cycle). The fixed points of $g = f(f(x))$ are

$$X_{1,2}^* = (\lambda + 1 \pm \sqrt{(\lambda+1)(\lambda-3)})/2\lambda.$$

Clearly they exist for $\lambda \geq 3$. Now, it is readily verified that $g'(X_{1,2}^*) = 1-(\lambda+1)(\lambda-3)$. Thus at the onset of the stable period-2 orbit when $\lambda = 3$, we have $g'(X_{1,2}^*) = +1$. As λ increases the algebraic slope decreases through zero to -1 at which the period-2 orbit bifurcates to a stable period-4 orbit. Indeed, setting $g'(X_{1,2}^*) = -1$ gives the value of the control parameter $\lambda_2 \approx 3.45 \ldots$, at which the stable period-4 orbit first appears.

Associated with the tangent bifurcation, there is a fascinating phenomenon of intermittency that we now briefly examine. Intermittency provides windows in time of stable periodic orbits in the parameter range of chaos ($\lambda_\infty \leq \lambda \leq 4$). It manifests ubiquitously as coherent, periodic oscillations interrupted by chaotic bursts in

the nonlinear systems — oscillators and fluid flows. Indeed, it is a common route to chaos. The basic idea is quite straightforward. Consider the map $X_{n+1} = f_\lambda(X_n)$ shown schematically in Fig.3.3(a) with two fixed points, one stable X_s and one unstable X_u for $\lambda \lesssim \lambda_c$. Let X_s and X_u coincide at X_c as $\lambda \to \lambda_c$ when the curve $f_{\lambda c}(X)$ is tangential to the diagonal line $X_{n+1} = X_n$. Now, by continuity, the map $f_\lambda(X)$ must lie just above the diagonal for $\lambda \lesssim \lambda_c$ as shown by the dotted line in Fig.3.3(b). Let us look at the trajectory constructed graphically as usual. It is clear that the phase trajectory

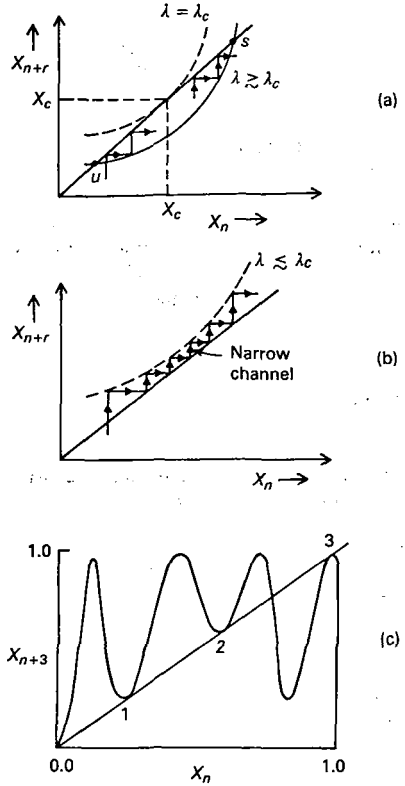

Fig.3.3(a) Intermittency when the return map approaches the tangent to the diagonal; **(b)** the phase point trapped in the narrow channel giving almost periodic, slow motion; (c) the third return map of logistic map at intermittency. Note tangency at three points 1, 2, 3 (schematic).

is trapped in the narrow channel between the map and the tangent line (diagonal) for a long time (i.e. for a large number of iterations) performing a regular motion (laminar phase). Of course, once it emerges out of the channel it wanders chaotically (bursts) until it is trapped again in a similar channel. The situation shown in Fig.3.3(c) is realized, for example, if we look at the third return map $g_\lambda = f_\lambda^3(X)$ of the logistic map. One can readily verify that the stable period-3 orbit starts at $\lambda = \lambda_c = (1 + 2\sqrt{2})$. The plot in Fig.3.3(c) shows $f_{\lambda_c}^3(X)$ which is tangent to the diagonal $X_{n+3} = X_n$ at three points. For $\lambda \gtrsim \lambda_c$ we get a period-3 stable orbit through the tangent bifurcation. The situations described in Figs.3.3(a) and (b) develop in the neighbourhood of these three points as λ crosses λ_c. To be precise, this is what is known as *Type-I intermittency*. However other variations are also known to exist.

Intermittency brings in unexpected richness to the logistic map in the so-called chaotic regime $\lambda_\infty < \lambda < 4$. There is an infinity of stable periodic windows, the periodic attractors, besides the strange attractors in this regime. In fact they are dense in that a periodic attractor can be found arbitrarily close to any strange attractor in this parameter regime. For any *given* value of $\lambda > \lambda_\infty$, however, there is only one attractor. There is also an infinity of unstable periodic orbits for each $\lambda > \lambda_\infty$, but these will be almost always missed in a numerical simulation. Some of this fine structure is too fine for computers (with their approach of rounding off errors) to resolve.

The Nature of the attractor set, whether a strange attractor, a stable periodic attractor, or an unstable periodic repeller, is measured quantitatively by its Lyapunov exponents, fractal dimensionalities and the power spectra. We will return to these rather technical issues later on.

3.2 Circle map

While the logistic map is prototypical of chaotic dynamics in that it exhibits sensitivity to initial conditions, stretching-out and folding-back of trajectories, period-doubling, intermittency and a fractional dimensional attractor (the strange attractor), it misses some of the other commonly observed and fascinating features of recurrent motions, such as *phase locking* and *quasi-periodicity*, because of its being a one-dimensional map and possessing just one control parameter. We, therefore, introduce and discuss briefly yet another standard map called the *circle map* which is a two-parameter map. It is derivable in some approximation from a two-dimensional map

representing the Poincaré section for a damped driven pendulum. The phase locking here means that the ratio of the frequency of the driven pendulum motion to that of the external drive remains pinned at the ratio of two integers ($r = p/q$ = a rational number) for a *range* of values of the control parameter α which is the ratio for the undriven pendulum (i.e. for drive amplitude zero), and that the range increases with the amplitude β of the drive.

The equation of motion for the angular displacement θ of a damped driven pendulum can be reduced to the motion in a three-dimensional phase space (θ, ω, ϕ) by introducing an additional variable $\phi = \omega_0 t$, where ω_0 is the circular frequency of the external drive. Thus, we have the autonomous system of equations:-

$$\begin{aligned} \dot{\omega} &= -\eta\omega - \sin\theta + f\cos\phi \\ \dot{\theta} &= \omega \\ \dot{\phi} &= \omega_0 \end{aligned} \tag{3.2}$$

Here the overdot indicates time derivative, η measures friction and f is the amplitude of the periodic cosinusoidal driving force. Clearly, ϕ and $\phi + 2\pi$ are to be identified. The same is true of θ. We can now resort to dimensional reduction from three to two dimensions by constructing a Poincaré section obtained by strobing the values of ω and ϕ at equal time intervals of $2\pi/\omega_0$ ($\equiv$ period of the drive). This gives a two-dimensional Poincaré map of the type:-

$$\begin{aligned} \theta_{n+1} &= f_1(\theta_n, \omega_n) \\ \omega_{n+1} &= g_1(\theta_n, \omega_n) \end{aligned} \tag{3.3}$$

Further reduction to a one-dimensional map takes place if the set (θ_n, ω_n) fills out a smooth curve on the *surface of section*. Now, the curve must, of course, be bounded. This could imply that ω_n is a smooth function of θ_n, and thus the map reduces to a one-dimensional map $\theta_{n+1} = g(\theta_n)$, for the angle θ with $\theta \equiv \theta + 2\pi$. This is obviously the map of a circle to itself. Hence the name *circle map*.

A widely studied circle map in the standard form is the two-parameter (α, β) map

$$X_{n+1} = X_n + \alpha - (\beta/2\pi)\sin(2\pi X_n) \pmod 1, \tag{3.4}$$

where we have set $X = \theta/2\pi$, the normalized angle, so that the unit interval is now mapped to itself. Here the parameter α is called the rotation frequency. It is equal to the winding number γ for $\beta = 0$ (to be introduced shortly). Finally, β measures the

nonlinear coupling of the pendulum to the periodic external force. It is essentially the amplitude of the periodic drive.

To see the physical significance of the rotation frequency parameter α, we set $\beta = 0$. Then α is nothing but the increment of the normalized angle per iteration. Thus, for a rational $\alpha(= p/q)$, q iterations will return the normalized angle X to its starting value after making p rounds of the unit interval, i.e. $X_{n+q} = X_n$. We get a periodic orbit. For an irrational α, however, X_n never quite hits the starting value, though it will pass arbitrarily close to it. We have here quasi-periodicity — "quasi" reminding us of the near hits. All this is familiar from the stroboscopic viewing of a mark on a spinning wheel. One can, for instance, trivially freeze the mark by making the period of the strobe light equal to that of the spinning wheel, or generate other stationary multimark patterns by keeping the ratio of the two periods rational. For an irrational ratio, however, the mark will appear to advance or retrograde because of the 'closure-failure'.

Now if we turn on the nonlinear coupling β, we have a whole range of fascinating behaviours. The sinusoidal term in the circle map gives some additional oscillatory contribution (to the otherwise constant increment α per iteration) which *depends* on the current value X_n of the state variable X. In other words, it nonlinearly modulates the steady rotation. This perturbation may be expected to foul up the harmony of the periodic motion noted above for a rational value of $\alpha = p/q$. On the contrary, it turns out, however, that the very nonlinear nature of this X-dependent oscillatory perturbation provides the necessary play, or shall we say elbow room, to absorb the 'misfit' and maintain the periodic motion even for an irrational α as the frequency parameter (α) is varied continuously over a finite interval that contains necessarily mostly irrationals. We say that the oscillations are *phase-locked.* In fact they are locked-in to a rational approximant of the now irrational α. In terms of the original system of a driven damped pendulum, the frequency of the pendulum is entrained to a rational multiple of the driving frequency. This is indeed a rational or harmonious dynamical compromise between the system trying to oscillate at its natural frequency as well as at the frequency of the external drive. Any quasi-periodic motion is then the result of a possible frustration to reach this compromise. This highly intriguing and important phenomenon is variously called phase locking, mode locking, frequency entrainment, or resonance. The tendency of a nonlinear driven oscillator to phase-lock makes synchronization a robust possibility and not just a hard-to-achieve coincidence. It occurs widely in real life. Indeed, it enables the rational numbers

to physically beat the irrationals that otherwise outnumber them zero to one in the strict mathematical sense!

As mentioned earlier, frequency entrainment was noticed by Christiaan Huygens way back in the 17th century when he found that two clocks mounted back-to-back on the same wall tend to become synchronized. There is complete phase locking of the lunar spin and the orbital motion, so that one side of the moon always faces the earth. The spin–orbit coupling here is due to the moon's elongation towards the earth. Phase locking enables the synchronization of the giant electric power generators coupled via a common grid. Commercial lock-in amplifiers and the driven nonlinear oscillators, such as the van der Pol oscillator, work on the principle of phase locking. One could have an acoustically-entrained cyclic chemical reaction. Indeed, David Jones in *Daedalus* speculates on such an entrainment of the crucial *Krebs cycle* of glucose oxidation to regulate the metabolic rate to advantage (see *Nature*, 354, 192 (1991)). But the example, perhaps closest to our heart, is that of a *Pace Maker* that entrains the irregular heartbeats of an arrhythmia patient.

As we vary the frequency parameter α for a fixed amplitude β, we pass through both the periodic (phase-locked) and the quasi-periodic motions. Indeed, there are infinitely many such periodic windows of phase-locked motion associated with ranges of α values. Their widths ($= 0$ at $\beta = 0$) increase monotonically with increasing nonlinear coupling β. Thus, in a (β, α)-plot, these windows appear as the so-called *Arnold's tongues* or *horns* (Fig.3.4) within which the orbits are phase locked periodically. In order to fully grasp these windows of phase-locked motion despite α being irrational, we must introduce another quantity γ ($\equiv$ the winding number = phase change per iteration averaged over many iterations). For the driver amplitude $\beta = 0$, obviously, the winding number $\gamma = \alpha$, the frequency parameter. For $\beta \neq 0$, however, the phase modulation due to the nonlinear forcing term makes them unequal. Thus even for α irrational, the averaged winding number γ may maintain its rationality and hence the periodic motion. This would lead to plateaus in the plot of γ versus α for a given β. That is to say, that while the winding number γ indeed increases with increasing α, it does so in a stick-slip manner. These plateaus resulting from the rational winding numbers in the $(\gamma - \alpha)$ plot for a fixed β give it the appearance of an incomplete staircase. For the critical value of the driving amplitude $\beta = 1$, the plateaus form a complete staircase in that they exhaust the measure of the full range of α values. Further, the staircase is self-similar in that any part of it when viewed under high resolution looks like the whole — it becomes the so-called *devil's staircase* (Fig.3.5). Properly viewed, phase locking is a

nonlinear generalization of the concept of resonance where the natural frequency of the driven system is not necessarily equal to that of the driver. It may be an integral multiple (ultraharmonic), a submultiple(subharmonic), or a rational multiple (subultraharmonic) of the driver frequency. The operative point is that the resonance persists over a finite range of the driver frequency parameter α for a given driving amplitude, or the nonlinear coupling β.

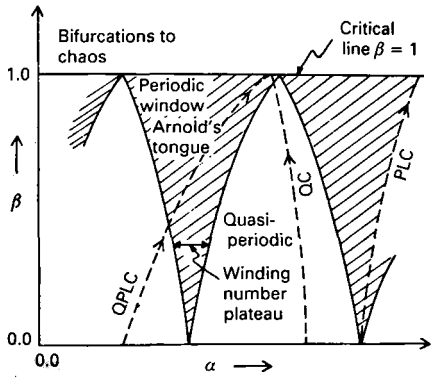

Fig.3.4 A few Arnold's tongues (hatched) for circle map on the amplitude (β)–frequency (α) plot. Winding number γ stays a constant rational across the tongue giving phase locking. Chaos co-exists with regular motion for $\beta > 1$. Three routes to chaos shown (schematic).

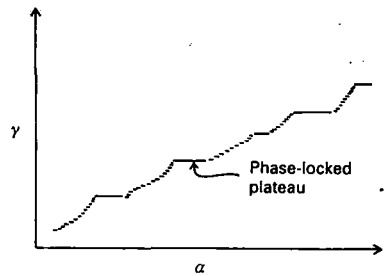

Fig.3.5 Devil's staircase plot for winding number (γ) versus the frequency (α) for the standard circle map with drive amplitude $\beta = 1$ showing plateaus at rational γ. Plot is self-similar (schematic).

Simple stability analysis can now reveal the route to chaos. Rewriting the circle map as

$$X_{n+1} = f(X_n)$$

with

$$f(X) = X + \alpha - \left(\frac{\beta}{2\pi}\right)\sin(2\pi X) \pmod 1, \tag{3.5}$$

we readily verify that $f'(X) = 1 - \beta\cos(2\pi X) > 0$ for $\beta < 1$, and hence the map is *invertible* for $\beta < 1$. Therefore, for $\beta < 1$ no chaos is possible; all one has is either phase-locked periodic orbits or quasi-periodic orbits, and transition from one to the other. The fixed points (X^*) of the map (3.5) are

$$\alpha - \left(\frac{\beta}{2\pi}\right)\sin(2\pi X^*) = \text{integer } (m) \tag{3.6}$$

The slope at any one of these points is

$$f'(X^*) = 1 - \beta\cos(2\pi X^*) \tag{3.7}$$

The stability condition $-1 < f'(X^*) < 1$ then gives (for $m = 0$, for instance)

$$\beta = \sqrt{4 + (2\pi\alpha)^2} \tag{3.8(a)}$$

for period-doubling bifurcation transition, and

$$\beta = \pm 2\pi\alpha \tag{3.8(b)}$$

for tangent bifurcation, or transition, to an infinite period which is quasi-periodic for small β.

This reveals three routes to chaos possible for $\beta > 1$ as shown schematically in Fig.3.4. Also note that for $\beta > 1$ the map $f(X)$ is bimodal, i.e. double-humped. It has two critical points where $f'(X) = 0$. Bimodality admits co-existence of attractors with their own *basins of attraction* (i.e. the phase space has more than one basin of attraction for a given parameter value. By contrast the logistic map was unimodal and hence there was only one basin of

attraction for a given value of the control parameter). Thus, both chaotic and periodic orbits are possible for $\beta > 1$ depending on the initial conditions.

The three-fold way to chaos is:

QPLC $\equiv$ quasi-periodic $\rightarrow$ phase-locked $\rightarrow$ bifurcation to chaos on crossing the critical line $\beta = 1$; QC $\equiv$ quasi-periodic $\rightarrow$ meets junction of two phase-locked modes at $\beta = 1$ and turns chaotic; PLC $\equiv$ phase-locked $\rightarrow$ period-doubling cascade to chaos beyond a point greater than $\beta = 1$.

Note that the periodic windows (the Arnold's tongues) containing the phase-locked or resonant modes overlap at the critical value of the driver amplitude $\beta = 1$.

3.3 Routes to deterministic chaos

We have just discussed the period-doubling bifurcation route to chaos in some detail. The physical example of the leaking faucet discussed earlier obviously follows this route. So also is the case for convective turbulence (Rayleigh–Bénard instability) where the temperature fluctuations at any point in the cell follow the period-doubling scenario. Both these rather different physical systems belong to the same universality class. But there are other bifurcation routes to chaos too. We have, for example, the quasi-periodic route to chaos. Here, the system starts with an equilibrium, a stationary point (the zero-dimensional attractor, or the stable fixed point) that becomes unstable at a threshold value of the control parameter, and bifurcates to a singly-periodic limit cycle which is a one-dimensional attractor (we call it the *Hopf bifurcation*). The limit cycle then bifurcates to a doubly-periodic torus (a two-dimensional attractor) which in turn bifurcates to a chaotic attractor of fractal dimension greater than two. This route to chaos is seen in the turbulence in a fluid flow confined between two co-axial cylinders with the inner cylinder rotating (the so-called *Couette–Taylor flow*). The control parameter here is the speed of rotation of the inner cylinder. There is yet another route to chaos, called the *intermittency route*, but we will let it pass. It seems very reasonable to suppose that as the control parameter is raised, the lower dimensional attractors get destabilized in favour of the higher dimensional attractors and this eventually leads to chaos.

Below, in Table 3.1, we give two of the common routes to chaos (see also Fig.3.6).

Table 3.1 Some common routes to chaos

ROUTE	MECHANISM
Period-doubling	
Stationary (Fixed point) → Hopf bifurcation → Limit cycle Singly-periodic → (Period T) Pitchfork bifurcation → Singly-periodic (Period 2T) → Pitchfork bifurcation → Singly-periodic (Period 4T) → ... → CHAOS	
Quasi-periodic	
Stationary (Fixed point) → Hopf bifurcation → Doubly-periodic Torus → Hopf bifurcation → ... → Limit cycle Singly-periodic → CHAOS →	

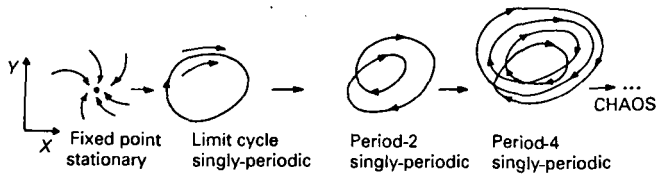

(a)

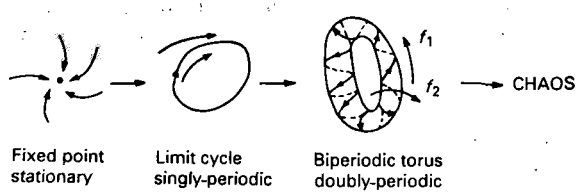

(b)

Fig.3.6 (**a**) Period-doubling route to chaos; (**b**) quasi-periodic route to chaos.

4 *Strange Attractors*

We have now become acquainted with attractors. These are geometrical structures, or limit point sets in the phase space on which the trajectories settle down eventually. The fixed point, the limit cycle and the biperiodic torus are all regular attractors and correspond to equilibrium or regular periodic motions. They have dimensions less than that of the phase space in which they are embedded. Their dimensions are, of course, integral. The chaotic motion is, on the other hand, irregular and aperiodic. It was shown by David Ruelle in 1971 that the attractor underlying the chaotic motion is a geometrical object whose dimension is fractional. Besides its strange 'fractal' geometry, this attractor is strange also in the dynamical terms of how this object is traversed by the phase trajectories. The trajectories are attracted *to* this attractor, but they are unstable *on* it, and thus show the sensitivity to initial conditions (or, SIC-ness) that characterises deterministic chaos. No wonder then that it has been named strange attractor.

Let us see how such a fractal attractor arises naturally as a result of the contradictory demands of dissipation (i.e. diminishing phase volume), sensitivity to initial conditions (exponential divergence of neighbouring trajectories), and confinement to a bounded region of the phase space in which it is embedded.

To fix ideas, consider a three-dimensional phase space (or state space) of a dissipative dynamical system. Inasmuch as the flow is dissipative, the trajectories must converge eventually to a geometrical object of dimension less than three so that its volume is zero. This would normally mean either a fixed point (equilibrium state), a limit cycle (singly-periodic motion), or a biperiodic torus (doubly-periodic motion) having integral dimensions 0, 1 and 2 respectively. But all these are, of course, regular motions and, therefore, cannot represent the aperiodic, chaotic dynamics. The only possibility is to relax the Euclidean hang-up of integral dimensions. The dimension must be between 1 and 3 in this case.

Next, let us see how a strange attractor reconciles the divergence of trajectories (SIC) with their convergence and confinement to a bounded region. It does so through the alternation of stretching-out and folding-back. Figure 4.1(a) schematically shows a

three-dimensional phase flow along the Z-axis in the mean, but diverging in the XX'-direction while converging in the YY'-direction. Figure 4.1(b) is a section of the flow, perpendicular to the Z-axis, and clearly shows the divergence (stretching) and the convergence (folding-back) of the trajectories characteristic of a saddle point. Figures 4.1(c) and 4.1(d) show the exponential divergence of neighbouring trajectories to nearly double their initial separation and their subsequent folding-back to confine them to a bounded region giving SIC. And finally, Fig.4.1(e) shows the fully-developed chaos (strange attractor), called the *Rössler attractor* for a three-dimensional flow. The Rössler attractor is quite common

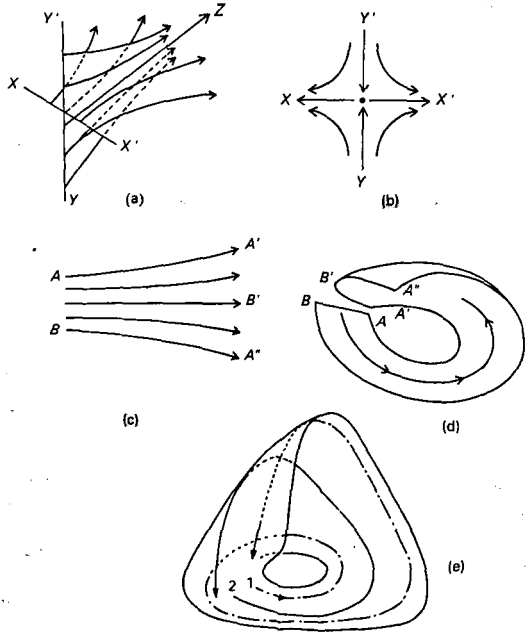

Fig.4.1 (a) Phase flow along Z-axis, diverging in the XX'-direction and converging in the YY'-direction; (b) cross section showing saddle point; (c) divergence of trajectories; (d) folding-back of trajectories; (e) the Rössler strange attractor.

and has been observed in fluid flows and chemical reactions. The phase flow underlying the Rössler attractor is described by the three coupled equations $\dot{X} = -Y - Z$, $\dot{Y} = X + aY$, and $\dot{Z} = b + Z(X - c)$. For typical values, $a = b = 0.2$ and $c = 5.7$, one has chaos.

As our second and last example, let us now consider the *Lorenz attractor*, named after its discoverer Edward Lorenz, who detected it in his computer modelling of weather as atmospheric convection way back in 1961, long before the idea of strange attractor was developed formally by David Ruelle. Here the phase space is three dimensional, (X, Y, Z), where X measures the intensity of convection (i.e., circulatory fluid motion), Y the temperature difference between the ascending and the descending currents, and Z the deviation of the vertical temperature profile from linearity. This is obviously a highly truncated version of convection, a synthetic convection if you like. The flow equations are

$$\dot{X} = \sigma(Y - X),\ \dot{Y} = -XZ + rX - Y \text{ and } \dot{Z} = XY - bZ \qquad (4.1)$$

Here σ, r and b are the control parameters and are necessarily positive. More explicitly, $r = R_a/R_c$ = Rayleigh number R_a normalized with respect to its critical value R_c with $R_a = \alpha g d^3 \Delta T/\nu a$, where α = thermal expansion coefficient, g = acceleration due to gravity, d = vertical distance between the two horizontal plates, ΔT = temperature inversion (the temperature of the lower hotter plate minus the temperature of the upper colder plate), a = thermal diffusivity = thermal conductivity divided by the specific heat, and $\nu = \eta/\rho$ (the Stokes kinematic viscosity where η = dynamic shear viscosity and ρ = density of the fluid). The parameter $R_c = \pi^4(1 + a_0^2)^3/a_0^2$ with a_0 = a dimensionless parameter defining the wavelength of the convective rolls. Here, time is measured in units of $d^2/\pi^2(1 + a_0^2)a$. Physically, the Rayleigh number R_a measures the ratio of internal energy released by the buoyancy to the kinetic energy dissipated by the viscosity, and drives the nonlinearity. Also $\sigma = \nu/a$ is a material property (the Prandtl number $\simeq 0.7$ for air and $\simeq 7$ for water) and $b = 4/(1 + a_0^2)$, a geometrical factor. In practice, one varies only the control parameter r, keeping σ and b fixed. Thus, Lorenz had set $\sigma = 10$, and $b = 8/3$ and obtained chaos. In most numerical simulations the values set are the same.

Let us now have a closer look at this strange flow. First, it is readily verified that the flow is dissipative; in other words, the divergence of the velocity field is negative. It can be represented as,

$$\frac{\partial \dot{X}}{\partial X} + \frac{\partial \dot{Y}}{\partial Y} + \frac{\partial \dot{Z}}{\partial Z} = -1 - b - \sigma < 0 \qquad (4.2)$$

and hence the contraction of the phase-space volume as $\Gamma(t) = \Gamma_0 \exp(-(1+b+\sigma)t)$. Next, it is quite straightforward to perform a linear stability analysis for the Lorenz equations. Note that there are three critical points obtained by just setting all the velocities $\dot{X} = \dot{Y} = \dot{Z} = 0$. These are $X = Y = Z = 0$ (labelled as O) and, additionally for $r > 1$, $X = Y = \pm\sqrt{b(r-1)}$, $Z = r-1$ (labelled as $C_\pm$). The critical point O represents no fluid flow (stagnation) — there is just heat conduction by molecular diffusion. The pair of critical points $C_\pm$ has each associated with it a steady circulatory convection. Now, linearising the nonlinear Lorenz equations about the critical point O yields the stability (or the 'plant', or the local Jacobian) matrix with eigenvalues 's' given as the roots of the equation $(s+b)(s^2+(1+\sigma)s+\sigma(1-r)) = 0$. One can easily verify that all the eigenvalues are real and negative for $r < 1$. Thus, for $r < 1$, O is a stable fixed point (a global attractor) as $C_\pm$ are unphysical for $r < 1$. For $r > 1$, however, one of the roots becomes positive making O unstable (a repeller). This is the Rayleigh–Bénard convective instability. Thus $r = 1$ marks the onset of steady convective circulation governed by the pair of critical points $C_\pm$ that now attract the orbit for $r > 1$. C_+ and C_- correspond to oppositely directed convective circulations. One has here a pitchfork bifurcation $O \rightarrow C_+ + C_-$ at $r = 1$, in which a fixed point becomes unstable, generating a pair of stable fixed points (foci). Next, we must examine the linear stability of $C_\pm$ by linearizing the Lorenz equations about C_+ and C_- (it is sufficient to analyse just one of them because of the obvious symmetry). Proceeding as before, we obtain the eigenvalues 's' of the stability matrix as given by the equation $s^3+(1+b+\sigma)s^2+b(\sigma+r)s-2b\sigma(1-r) = 0$. One eigenvalue is necessarily real and the other two are complex conjugates. Now, for the stability of these two convecting equilibria ($C_\pm$), the roots must have negative real parts. The necessary and sufficient condition for this can be shown to be $b(1+b+\sigma)(\sigma+r) \geq 2b\sigma(-1+r)$. When this is so, both $C_\pm$ are asymptotically stable equilibrium points. Further, these steady convective rolls become unstable for $r > \sigma(3+b+\sigma)/(-1-b+\sigma) = r_c$, say, and $\sigma > 1+b$. Then all the equilibria are unstable and chaos results. For the typical choice of parameters ($\sigma = 10$ and $b = 8/3$), we get $r_c = 24.74$. Thus, for $r < 1$, there is stagnation, and for all initial conditions the system settles down to the stable fixed point O without any macroscopic fluid motion, i.e. without convection. For $r > 24.74$, we have eventually chaotic orbits for all initial conditions. The situation is rather subtle for $1 < r < 24.74$. It turns out that for $1 < r < 24.06$, all initial conditions relax to one of the two asymptotically stable convective equilibria. For $24.06 < r < 24.74$, however, depending on the

initial conditions the orbit settles down either to one of the two stable convective equilibria, or to chaos — hence the possibility of hysteresis. [In fact the motion is much more fine structured in the parameter space, with the possibility of chaos (strange attractor) co-existing with the condition of asymptotic stability (equilibrium).] The chaotic regime, $r > r_c$, is characterized by bounded motion comprising random alternate sequence of windings around the two unstable foci $C_{\pm}$.

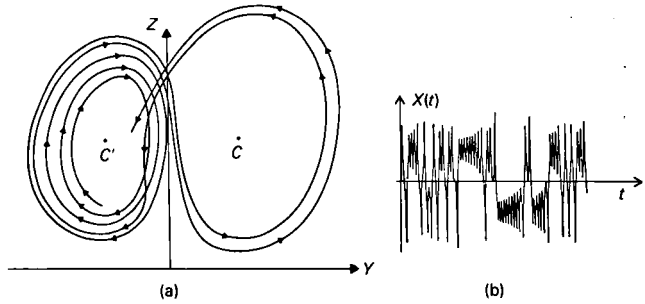

Fig.4.2 (**a**) Lorenz Attractor projected on YZ-plane; (**b**) signal $X(t)$ (schematic).

In Fig.4.2(a) we have shown the projection of the trajectory for this strange attractor on the Y–Z plane. The trajectory is seen to wind around the unstable fixed point C_+, spiralling out till it exceeds some critical distance, and then flips over and starts winding around the other unstable fixed point C_-. If we were to list the number of times it winds around C_+ before flipping to C_-, the sequence so generated will be as random as the heads and tails in the tossing of a true coin. Figure 4.2(b) gives a trace of $X(t)$ as a function of time and clearly shows the above random flippings between C_+ and C_-. The trajectory seems to live on a surface, but actually the surface has finite thickness within which there is an intricate multilayered fine structure like the foliations of an onion shell. If we were to pass a line through this surface, the points of intersection would form a set of fractional dimensions lying between 0 and 1. The strange attractor is a fractal.

The Lorenz attractor is the archetype of strange attractors. Its owl-like double scroll (or the *Cantor-book* like) appearance decorates the cover pages of many a monograph on chaos.

One must remember that the real physical problem of a fluid heated from below involves solving equations of fluid dynamics (the

Navier–Stokes equations) together with the heat-flow equations — the heat is advected by the fluid motion as well as conducted by the molecular diffusion (the *Fourier equation*). These are partial differential equations and, therefore, correspond to infinitely many degrees of freedom. The Lorenz equations are a highly truncated version of these differential equations where only a small number of coupled, spatial Fourier components (modes) of the flow field has been retained. In fact the truncated set (*Lorenz model*) is a rather bad approximation in the physically interesting domain of parameters. Still, it has become a laboratory for numerical work on deterministic dissipative chaos. It turns out, however, that the model describes rather well the dynamics of a three-level laser action with X = electric field, Y = polarization and $(r - Z)$ = the population inversion.

We should emphasize here, that despite its intricate mixed-upness, the strange attractor is highly structured and organized. It is also very robust — it is stable against local perturbations. Admittedly, a strange attractor, particularly a higher-dimensional one, is hard to determine experimentally. It is, however, possible to partially reconstruct it from the measurement of any single variable, $X(t)$ say, as a function of time, for example the temperature or the velocity component at a point. The point is that the very mixed-upness of the strange attractor makes it a kind of 'implicate' universe in which every variable affects and is, therefore, implied in every other variable to an extent. Hence, measuring any one of them as a function of time can tell us, for example, how many variables there are that constitute the whole. This reconstruction is done by constructing an artificial phase space from the measured signal $X(t)$. It is like being able to tell the number of factors affecting the disturbed (or fibrillating) heart of a patient from the single ECG trace (see Chapter 6 for details).

The strange attractor is a geometrical object in phase space which is neither point-like nor space-filling. Once on it, the phase point remains confined to it and appears to walk randomly, coming eventually arbitrarily close to every point of the attracting set. Its orbit is unstable everywhere on the attractor, but the strange attractor as a whole is robustly stable.

5 *Chaos Without Dissipation: Hamiltonian Chaos*

Until now, we have looked for chaos in dissipative dynamical systems. The chaos we found there resulted from a conflict between the continual contraction (dissipation) of the phase-space volume towards zero measure on the one hand, and the absence of an attractor, such as a fixed point or a limit cycle to converge to, on the other. This conflict is resolved by the phase trajectory converging to, and wandering endlessly on, a limit set of fractional (fractal) dimension that fills a finite region of the phase space densely, but has measure zero — the so-called strange attractor, the engine that drives chaos. Such a behaviour, i.e. wandering endlessly, is caused by local instability which is marked by the presence of saddle points in the phase portrait. We recall that the saddle point, also referred to as the hyperbolic point, stretches the trajectories along an unstable (repelling) direction, and folds them back along a stable(attracting) direction which is perpendicular to the former, generating thereby SIC-ness and hence chaos.

There are, however, dynamical systems that do not dissipate. We call them conservative — their motion keeps the associated phase-space volume constant in time. The commonest among them, and by far the best studied, are the Hamiltonian systems that obey the classical Newton's laws of motion without friction. Thus, we have the celebrated three-body problem of the Moon–Earth–Sun system bound by gravitation. It is obviously of great interest, and of some concern whether this system is really locked in an eternally stable regularity of motion, or if the earth (or the moon), under the perturbing aspects of the other planets, may after all tumble chaotically in the long run and wander too close to, or too far from the sun for human comfort. Approximate calculations giving short-term stability over the time-scale of 10^3 years set by the strength of the planetary perturbations will not do. What is really in question is the long-term stability on the time-scale of 10^9 years! We could also consider star clusters, or clusters of whole galaxies. There are still other such Keplerian systems that have held great fascination for astronomers in the past. Thus we have the enigmatic rings of Saturn, discs of

particulate matter in orbit, divided by possibly the periodic perturbation of one of the saturnine moons, the Mimas. Astronomers call these the *Cassini divisions*. Similarly the asteroid belt between Mars and Jupiter, again with systematic absences called the *Kirkwood gaps* in their orbital periods. As we will see later these gaps, generically the KAM gaps, are the flip side of chaos. Then, there are the man-made satellites orbiting the earth and other lesser systems in the laboratory down here on earth. Thus there is the motion of charged particles trapped in the electric and magnetic fields in the storage rings of giant particle accelerators, or the plasmas confined magnetically in Tokamaks, or just a heavy gyroscope (remember the uncanny upending Tippe Top that fascinated great physicists like Sir William Thompson, Niels Bohr and Wolfgang Pauli no end! See, e.g., Richard J. Cohen, *American Journal of Physics*, **45**, 12 (1977).). In all these systems, the friction (e.g., the tidal friction for planetary motions) can be almost always neglected in the zeroth approximation. We, therefore, turn now to such conservative systems and explore the possibility of observing chaos there.

Conservative systems are qualitatively different from their dissipative counterparts. First, the dissipative system must be driven, otherwise it will run down due to dissipation — it is an open system. But a conservative system can move perpetually on its own — it is a closed system, though we will often consider it perturbed periodically by an externally applied force, e.g., a periodically kicked pendulum. A dissipative system can have asymptotically stable fixed points, or limit cycles. The conservative system, with its constancy of phase-space volume cannot have these linearly stable attractors. It can have an orbitally stable centre on the other hand, which is denied to a dissipative system. Unlike as in the dissipative systems, chaos in the conservative or the Hamiltonian systems is associated with these centres (elliptic points) bifurcating into a saddle point (the hyperbolic point) and two elliptic points. As we will see, a Hamiltonian system can be chaotic provided the system is *non-integrable*. Integrable Hamiltonian systems have no chaos. Such a non-integrable Hamiltonian chaos is 'soft' in the sense that the 'stochastic sea' (of chaotically wandering trajectories) will co-exist with 'islands of stability' (containing periodic orbits) in the phase space, and the latter gradually shrink to a negligible measure as the non-integrable Hamiltonian perturbation is turned on. But first we must briefly recall the elementary lessons of Hamiltonian dynamics and introduce the important ideas of the integrable system and the associated invariant tori, their gradual destruction by a non-integrable perturbation and the great KAM theorem. These are matters of great technical complexity. We can only hope to get

a flavour of the essentials here. We will follow our intuition that physics is closer to geometry than to algebra, and appeal freely to our sense of visual continuity that maps neighbourhoods into neighbourhoods. Any kind of derivation or completeness is frankly out of the question here.

5.1 Hamiltonian dynamics

Consider a dynamical system of N degrees of freedom with coordinates q ($\equiv q_1, q_2, \ldots, q_N$) and their conjugate momenta p ($\equiv p_1, p_2, \ldots, p_N$). The motion in the $2N$-dimensional phase-space is now governed by the Hamiltonian h (q, p) which is nothing but the total energy of the system expressed in terms of q and p. The Newtonian laws of motion are then expressed by the Hamiltonian equations

$$\dot{q}_i \equiv \frac{dq_i}{dt} = \frac{\partial h}{\partial p_i}$$

$$\dot{p}_i \equiv \frac{dp_i}{dt} = -\frac{\partial h}{\partial q_i} \tag{5.1}$$

Inasmuch as there are $2N$ first-order differential equations, with the right-hand sides single-valued functions of (q, p) without explicit time dependence (i.e. autonomous equations), there is a unique non-self-intersecting trajectory passing through any given point of the phase space. What is more, the phase flow conserves the phase-space volume. Hence the conservative system. Indeed, if we regard $(\dot{q}, \dot{p})$ as a $2N$-dimensional phase velocity vector field, $\dot{r}$ say, then the first assertion is obvious as $\dot{r}$ is defined uniquely at each point of the phase space through the Hamiltonian equations of motion, while the second assertion about the conservation of the phase-space volume follows at once by noting the vanishing of the divergence of the velocity vector field $\dot{r}$:

$$\text{Div } \dot{r} = \sum_i \left(\frac{\partial \dot{q}_i}{\partial q_i} + \frac{\partial \dot{p}_i}{\partial p_i} \right) = \sum_i \left(\frac{\partial^2 h}{\partial q_i \partial p_i} - \frac{\partial^2 h}{\partial p_i \partial q_i} \right) = 0 \tag{5.2}$$

where we have used the Hamiltonian equations for the velocities $\dot{q}_i$ and $\dot{p}_i$ and interchanged the order of partial differentiations. This is essentially the celebrated Liouville theorem. It helps us visualize this geometrically. Consider, for example, a 'drop' of the phase fluid at time $t = 0$ corresponding to all the possible initial conditions $(q(0), p(0))$ lying within the 'drop'. Then Eqn.5.2 asserts that as the drop moves under the Hamiltonian dynamics of its

constituent phase points, the volume enclosed by its boundary (surface of the drop) will remain unchanged (invariant). The shape of the 'drop' may, of course, change greatly. The 'drop' may send out fingers, become irregular and highly in-folded. Indeed, if we imagine the phase 'drop' coloured, and coloured differently from the rest of the phase fluid initially outside the phase 'drop', we could eventually have 'bubbles' of the outer phase fluid included within the now highly deformed phase 'drop'. In fact, while the detailed volume of the 'drop' proper, visualized and tagged by its colour, should have remained unchanged, the unresolved coarse-grained volume enveloped by the now highly rarified phase 'drop' may have increased manifold, even exponentially with time. This is the local instability which is key to *mixing* and to Hamiltonian chaos despite the rigorous 'conservatism' of the phase-space volume. We will return to this point later.

Under Hamiltonian dynamics, any phase function $f(q, p)$ changes in time implicitly through the time evolution of (q, p) as

$$\frac{df}{dt} = \sum_i \left(\frac{\partial f}{\partial q_i} \frac{\partial h}{\partial p_i} - \frac{\partial f}{\partial p_i} \frac{\partial h}{\partial q_i} \right) \equiv [f, h] \tag{5.3}$$

where

$$[A, B] \equiv \sum \left(\frac{\partial A}{\partial q_i} \frac{\partial B}{\partial p_i} - \frac{\partial A}{\partial p_i} \frac{\partial B}{\partial q_i} \right)$$

is called the *Poisson bracket*. Thus $[q_i, p_j] = \delta_{ij}$ ($\equiv$ *Kronecker delta* $= 1$ for $i = j$, and $= 0$ for $i \neq j$), and $[q_i, q_j] = [p_i, p_j] = 0$. Clearly, $dh/dt = 0$ implying that the energy is a constant of motion. Thus, for the Hamiltonian system [and with $h(q, p)$ having no explicit time dependence], the energy of the system is a constant of motion and, therefore, the trajectories lie on the $(2N-1)$-dimensional constant energy surface in the phase space.

With these basics of mechanics in mind, we are now prepared to address the Hamiltonian chaos. But one final remark. Recall how we often simplify a dynamical problem by going over to (transforming to) new bases, coordinate systems or the frames of reference, conveniently adapted to the symmetry that may be there. Thus, e.g., for the motion in central force fields (Keplerian or Coulombic problems) we use the spherical polar coordinate system — it would be perverse to use the cartesian coordinates here. In a similar spirit, it is often apt to go over to new phase-space variables (Q, P) that are physically *at par* with the old variables (q, p), but more convenient. 'Physically *at par*' has a well-defined meaning

here: If under the transformation $(q, p) \rightarrow (Q, P)$ we have the Hamiltonian $h(q, p) \rightarrow H(Q, P)$, then the equations of motion in terms of (Q, P) and $H(Q, P)$ must have the same form as in terms of the old variables namely, Eqn.5.1. Thus, all the Poisson brackets must remain formally unchanged. Such a change of variables is called a *canonical transformation.*

Unfortunately, the simplifying symmetries are often of a dynamical Nature, rather hidden, and are not easy to visualize. This makes the choice of the canonical transformation highly non-trivial.

5.2 Integrable and non-integrable systems

For a conservative system such as a Hamiltonian one with the Hamiltonian $h(q, p)$ not explicitly dependent on time, the energy $(E = h(q, p))$ is a constant of motion. Such a constant of motion defines a surface $E = h(q, p)$ in the phase space. The trajectories are, therefore, confined to this $(2N-1)$-dimensional subspace, the constant energy surface of reduced dimensions $(2N-1)$ embedded in the full $2N$-dimensional phase space. This reduction of dimensions restricts, and thereby simplifies the motion. The question naturally arises — Are there more such obliging constants of motion? By a constant of motion (also called a *first integral or invariant*) we mean a function, $f(q, p)$ say, not explicitly involving time that remains constant even as the coordinates and momenta (q, p) change in time according to the canonical equations of motion, Eqn.5.1. It is clear geometrically that the trajectory will have to lie on the intersection of these invariant surfaces defined by these constants of motion. The greater the number of such independent constants of motion, the smaller the dimension of the intersection subspace, and, thus, the simpler the motion.

It turns out that the motion is simplest if a system of N degrees of freedom has exactly N independent constants (invariants) of motion including energy, assumed to be mutually compatible as defined later. For then, the system is reducible essentially to that of N non-interacting degrees of freedom — like N free particles moving uniformly along straight lines with constant momenta. In short, N constants of motion are a straitjacket! Such a Hamiltonian system is said to be integrable. Obviously, integrability excludes chaos. Let us have a closer look at this wonderful idea of integrability.

Assume that the system admits a canonical transformation from the old (q, p) to the new (θ, J) coordinates-momenta such that the transformed Hamiltonian depends only on the N momenta, $J (\equiv J_1, \ldots, J_N)$. That is $h(q, p) = H(J)$. Recalling now the

form invariance of the Hamiltonian equations of motion under a canonical transformation, we must have

$$\frac{dJ_i}{dt} = -\frac{\partial H(J)}{\partial \theta_i} = 0, \quad \text{giving } J_i = \text{constant} \tag{5.4}$$

$$\frac{d\theta_i}{dt} = \frac{\partial H(J)}{\partial J_i} \equiv W_i(J), \quad \text{giving} \quad \theta_i(t) = W_i(J)t + \theta_i(0)$$

Thus the set of N momenta J_i ($i = 1, 2, \ldots, N$) are the N constants of motion, and the N coordinates θ_i ($i = 1, 2, \ldots, N$) increase linearly with time as angles of uniform rotation.

These are the celebrated *action (J) – angle (θ)* variables. But what about the unbounded growth of $\theta_i(t)$ as $t \to \infty$? Well, for the motion to remain bounded in phase space, we must physically identify θ_i and $\theta_i + 2\pi$. This periodic boundary condition renders the motion multi-periodic with the periods $T_i = 2\pi/W_i$. Thus, we have reduced our system to N non-interacting degrees of freedom θ_i (t) corresponding to free motions with constant momenta J_i. All this was possible only because we had N momenta J_i as constants of motion. Such a system is called an *integrable system*. We can rephrase it as follows. A Hamiltonian system of N degrees of freedom is said to be integrable, if there are N constants of motion. We can then identify these constants of motion (or their combinations) as the N action variables J_i. We must, of course, insist that these constants of motion be functionally independent. For instance if $J_2 = (J_1)^2$, then J_1 and J_2 are not functionally independent. For functional independence of J_1 (q, p) and J_2 (q, p), say, it must not be possible to eliminate (q, p) in favour of a functional relation between J_1 and J_2 such as $J_2 = f(J_1)$. We must also demand that these constants of motion be *compatible*. After all they must act as momenta and hence the canonical Poisson brackets must be preserved, i.e. $[J_i, J_j] = 0$. (Also $[J_i, H]=0$ because J_i is constant in time.) We say then that the J_i's are in *involution*. The latter has a geometrical meaning, namely that the surfaces J_i (q, p) = constant define an intersection that is smooth enough. (There is also a regularity condition on the Jacobian matrix $(\partial^2 H/\partial J_i \partial J_j)$, but we will let it pass.) Existence of N such invariants in involution ensures the construction of a solution by quadrature (integration).

But then, requesting integrability is in fact a tall order. Also, there is no simple method of determining whether a given system is integrable, and if so, what the N constants of motion in involution might be. Their existence is related to the symmetries (kinematic and dynamical) of the system that are often well hidden. The fact

of the matter is that integrable systems are rare for $N > 2$. (The $N = 1$ case is always integrable because the energy is naturally the single constant of motion required for integrability.) Indeed, it comes as a surprise that until the middle of the 20th century, much of classical mechanics was preoccupied with integrable systems — the harmonic oscillator, the Coulomb and the Keplerian problems, the free motion on a triaxial ellipsoid, the hydrogen molecular ion and the spinning top. For the spinning top, $N = 3$ and the three regular first integrals are the energy and the two angular momenta. But the three-body Moon–Earth–Sun problem is already non-integrable. The rarity of integrable systems is best illustrated by the following comparison. We know that rational numbers on a unit real interval are (countably) infinite, but they occupy no length (measure). The entire length is occupied by the (uncountable) infinity of irrational numbers. Still, the rational numbers are dense in the interval in the sense that any irrational number can be approximated arbitrarily closely by a sequence of rational numbers. Now, the integrable systems are too rare to be dense in this sense. So much so that to look for a non-integrable Hamiltonian is like looking for a 'non-elephant' animal!

Given this rare occurrence and the fact that integrability negates chaos, one may rightly ask — Why should we have to devote so much space to discussing integrable Hamiltonians? Well, the point is that the Hamiltonian chaos is best described and analysed as a gradual disruption of the simple integrable trajectories as we turn on a non-integrable perturbation. Thus prepared, we now turn to chaos in non-integrable Hamiltonian systems.

5.3 Invariant tori: Resonant and non-resonant

Let us once again return to our integrable Hamiltonian systems with the action-angle variables (J_i and θ_i) with $i = 1, 2, \ldots, N$. It is easy to view each pair (J_i, θ_i) as polar coordinates describing a circle with J_i = constant (as the radius) and $0 \leq \theta_i \leq 2\pi$ as the angle. Then N such independent and simultaneous circular motions together describe a trajectory of the phase point lying on an N-torus, embedded in the $2N$-dimensional phase space in general. Thus, for $N=1$, the torus collapses to just a circle in the two-dimensional phase space. For $N=2$, the 2-torus can be readily visualized as a doughnut-like surface embedded in a three-dimensional subspace. The latter is defined by the constant energy surface in the full four-dimensional phase space. Here W_1 and W_2 are, respectively, the circular frequencies for motion round the meridional (poloidal or minor) ϕ-circle and the longitudinal (toroidal or major) θ-circle

as shown in Fig.5.1. And so on for the N-torus. One may, however, ask — Why a torus and not a sphere? This is a rather deep question of topology. But the essential point of the argument is just this. The N-constants of motion in the $2N$-dimensional phase space define an N-dimensional surface on which the trajectories must lie. This defines an N-component velocity vector field tangential to the surface. Now, it is readily appreciated that it is impossible to have a vector field lying on (tangential to) the surface of a sphere wrapping it smoothly and completely. One must have singularities — e.g. nodes, focal points, or saddle points, where the direction of the vector field is ill-defined, or the field itself vanishes. This is in fact a non-trivial theorem in topology: You cannot comb the hair on a sphere! (Here each individual hair combed so as to lie tangentially to the sphere, represents the vector field locally. Thus, clearly, if the hair is combed along the longitudes, say, then it will define the direction of the vector field uniquely at each point, except at the two poles where the longitudes converge to a point. Again, if the hair is combed along the latitudes, we will still have

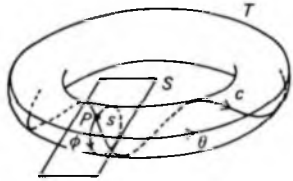

(a)

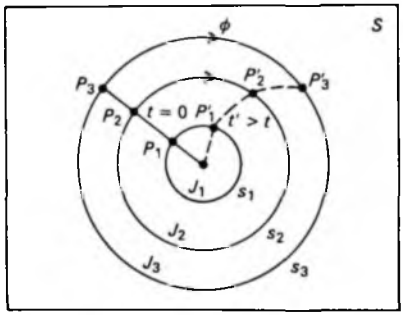

(b)

Fig.5.1 (a) Invariant 2-torus showing meridional surface of section S. The trajectory c generates Poincaré section s by intersections P ; (b) twist map showing relative ϕ-shifts of initially aligned intersections with S of trajectories lying on three nested tori.

the directional ambiguity at the polar points where the circular hair lines dwindle to points. In fact this ambiguity persists no matter how the hair is combed.) The velocities here are $\dot{\theta}_i = W_i$ and of course, $\dot{J}_i = 0$. An N-torus with its multiple connectivity resolves this frustrating conflict.

Thus we conclude that the trajectories of an integrable Hamiltonian system are confined to N-tori, each of which is labelled by the N constants of motion, the N actions J_i. We aptly call these *invariant tori*. Now, it may happen that the N frequencies W_i are commensurate, i.e. rationally related. That is to say we can have $k_1W_1+k_2W_2+\ldots+k_NW_N = 0$ for some integral coefficients $k_1, k_2, \ldots, k_N$. This means that the trajectory will exactly close on itself after a finite period of time which would be the lowest common multiple of the N periods $2\pi/W_i$. A closed Lissajous figure! We have a periodic, or more precisely, a multiperiodic orbit. Accordingly, we call these invariant tori the *rational tori*. Indeed, the rational condition on the frequencies W_i ($\equiv d\theta_i/dt$) gives $k_1\theta_1 + k_2\theta_2 + \ldots + k_N\theta_N$ = constant, implying that the torus effectively has one dimension less. Hence also the name *resonant tori*. Celestial mechanics is full of such resonances. On the other hand, if the frequencies are incommensurate, i.e. not rationally related, the trajectory will wind eternally round the torus, never quite closing, never self-intersecting but passing arbitrarily close to any point on the torus — a kind of endless Lissajous figure. We call these invariant tori the *irrational tori*, or the *non-resonant tori*. Correspondingly, the motion is said to be conditionally periodic, or quasi-periodic. In Fig.5.1 we have shown schematically the invariant tori for the case $N=2$, with energy as one of the two constants of motion. The 2-torus can, therefore, be visualized as embedded in a three-dimensional subspace — a surface of constant energy. For the rational torus, a trajectory intersects a Poincaré surface of section, taken in the meridional plane, at a finite set of points; for the irrational torus it fills out a continuous curve.

5.4 KAM theorem

The distinction between the rational and the irrational tori may appear to be mere nitpicking, inasmuch as the rational numbers (periodic orbits) are dense in real numbers and any irrational number (quasi-periodic orbit) can be approximated arbitrarily closely by a sequence of rational approximants. It turns out, however, that these two types of motion differ qualitatively as regards their stability against a small non-integrable perturbation. And thereby hangs the question of existence of chaos in Hamiltonian systems. The question was answered in a celebrated theorem proved and

elaborated by Andrei Kolmogorov, Vladimir Arnold and Jurgen Moser around the middle of the 20th century. This is the awe-inspiring *KAM theorem*. Simply stated, the theorem proves that under fairly general conditions of regularity, addition of a sufficiently small non-integrable perturbation term to an integrable Hamiltonian system leaves most irrational (non-resonant) tori intact, though slightly deformed. Thus, the invariant tori persist in the phase space of the perturbed system, densely filled out with quasi-periodic trajectories. The number of independent frequencies equals the number of degrees of freedom. We call these eternally stable tori the *KAM tori*, or the *KAM surfaces*. They are robust. There may be, however, a set of initial conditions on the tori that lead to trajectories wandering over the entire constant energy surface. But their measure is negligibly small for a small perturbation. It is only the resonant tori that get destabilized first. We will now explore this process with the help of what is known as the *twist map*.

5.5 Twist map

Let us reconsider an integrable Hamiltonian system of two degrees of freedom ($N = 2$) with the corresponding invariant, rational 2-tori as shown in Fig.5.1. Let J_1 and J_2 be the two action variables defining a torus and W_1 and W_2 the corresponding circular frequencies of motion along the meridional (ϕ) and the longitudinal (θ) circles of radii J_1 and J_2. Let $W_1/W_2 = p/q \equiv \alpha$, with p and q integers. Here α is the rotation (winding) number. The intersection of phase trajectories with the Poincaré surface of section shows concentric closed curves (circles), corresponding to the nested tori with different values of actions. It is important to note, however, that a particular trajectory on a given torus ($W_1/W_2 = p/q$) generates only a finite set of q points on the continuous curve (circle) on the meridional surface of section. It is convenient and sufficient to study now the Poincaré map so generated. Inasmuch as energy is the only constant of motion, it is sufficient to consider the 2-torus embedded in a $2N-1 \equiv$ three-dimensional subspace (constant-energy surface) and label the different tori by just one action variable J with $W_1 = W_1(J)$ and $W_2 = W_2(J)$, giving the angles $\phi = W_1(J)t + \phi_0$ and $\theta = W_2(J)t + \theta_0$. The successive ϕ intersections on the meridional surface (plane) of section are then related by

$$\phi_{n+1} = \phi_n + 2\pi\alpha(J_n) \qquad (5.5(a))$$

$$J_{n+1} = J_n,$$

where $\alpha(J_n) = W_1(J_n)/W_2(J_n) \equiv$ rotation (winding number). This

recurrence relation is one of the standard maps, called the twist map, for conservative systems (verify that the Jacobian $\partial(\phi_{n+1}, J_{n+1})/\partial(\phi_n, J_n) = 1$). It is called the twist map for the obvious reason that, the rotation number α being different for different tori, the points of intersection of trajectories with the surface of section on different circles initially aligned radially (same phase angle ϕ) will be phase-shifted relatively at later intersections (Fig.5.1), in much the same manner as the runners on the circular tracks in a field.

Now we come to the most important consideration of what happens to the rational tori when we add a sufficiently small non-integrable perturbation (V) to the integrable Hamiltonian (H_0). In general, this amounts to adding a term $\epsilon V(J_1, \phi_1, \ldots, J_N, \phi_N)$ to H_0. All we have to do now is to modify the twist map as

$$\begin{aligned} \phi_{n+1} &= \phi_n + 2\pi\alpha(J_n) + \epsilon V_1(J_n, \phi_n), \\ J_{n+1} &= J_n + \epsilon V_2(J_n, \phi_n) \end{aligned} \qquad (5.5(b))$$

with $\epsilon \ll 1$, and $\alpha = p/q$. Inasmuch as the system is still Hamiltonian, this map must be conservative (i.e. area preserving).

5.6 Destruction of the resonant tori and soft chaos

Let us focus on one particular rational torus, or rather on its Poincaré section (Fig.5.2(a)). Consider first the associated unperturbed twist map. It is clear that this rational torus (S) must be flanked by (indeed 'protected' by) the two nearest, necessarily irrational tori (the KAM tori), one on the inside (S_1) and one on

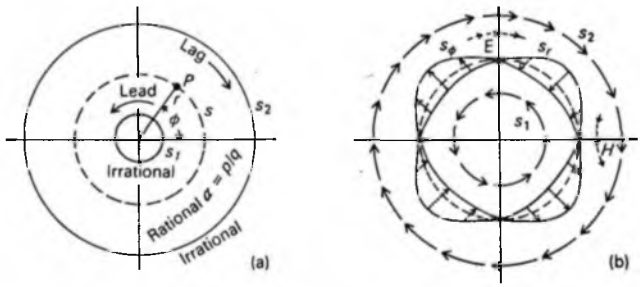

Fig.5.2(a) Poincaré section of rational $\alpha = p/q$ (S) and neighbouring irrational (S_1 and S_2) tori for $N = 2$ integrable system; **(b)** generation of elliptic (E), hyperbolic (H) fixed points due to small non-integrable perturbation of S to S_r and S_ϕ.

the outside (S_2). Let the small perturbation be switched on. Now, we have from the KAM theorem that these two non-resonant tori are to persist for a small enough perturbation. In order to see its effect on the resonant torus, just ask for the mapping of the unperturbed Poincaré section, the ϕ-circle(s), under the perturbed map and appeal to continuity. We must have it mapped on a closed curve then. Since, however, the map is conservative and the curve is closed, the latter must intersect the unperturbed circle an even number of times. The points of intersection will now be the fixed points of both the perturbed as well as the unperturbed map, and there will be 2 kq of these fixed points in general where k is an integer. Let us emphasize once again that the unperturbed circle J (= constant on the Poincaré surface of section of the rational torus ($\alpha = p/q$)) is a quasi-continuum of fixed points of period q in the sense that every trajectory intersecting the section at *any* point on the circle will re-intersect it at the same point after q rounds. However, any *given* point on it generates only a *finite* set of q points under the Poincaré map. Half of these 2 kq will be elliptic, and half hyperbolic (see Appendices C and D). Let us see how this comes about.

Let us assume that the winding number $\alpha(J)$ increases radially inward. Then we can see from the twist map that the quasi-periodic trajectory on the KAM torus just outside (inside) of the resonant torus will lag (lead) relative to the resonant trajectory. On successive iterations of the Poincaré map what happens to our rational torus between these two nested, robust, irrational tori? That is the question. Clearly, a point (r, ϕ) on the unperturbed curve S will, after q iterations of the perturbed map, get mapped to its own neighbourhood on the section S. Now, by continuity, it must be possible to find a nearby point (r_0, ϕ_0) such that after q rounds of iteration (of the Poincaré map, corresponding to q successive intersections with S of the trajectory on the perturbed torus), the angle ϕ is returned to its initial value ($\phi_q = \phi_0$). The locus of such points (r_0, ϕ_0) then generates a closed curve, S_ϕ on S. Of course, $r_q \neq r_0$ in general and, therefore, the curve S_ϕ is not invariant under the q iterations. It will be transformed into yet another closed-curve, S_r, say. Conservation of phase-space volume (area here) and closure of the curves S_ϕ and S_r would require an even number of their mutual intersections, and each such intersection (and its iterates) shall be fixed points of period q.

Further, simple considerations of flow directions in the vicinity of these fixed points show that the hyperbolic fixed points (H) alternate with the elliptic fixed points (E) as we go round the curve of section. Inasmuch as the hyperbolic (elliptic) points can get

mapped only onto hyperbolic (elliptic) points, we have in general $2kq$ such alternating fixed points in all where k is an integer.

As the perturbation is increased, the elliptic points keep bifurcating, each into two elliptic points and a hyperbolic point, and the intersecting curves S_r and S_ϕ become more wiggly. These bifurcations cause period doubling and the period of the orbit subtending the $2k$ elliptic points is $2kq$ after k bifurcations. Now the orbits originating close to the hyperbolic points are known to be chaotic while those near the elliptic points will be periodic, or quasi-periodic on invariant tori. The chaotic region progressively submerges more and more of the occupied region of the phase space while the islands of regular (periodic or quasi-periodic) motion dwindle. This is the *soft chaos*. At any stage, the stable KAM tori form barriers to penetration by the irregular trajectories, harnessing thereby the tendency towards total chaos.

Thus we have on the Poincaré section closed curves, islands of stability (stable, regular, periodic orbits) corresponding to the elliptic fixed points surrounded by the robust KAM irrational tori. On the other hand, and co-existing with these islands of stability, are the neighbourhoods of the hyperbolic points (saddle points) that correspond to highly irregular, aperiodic motions that show up in the Poincaré section as a dust of points. All this is due to the SIC-ness, so very characteristic of the neighbourhoods of separatrices of the saddle points. In fact, the KAM theorem sharpens the question of stability of the non-resonant (irrational invariant) tori by quantifying the degree of irrationality of the winding number. It asserts that for the non-resonant tori to persist despite non-integrable perturbation, we must have $|(W_1/W_2 - p/q)| > c/q^\nu$, where the small constant c measures the strength of the non-integrable perturbation and the exponent ν is sufficiently large, e.g., $\nu = 2.5$. This condition covers majority of trajectories. The KAM theorem is perhaps the finest application of the purest of mathematics, the *number theory*.

A direct consequence of the KAM theorem is that in the vicinity of the highly rational numbers there will be no invariant tori. These absences are known as the KAM gaps and provide an understanding of the Cassini divisions and the Kirkwood gaps in astronomy referred to earlier.

As a rule, the 'more irrational' α is, the more robust is the torus against a given perturbation. Now, the most irrational number (i.e. most distant from rational numbers) in the strict mathematical sense is the so-called golden ratio $r = (\sqrt{5} - 1)/2$ of the ancient Greeks. Thus, the last irrational torus to be destabilized is the one with $\alpha = r$. These KAM tori are effective barriers against the random wandering of the trajectories originating near the resonant rational

tori. This phase-space localization, however, is absolute only for the case $N = 2$. In higher dimensions, when $N=3$ for instance, the three-dimensional KAM tori do not partition the five-dimensional constant energy surface into disconnected spaces. Hence the possibility of (ultra slow) irregular wandering or percolation from one resonant torus to another, leading to what is called the *Arnold diffusion*.

5.7 Standard map

As an example of a conservative map, consider the map generated by a periodically impulsively kicked rotator with angular momentum J_n and position θ_n just before the n^{th} impulse. The rotator rotates uniformly in between the kicks. The map is

$$J_{n+1} = J_n + K \sin \theta_n \tag{5.6(a)}$$

$$\theta_{n+1} = \theta_n + J_n$$

The Jacobian $\partial(J_{n+1}, \theta_{n+1})/\partial(J_n, \theta_n)$ equals unity. This is the famous *standard map*. Physically, one can imagine a pendulum subjected to a gravity g which is switched on and off periodically but impulsively, i.e., $g \propto \sum_n \delta(t-n)$. Each impulse instantaneously changes the angular momentum of the pendulum by an amount proportional to the time integral of the tangential component (θ) of the vertically acting gravity. In between the impulses, the pendulum moves uniformly as a free rotator. The resulting 'stroboscopic' motion relating the angular momentum (J_n) and the angular position (θ_n), just before the n^{th} impulse, is precisely the standard map.

For $K=0$, one just has a twist map and a regular (periodic/quasi-periodic) motion, with $J_n/2\pi(=$ constant) acting as the winding number, rational or irrational. For a small but non-zero K, one has the trajectories locked in stable motion around the periodic orbits of the standard map forming chains of stability islands on the surface of section resulting from the progressive dissolution of the rational tori. These chains, however, remain separated by the KAM (irrational) tori that act as barriers. The KAM tori are progressively destabilized as K increases. The disappearance of the last KAM orbit beyond a critical value of K leads to global chaos.

5.8 Driven pendulum

Of course, we could also consider the pendulum to be driven sinusoidally. This too generates a conservative map (an area preserving

map) that describes a non-integrable Hamiltonian system. It is assumed here that the pendulum can have not only small amplitude ($-\pi < \theta < \pi$) oscillations about its usual position of stable equilibrium ($\theta = 0$), but can also rotate completely around the vertical circle passing through the point of unstable equilibrium ($\theta = \pm\pi$). This system has a rich phase portrait and exhibits transition from the bounded oscillations (vibrations or librations) to unbounded rotation modulated by oscillations and a host of phenomena such as periodic orbits, intermittency, and chaos as we tune the two parameters, namely, the ratio of the natural frequency of small amplitude oscillations to the driving frequency and the strength of nonlinear coupling. The original equation for an undamped driven pendulum suitably normalized reduces to the standard form

$$\ddot{\theta} + \sin\theta = \epsilon \cos\omega_0 t \qquad (5.6(b))$$

Introducing θ, $\omega = d\theta/dt \equiv \dot{\theta}$ and $\phi = \omega_0 t$, we have the autonomous set of equations

$$\dot{\omega} + \sin\theta = \epsilon\cos\phi,\ \dot{\theta} = \omega,\ \dot{\phi} = \omega_0 \qquad (5.6(c))$$

This has a three-dimensional phase space, or N=3/2 as there is no momentum conjugate to ϕ and hence only half a degree of freedom is reckoned for ϕ. The flow is clearly conservative.

In Fig.5.3, we show the phase portrait in the $\theta - \omega$ plane for the undamped pendulum without the drive. One can readily identify the

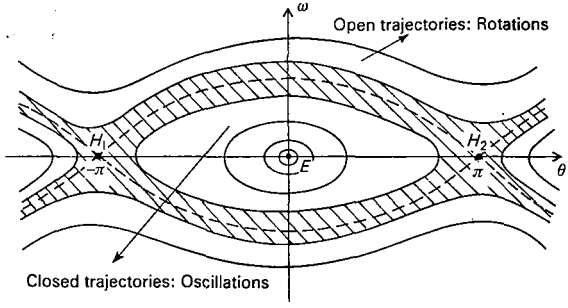

Fig.5.3 Phase portrait of an undamped pendulum without drive. Notice the elliptic fixed point (E: oscillations) and the hyperbolic points (H_1, H_2: rotations) and separatrices (dashed lines) through H_1 and H_2. Periodic perturbation destroys separatrices and creates a stochastic layer containing chaotic trajectories and stability islands, shown hatched in Poincaré section (schematic).

elliptic centre (θ=0, ω=0) attracting the bounded oscillations around the stable equilibrium with zero angular velocity on the average. One can also identify the hyperbolic points (saddle points) at $\theta = \pm\pi$, $\omega = 0$, corresponding to the unstable equilibrium, and the two separatrices joining these two hyperbolic points (hence the heteroclinic orbit, see Appendix D) separating the oscillating motion from the unbounded rotation with non-zero average velocity.

Now, what happens when the periodic drive ϵ is turned on? Well, it is quite similar to the case of the standard map. All one has to do is to view the phase portrait (Fig.5.3) doubling now as a guide to the eye for the points of intersection of the trajectories with the $\omega - \theta$ plane as the surface of section. The instability in the neighbourhood of the separatrices leads to the formation of stochastic layers around them with chaotic motion within the layers. A layer contains, however, islands of stability impervious to stochastic trajectories. The interior of an island repeats the above structure at a finer level as energy E is increased, and the islands shrink, and the stochastic layer gradually spans nearly the entire phase space. This is the route to soft chaos, with coexisting islands of stability and stochastic regimes.

A characteristic feature of this soft chaos is intermittency. A chaotic trajectory passing near the boundary of a stability island (which it cannot penetrate) performs temporarily a regular motion there, approximating the nearby periodic orbit, and then wanders off chaotically. The brief encounters of regularity interrupting the chaotic wandering constitute intermittency. We had come across the phenomenon of intermittency earlier while discussing the dissipative logistic map. Intermittency is a common characteristic of Hamiltonian chaos and, indeed, it distinguishes it from a purely stochastic, random process. In turbulent flows it seems associated with the 'coherent structures' that coexist with turbulence. It is seen in rivers as 'boils', known as *Mark Twain boils* after Mark Twain who is reported to have noticed them in the Mississippi.

Finally, we have briefly described above just two specific models of Hamiltonian chaos. We could include many, e.g. two-coupled pendulums etc. But the point is that the main features of nonlinear dynamical systems in compact domains with at least two degrees of freedom are quite generic. This is due to the *structural stability* of the governing equations that preserve the global behaviour and the phase portrait despite small changes of parameters. There are also some purely geometrical models of chaos, for example the *Sinai billiard-ball* models, that mimic hyperbolic systems leading to SIC-ness and mixing of trajectories. Thus, the motion of a ball (hard elastic sphere) moving freely on a flat annulus with a circular

hole and undergoing specular reflections at the boundaries leads to chaotic mixing due to the defocussing effects of the convex boundary of the hole. The same is true for the *Sinai stadium* — two semi-circles capping a rectangle. And the free motion on a pseudosphere — a surface of constant negative Gaussian curvature (a saddle point all the way!). Indeed, these Hamiltonian chaotic systems have provided deeper insights into the postulates of equilibrium statistical mechanics (such as mixing and ergodicity) and reveal the emergence of statistical laws in a deterministic dynamical system. By ergodicity all we mean is that the phase trajectory will have eventually passed through almost all points (or rather arbitrarily close to all the points) on the constant energy surface, spending equal time in the phase-space cells (pixels or voxels) of equal volume (it visits 'every hamlet' so to say). This allows us to equate the time averages with the phase-space averages. The *Ergodicity problem* has associated with it names of the great founding fathers of statistical mechanics — Ludwig Boltzmann, James Clerk Maxwell, Josiah Willard Gibbs, Henri Poincaré and George David Birkhoff — from the late 19th and early 20th centuries. A related idea, but much stronger than ergodicity, is the condition of mixing (that again goes back to Gibbs) which is really responsible for the process of relaxation to equilibrium so very characteristic of all physical systems. As discussed earlier, it involves instability of the phase 'drop' leading eventually to a highly rarified shape that allows it to envelope the entire phase space at any instant of time in a coarse-grained manner. It was only as recently as 1963 that a gas of elastic hard spheres (the Lorentz gas) was shown by Ya Sinai to be ergodic as well as mixing. Hamiltonian chaos provides new insights into these deep problems.

6 *Fractals, Multifractals and Reconstruction of Strange Attractors*

We live in a three-dimensional space. To locate a point in this space we need to specify three numbers, the three Cartesian coordinates (X, Y, Z), say. A smooth surface is two-dimensional. To locate a point on it we need to specify two numbers, the latitude and the longitude, say. Similarly, the line is one-dimensional. We just have to give the distance of the point along the line from a given reference point on it, the origin. And of course the point has dimension zero. These Euclidean geometrical ideas can easily be generalized to higher dimensions. This idea of dimensionality has to do with the ideas of continuity and neighbourhood, of smoothness. We call it the topological dimension.

There is another sense in which we use the idea of dimensionality. It measures the content, or the capacity of a geometrical object — how densely it covers the space in which it may be embedded, though the dimensionality is intrinsic to the object. We call it the *metric*, or the *capacity dimension*. Thus, the cube has a volume, the square has an area and the line has a length. For conventional geometrical objects that are smooth, or regular on relevant length scales, this dimensionality is an integer and has the same value as the topological dimension. But, there are unconventional geometrical objects that are irregular on all length scales. Their capacity dimension defined appropriately may be a fraction. We call such a geometrical object a Fractal. The discovery of fractals is due to the IBM mathematician Benoît Mandelbrot who was led to this idea through his studies of complex geometric structures of irregular shapes and forms such as rough coastlines, lightning's zigzag paths, clouds and sponges that reveal self-similarity down to the finest length scales of interest. A fractal is how Nature explores or covers almost fully a volume with a surface, or an area with a line, or in general a higher dimensional space with something of a lower dimensionality, sparsely but quite efficiently. We should note in passing that the term capacity dimension, as determined by a box-counting algorithm to be discussed later, is due to the great Russian theorist A.N. Kolmogorov. It is now often

used interchangeably with the term fractal dimension. The latter was, however, introduced by Mandelbrot for yet another dimension, the Hausdorff dimension best known to mathematicians.

6.1 Fractal dimension

Let us take an operational viewpoint and measure the length of a line as shown in Fig.6.1(a). All that we have to do is to walk the curve with a divider, marking off equal divisions of size ϵ, where ϵ is the distance between the pointed ends of the divider, or the ruler length. Let $N(\epsilon)$ be the number of steps required to cover the curve. Then $\epsilon N(\epsilon)$ will be an estimate for its length. But not quite its length. This is because the chords subtended by the divider are necessarily shorter than the arc lengths. We are cutting corners! So what we have here is a polygonal approximation to the actual curve. Now make the step length ϵ sufficiently small so that the polygon nearly hugs the curve. This is always possible for a smooth curve, one that is locally straight. We call this a regular curve. It has a well-defined tangent at every point of it. Then, $\epsilon N(\epsilon)$ must tend to the length of the curve as ϵ tends to zero. In other words, $N(\epsilon) \sim \epsilon^{-D}$ as $\epsilon \to 0$, with $D=1$, the dimensionality of the curve as expected.

Consider now an irregular, kinky curve that zigzags down to the smallest length scales (Fig.6.1(b)). At higher resolutions (magnifications) the curve reveals progressively a finer structure similar to the one observed at the lower resolution. We say that the curve is self-similar. It is clear then that no matter how small ϵ is made, our polygonal walk will never quite hug the curve. It will always cut corners. However, we may still have the scaling $N(\epsilon) \sim \epsilon^{-D_0}$ as $\epsilon \to 0$, but now D_0 is a fraction in general. We call it the *fractal dimension* of the fractal curve (also called the *capacity dimension* D_c). Put a little more formally, D_0 = limit of $-\ln N(\epsilon)/\ln \epsilon$ as $\epsilon \to 0$. Here 'ln' denotes natural logarithm. It should be noted that D_0 is the property of the curve independent of the dimensionality d of the Euclidean space in which the curve happens to be embedded. Also, instead of the chords of length ϵ, we could have used d-dimensional balls of radius ϵ, or d-dimensional boxes of size ϵ on the side, to cover our curve without affecting the computed fractal dimensionality D_0 above (Fig.6.1(c)). Thus, the capacity dimension can be computed using some box-counting algorithm. Incidentally, all fractal objects need not have a non-integral dimension. It is amusing that the fractal dimension of the coastline of England is about 1.2, while that of the distribution of stars in the sky is about 1.23.

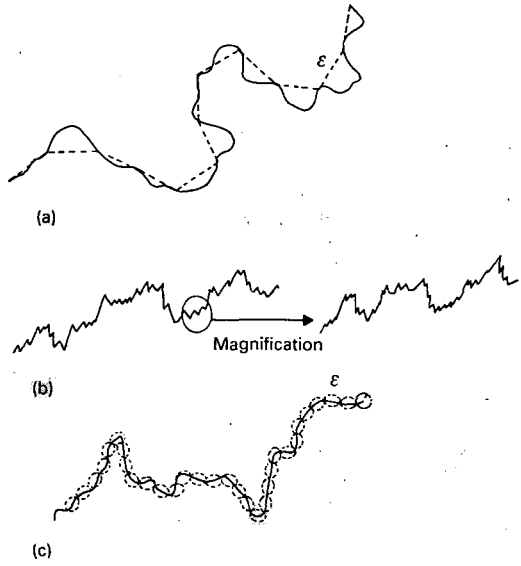

Fig.6.1 (**a**) Covering a line with scale ϵ; (**b**) self-similar fractal curve; (**c**) covering a line with ϵ-balls.

The above operational definition of the fractal dimension can now be applied to any set of points and, therefore to any geometrical object such as a strange attractor. Thus, for a set of points (or an attractor) in a two-dimensional phase space, as for the logistic map discussed in Chapter 3, all we have to do is to cover the set with $N(\epsilon)$ squares, measuring ϵ on the side, and apply the above formula. For the Lorenz attractor embedded in the three-dimensional phase space, we have to use ϵ-cubes instead of ϵ-squares. And so on.

6.2 Examples of fractals: Cantor dust, Koch snow flake

Cantor set (or *dust*) is the canonical example of a fractal that can be constructed following a simple rule. Take a straightline segment, a closed unit interval [0,1] say. Closed means that the end points are included in the interval. Open, by contrast, means that the end points are not included. Trisect the unit interval into three equal segments and omit the middle third open interval. Trisect the remaining two segments and again omit the two open middle

thirds. Iterate this operation ad infinitum and you will be left with a sparse dust of points — a Cantor set of uncountably infinite number of points, but of measure (length) zero (Fig.6.2), because $2^n(1/3)^n$ tends to zero as n tends to infinity. What about its dimension? Well, on each round of iteration the ruler length (ϵ) of the segments gets divided by 3 while the number $N(\epsilon)$ of segments is doubled. Hence the fractal (capacity) dimension $D_c = -\ln 2/\ln (1/3) = 0.630$. Of course, one could generalize this by replacing the fraction 1/3 by a fraction b, $0 < b < 1$. That is, remove the middle section of relative length b and get $D_c = \ln 2/\ln (2/(1-b))$.

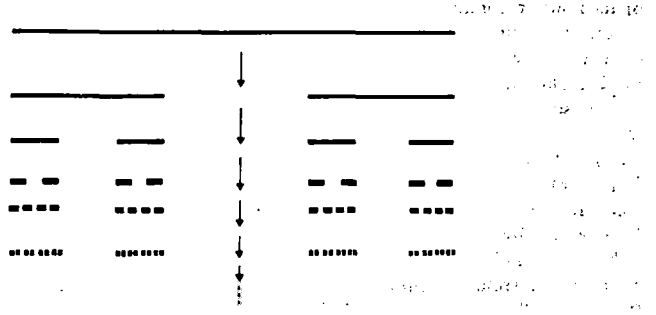

Fig.6.2 Cantor set construction by middle — third deletion. Fractal dimensionality = 0.630.

Other examples of fractals include the *Koch snow flake* (Fig.6.3) and the formation of ice crystals, river and vascular networks, and clusters of galaxies! We even have the fractal Nature of music, notably that of J.S. Bach! Incidentally, the fractal dimension of the attractor set for the logistic map at λ_∞ (onset of chaos) can be shown to be about 0.538 using the box counting algorithm. For $\lambda = 4$, however, the fractal dimension is 1. And for a finite set of points, $D_0 = 0$.

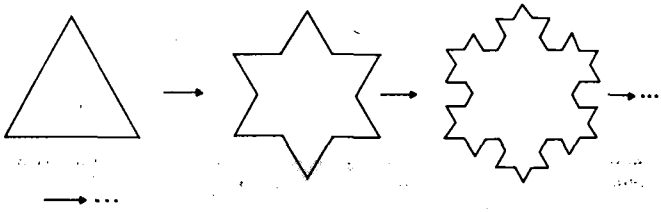

Fig.6.3 Koch Snow Flake or Triadic Island. Each side sprouts an equilateral triangle iteratively. Encloses finite area with infinite perimeter.

6.3 Correlation and information dimensions

As noted above, the fractal dimension defined above is also called the box counting, or the capacity dimension for obvious reasons and denoted by D_c. However, two fractals having equal fractal dimensions (which is a global, average concept) are not necessarily identical. They may differ locally in terms of their inhomogeneity, i.e. small-scale variations of the density of points of the fractal object. The geometrical object may be resolved as a superposition of many fractals much the same way as a function may be resolved in terms of its Fourier components or moments. One can actually define a spectrum of dimensionalities that fully characterizes such a fractal, or a multifractal to be precise. One such very useful dimension is the correlation dimension D_2, also called the frequency dimension, or the scaling dimension of a set of points. For this, count the fraction $C(\epsilon)$ of points on the average lying within a radius ϵ of any point on the fractal. Then D_2 is defined through the scaling form $C(\epsilon) \sim \epsilon^{D_2}$ as $\epsilon \to 0$. Here $C(\epsilon)$ is a correlation function that measures the typical number of neighbours a point has on the set. D_2 is generally more efficient to compute.

More formally, the set of N points in a d-dimensional state space define the correlation integral introduced by P. Grassberger and I. Procaccia (*Physical Review*, A28, 259, 1983):

$$C(\epsilon) = \lim_{N\to\infty} \frac{1}{N^2} \sum_{i,j=1}^{N} \theta(\epsilon - |X_i - X_j|) \tag{6.1}$$

where $\theta(x)$ is the Heaviside step function, $\theta(x)=0$ for $x < 0$ and $\theta(x)=1$ for $x \geq 0$. Here X_i is the position vector of the i^{th} point and $|X_i - X_j|$ the distance between the pair of points (i, j) measured according to the geometry of the d-dimensional embedding space.

Then D_2 is given by the initial slope:

$$D_2 = \lim_{\epsilon\to 0} \frac{\ln C(\epsilon)}{\ln \epsilon} \tag{6.2}$$

There is yet another dimension that is physically highly motivated – it is the *information (entropic) dimension* of the geometrical object and is denoted by D_1. It gives a physical substance to the geometrical content by asking how often, or densely, a neighbourhood is visited. Let the d-dimensional phase space be covered by m boxes (bins or pixels or voxels) of size (or resolution) ϵ on the side . Let N_i be the number of points of the geometrical object in the i^{th} box and

N the total number of points. Then one can introduce the measure of missing information (Shannon's entropy) as

$$I(\epsilon) = -\sum_i p_i \ln p_i \tag{6.3}$$

where $p_i = N_i/N$ is the relative frequency of occupation (or the probability) for the i^{th} box (this agrees with the usual idea of entropy, or missing information — it is greatest if all boxes are equally frequently visited or occupied implying complete uncertainty, and zero if just one box is occupied implying total certainty). The information dimension is now defined as the initial slope that measures how this information scales with the bin size ϵ:

$$D_1 = \lim_{\epsilon \to 0} (-I(\epsilon)/\ln \epsilon) \tag{6.4}$$

It turns out that D_0 (fractal), D_1(information) and D_2 (correlation) are the most important dimensions — the invariant geometrical features. However, one can generalize to D_q, the generalized dimension of order q as

$$D_q = lim_{\epsilon \to 0} \frac{1}{q-1} \ln \left(\sum_{i=1}^{m} p_i^q \right) \Big/ \log \epsilon \tag{6.5}$$

It is readily verified that D_q reduces to D_0, D_1 and D_2 for $q = 0$, 1 and 2 respectively [for $q = 1$ one must be a little careful and take the limit $q \to 1$ by writing $p_i^q = p_i p_i^{q-1} \simeq p_i(1 + (q-1)) \ln p_i +$ terms involving higher powers of $(q-1)$]. One can also verify that $D_q \geq D_{q'}$ for $q \leq q'$. Equality holds for the uniformly distributed point set.

6.4 Multifractals and the spectrum of singularities of local density of points: The $f(\alpha) - \alpha$ plot

Multifractal analysis is required to describe completely the small-scale variation of the density (non-uniformity of the point-set). It measures the inhomogeneity. A set may be a superposition of fractals, thus having a spectrum of fractal dimensions. Multifractal analysis is thus the analogue of fourier analysis, a distant analogy though.

Let the set (e.g., an attractor) be partitioned with resolution ϵ. Label the boxes (voxels) by $i = 1,2, \ldots, N$. Then one would expect a local scaling of the probability

$$p_i(\epsilon) = \epsilon^{\alpha_i(\epsilon)} \tag{6.6}$$

with $\alpha_i(\epsilon)$ the strength of the singularity as $\epsilon \to 0$. The scaling index (exponent α (ϵ)) measures the density of points on different subsets

of the attractor. Large α (ϵ) implies rarefied subsets, and small α (ϵ) implies densified subsets. Typically, one finds $\alpha_{\min} \leq \alpha \leq \alpha_{\max}$. Then $\alpha_{\max} - \alpha_{\min}$ measures the degree of inhomogeneity. Thus α is the spectral component. To find the intensity of the spectral component, we must count how frequently a given α occurs on the set. This will constitute a global characterization of the set — a global scaling of the density of points.

Now, we substitute for p_i (ϵ) from Eqn.6.6 in the expression for D_q (Eqn.6.5) and replace $\sum_i = \int n\ (\alpha, \epsilon)\ d\alpha$ by introducing a density-in -α (i.e., number of points per unit interval of α), $n(\alpha, \epsilon)$, which is then taken to scale as $n(\alpha, \epsilon) = \rho(\epsilon)\epsilon^{-f(\alpha)}$. Here $f(\alpha)$ is an index reflecting the local scaling of the density $n(\alpha, \epsilon)$ with ϵ as $\epsilon \to 0$. Straightforward saddle point integration then gives the saddle point condition

$$D_q(q-1) = |(q\alpha - f(\alpha))|_{q=df/d\alpha} \equiv \alpha(q) - f(\alpha(q)) \tag{6.7}$$

Here $q = df/d\alpha$ is to be solved for α as function of q. One can readily verify from Eqn.6.7 that

$$\frac{d}{dq}(D_q(q-1)) = \alpha(q) \tag{6.8}$$

This suggests that the Eqn.6.7 describes a Legendre transformation:

$$f(\alpha) = q\alpha - D_q(q-1) \tag{6.9}$$

where $D_q(q-1)$ is a 'Lagrangian', q the 'velocity', $\alpha(q)$ the 'momentum' and $f(\alpha)$ the 'Hamiltonian'. One readily verifies $\partial f/\partial q = 0$ as it should be. Thus, from the measured D_q one can calculate (α, $f(\alpha)$).

The Legendre transformation is the standard technique in mechanics and thermodynamics to formally change from one set of independent variables to another conjugate set of independent variables.

Thus we arrive at the $f(\alpha)$ versus α plot. This plot of spectrum of singularities (see Fig.6.4) has some universal features:

$$\frac{df}{d\alpha} = q$$

$$\frac{d^2 f}{d\alpha^2} < 0 \tag{6.10(a)}$$

It follows, therefore, that

$$\begin{aligned} &(a)\quad D_0 = f_{max}(\alpha) \\ &(b)\quad D_{-\infty} = \alpha_{\max} \\ &(c)\quad D_{+\infty} = \alpha_{\min} \end{aligned} \tag{6.10(b)}$$

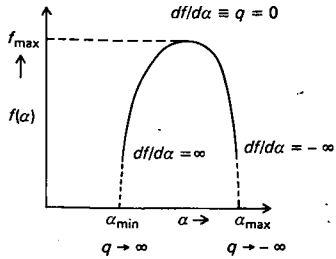

Fig.6.4 Multifractal spectrum of Singularities: $f(\alpha) - \alpha$ plot (schematic).

Finally, a highly illustrative and calculable example of the multifractal can be constructed recursively as follows. Consider a uniform distribution (of matter, say) having constant density of unity over the interval [0,1] (see Fig.6.5). Now, in the first round of recursion, redistribute the density by piling up the weight in the middle half as shown in Fig.6.5. Thus, the density is unity over the interval

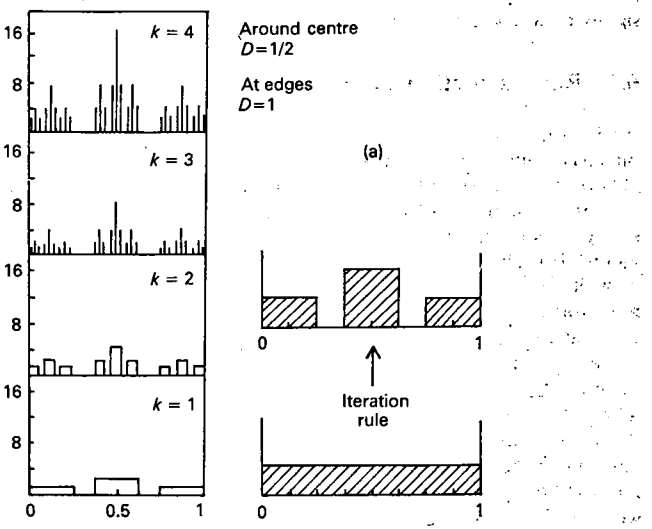

Fig.6.5 (a) Construction of a multifractal by iterative rule *Contd.*

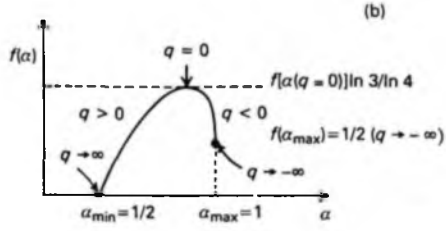

Fig.6.5 *Contd.* **(b)** Spectrum of singularities.

(0, 1/4), zero over (1/4, 3/8), two over (3/8, 5/8), zero over (5/8, 3/4) and again unity over (3/4, 1). Now repeat the same piling-up-by-redistribution procedure on each of the three piles so obtained. And so on, *ad infinitum*. This gives ultimately an inhomogeneous but self-similar distribution of the matter which is multifractal. The corresponding spectrum of the singularities, the $f(\alpha) - \alpha$ plot, is sketched in Fig.6.5. The spectral dimension varies from $D=1/2$ near the centre signifying a high density, to $D=1$ near the edges signifying a low density. A sandpile if you like!

6.5 Reconstruction of strange attractors

An important geometrical aspect of a strange attractor is its own dimensionality and the embedding dimensionality (the dimensionality of its phase space). There are also dynamical aspects, e.g., the Lyapunov exponents. The question is this — Can we reconstruct the strangeness of the strange attractor from a limited set of measurements? It is almost like asking, 'Can we hear the shape of a drum?' Now, it turns out that it is indeed possible to reconstruct the strange attractor, that is to extract certain invariant characteristics, dynamical and metric, of the nonlinear dynamics such as the Lyapunov exponents, the fractal dimensions and the embedding phase-space dimensions, from the measurement of just a single scalar quantity as function of time sampled so as to give a time series. This is the content of the remarkable theorem of Floris Takens — the embedding theorem. Formally, for the d-dimensional phase motion governed by d first-order differential equations $\dot{X}_i = f_i(X_1, \ldots, X_d)$, we can eliminate all but X_1, say, in favour of a single differential equation of order $(d-1)$ for X_1. Thus, it should be sufficient to study just any one of the d X_i's, X_1 say, without loss of information.

Instead of measuring all the state variables at one time, we have to measure one state variable at many times — a real trade off! This remarkable claim, however, becomes less unreasonable once we realize that all the dynamical state or phase-space variables of the chaotic system are necessarily *implicated* in that single time series. Thus, the entire multidimensional attractor is folded-in into the one-dimensional time series, and the question is merely that of unfolding it back into the full phase space. This is made possible by constructing an artificial phase space of sufficiently high dimension through the use of 'time-delayed coordinates' as described below. The strange attractor is indeed an implicate universe, we might say.

Let the scalar signal be sampled so as to give a time series

$$s(n) = s(t_0 + n\tau) \tag{6.11}$$

Here t_0 is some initial time and τ is the sampling time interval of the measuring instrument. The scalar signal may typically be a component of some fluid velocity at a point in a fluid measured by the *laser Doppler interferometric technique*, or by the hot-wire anemometry. The signal may also be the concentration of the bromide ions, say, in the BZ reaction that involves some 25 chemical species! From the time series we construct an N-dimensional vector

$$X(N) = (s(n)\ ,\ s(n+T)),\ \ldots\ ,\ s(n+(N-1)T) \tag{6.12}$$

where the delay T can in principle be anything. Here T is an integer.

Now let n take all integral values and use the resulting N-dimensional vectors to populate the artificial phase (state) space of N dimensions so constructed out of the time series. The resulting geometrical object, of course, will not be quite the same as the original attractor (because the components of $X(N)$ are not the original state variables but rather some nonlinear functions of them) but any smooth nonlinear change of variables should give an equally good set of coordinate bases as far as the invariant features are concerned. In particular, for large enough N, we expect a complete unfolding of the time series into the original attractor. Thus, for a chosen N, construct the artificial state space and populate it with the phase-points $X(N)$'s. Evaluate the corresponding dimension D_2^N of this point set following the Grassberger–Procaccia procedure (Eqn.6.1). Plot D_2^N against N. It should increase monotonically with N saturating to a limiting value. The integer $d = N_{\min}$ beyond which D_2^N saturates to the limiting value (fraction in general) is the embedding dimension of the attractor (i.e., dimension of the state space in which the attractor is embedded), and the saturation

value $D_2^{N_{\min}}$ is the correlation dimension D_2 of the attractor. And, of course $D_c \geq D_2$. It turns out that $D_2 = 1$ for a singly periodic motion (limit cycle), $D_2 = 2$ for a biperiodic torus and $D_2 > 2$ for a strange attractor. For a truly stochastic noise, $D_2 = \infty$.

But D_2 is not the only dimensionality to be recovered from the time-series. We can recover the entire spectrum D_q of generalised dimensionalities of order q introduced earlier. For this consider the generalization of the correlation function

$$C^q(\epsilon) = \lim_{N\to\infty} \left[\frac{1}{N} \sum_{i=1}^{N} \left[\frac{1}{N} \sum_{j=1}^{N} \theta(\epsilon - |X_i - X_j|) \right]^{q-1} \right]^{((1/q)-1)} \tag{6.13}$$

Then, it can be shown that

$$D_q = \lim_{\epsilon\to 0} \left(\frac{\ln C^q(\epsilon)}{\ln \epsilon} \right) \tag{6.14}$$

Thus it is possible to reconstruct the attractor by finding D_q's of an artificial phase-space of *sufficiently high-dimension* constructed from the time-series of a *single* measured variable — again the embedding theorem of Takens.

Reconstruction of low-dimensional strange attractors from a time-series by the embedding method has been carried out successfully in many cases now. Notable among these are the chemical chaos in the BZ reaction; the cardiac chaos from the ECG; the neuronal (brain) chaos from the EEG giving *lower* dimensionality for the epileptic state compared with the normal state; chaotic epidemics like measles; in some types of fully developed turbulence, and the X-ray luminosity of the neutron star Her-$X1$. There is however, sometimes, the complication due to the really stochastic noise obscuring deterministic chaos.

Aside from these metric properties discussed above, the strange attractor has dynamic properties too, which are characterised differently. One could, for instance, Fourier analyse the time-series $X(t)$, $X(t+\tau)$, $X(t+2\tau)$, ... The square of the absolute value of the Fourier coefficient then gives the power spectrum of the motion. For this one often resorts to the technique of *fast fourier transform*. For a regular attractor, the periodicities will show up as sharp peaks (lines) in the spectrum. For the strange attractor, however, the spectrum is continuous and rather flat corresponding to the aperiodicity of the motion.

There are other equally characteristic invariant dynamic properties of the strange attractor that measure, for instance, the rate of

exponential divergence of neighbouring trajectories (the Lyapunov exponents) or the related dynamic entropy (the rate of information change or the Kolmogorov entropy). These quantify the stretching-out and the folding-back of the phase-space trajectories so very characteristic of deterministic chaos (see Appendix A).

7 *Concluding Remarks*

Most real physical systems show chaos for some initial conditions and ranges of the control parameters. Essential for chaos is nonlinearity that can lead to exponentially sensitive dependence on initial conditions and to orbit complexity. The chaotic trajectory is unstable all along it, but chaos itself is robust. Much of our discussion of deterministic chaos in the preceding pages has been limited to dissipative dynamical systems with continually contracting phase-fluid volume. Indeed, chaos resulted as subtle resolution of the apparently contradictory demands of diminishing phase volume, non-intersection of the phase trajectories and the exponential divergence of the once neighbouring trajectories (sensitivity to initial conditions, or SIC). However, as we have also discussed, non-dissipative (that is conservative, or Hamiltonian) systems with phase volume constant in time can and do show chaos too. For this we need non-integrable Hamiltonian systems. (A Hamiltonian system is said to be integrable if, roughly speaking, the number of constants of motion equals the number of degrees of freedom — such systems are reducible to as many independent, non-interacting degrees of freedom through certain transformations well-known in classical mechanics. Hence no mixed-upness, and no chaos therefore.) Two nonlinearly coupled harmonic oscillators (the Hénon–Heiles system) is one such example that shows chaos when excited beyond an energy threshold. So is possibly the case with a gravitating stellar cluster. Chaos with a low dimensional strange attractor has been detected in the accreting neutron star Her-$X1$, and reconstructed from the time-series analysis of its X-ray emission. Examples abound. Indeed, classical mechanics has received a new lease of life from the (*non-integrable*) Hamiltonian chaos. The latter is, in a way, the missing link between classical mechanics and statistical mechanics — it may provide a rationalization of the Boltzmannian hypothesis of molecular chaos (the statistical assumption), of ergodicity and mixing.

Perhaps the greatest challenge facing the chaos theory is the one posed by the originally motivating problem of turbulence of a fluid flowing through a pipe and particularly the open flow past obstacles, the wake. The problem remains partially solved. Fully developed

turbulence certainly has a strange attractor at the heart of it, but many non-universal aspects of turbulence remain open questions. The original idea of Landau that turbulence results from a cascade of instabilities, with new incommensurate modes appearing one at a time, does not work. Turbulence remains the last unsolved problem of classical mechanics.

Two-dimensional incompressible flow, however, can be reduced to the Hamiltonian form. It shows the characteristic coexistence of the ordered islands of stability, e.g., vortices and jets, and the chaotic regions in the phase space which is the physical space of the mixing process itself. The two are separated by the KAM-type barriers (e.g., undulating jets) that obstruct mixing by advection. One believes that the gulf stream (jet) on Earth and the great red spot (vortex) on Jupiter are examples of such traps. Indeed, it has been suggested that a spectacular example of such a trapping zone exists in the form of 'meddies', the vortices that originate in the Mediterranean and drift across the Atlantic carrying with them the Mediterranean marine life unmixed and trapped for a year, or even more. The persistence of such barriers to mixing despite weakly turbulent flows as predicted by the KAM theorem, and the possibility of realizing efficient mixing by chaotic advection, are serious matters of relevance to problems of pollutant dispersal in the environment and of mixing in chemical reactors. After all, gentle chaos with sensitivity to initial conditions is energetically much more cost-effective than the brute-force stirring to create mixing by turbulence.

Many more, rather subtle, applications and manipulations of chaos based on its very exponential sensitivity and orbit complexity are being experimented with — chaos *control*, *encoding* of digital information, and *targeting* — among others. Let us consider these briefly. (For a very readable discussion, see E. Ott and M. Spano, *Phys. Today*, **48**, 35 (1995); T. Shinbrot, C. Grebogi, E. Ott and J.A. Yorke, *Nature*, **363**, 411 (1993).)

Controlling chaos, when it is unavoidably present, exploits its hidden order — namely the many unstable periodic orbits embedded in the chaotic attractor. As we have learnt in Chapters 3 and 5, a free-running chaotic trajectory shall, in the course of its random walk, approach any given unstable periodic orbit arbitrarily closely, follow it for a few cycles, and then wander off. Now, one of these periodic orbits may be desirable for an optimal system performance. Chaos control then simply means that we give suitable kicks to the system so as to reset it back to the unstable periodic orbit, i.e., we stabilize the latter. In practice it calls for a control loop where the deviation from the desirable periodic orbit, as reflected

in the deviation from the optimal system performance, is sensed as an error signal which is then fed back negatively. Because of the exponential sensitivity, these control signals need only be small. The other main advantage of chaos control, when possible, is the unlimited choice of unstable periodic orbits to lock-in to. Usually, chaotic attractors of low dimensions (less than 5) are to be harnessed. Such a chaos control has been devised for a solid-state laser, for mechanical and electronic oscillators, and for the arrhythmic heart of a rabbit (in vitro). It is being attempted for the ventricular fibrillation of a canine heart.

The use of a chaotic attractor for encoding and transmitting digital information is best illustrated with the example of a chaotic oscillator whose attractor is a 'double-scroll': the phase trajectory traces a number of loops in the left lobe, say, wanders off to the right lobe, traces a number of loops there, wanders back to the left lobe and so on, much the same way as for the Lorenz attractor in Fig.4.2(a). The sequence of the left-lobe and right-lobe windings may be represented by an 'apparently' random string of binary digits, 0 and 1. Now, because of exponential sensitivity, it is possible to give small but calculable kicks to the chaotic oscillator that change the sequence in a computable manner in the short run so as to encode the digital information. Again, the advantage is the smallness of the control signal, even though the chaotic oscillator (a powerful transmitter perhaps) itself may have a large output.

Targeting means coaxing the dynamical system to go quickly from a given initial condition to a final desirable condition (target region) within the phase space of the attractor. Again, the exponential sensitivity makes this possible through a careful choice of perturbations that need be only small. A spectacular implementation of such a targeting was the redirecting by the NASA scientists of the Sun–Earth Explorer-3 Spacecraft from its near-Earth orbit towards a distant cometary encounter with a minimum of fuel consumption. This was done using the sensitivity of the Earth–Moon–Spacecraft three-body system which is known to be non-integrable.

Applications of the ideas from chaos and strange attractors outside the physical sciences, in particular in life sciences (biology and medicine) are very encouraging. The possibility of reconstruction of the attractor from the measured time-series (the ECG and EEG traces, for example) has opened up new diagnostic routes. For an excellent account of these, see *Fractal Physiology and Chaos in Medicine* by Bruce J. West, World Scientific, Singapore, (1990). It is strongly indicated, for example, that disorders such as schizophrenia can be modelled by strange attractors associated with the middle layer of the forebrain, the limbic brain (which is the seat of emotions),

causing chaotic oscillations between thought and emotions. Similarly, for the case of epilepsy it is significant that the normal neural activity of the brain has a chaotic attractor of higher dimension than that of the epileptic brain! Indeed one has $D_0 \sim 6.1$ (quiet awake); $D_0 \sim 8.2$ (rapid eye movement, or REM, sleep); $D_0 \sim 4.05$ for deep sleep; and for the epileptic state $D_0 \sim 2.05$.

Finally, there is the rapidly expanding field of quantum chaos in the highly excited states of atoms and molecules that we have not touched upon at all. What happens to a classically chaotic system when we quantize it? It has been found that the regular-to-chaotic transition in a quantum system is marked by a qualitative change in the statistics of the energy-level spacings: in the chaotic-case the levels 'repel' each other. The Heisenberg uncertainty principle, however, blurs the classically sharp trajectories. It is not clear how the fine structure of a strange attractor will tolerate this quantum diffusion. These are some of the deep questions that remain to be fully answered. It may even provide deeper insights into quantum mechanics.

Strange attractors encountered in Nature are often low-dimensional despite the large dimension of the phase space in which they may be embedded. Obviously, most degrees of freedom are damped out, leaving just a small number of macroscopic degrees of freedom that make up the eventual attractor. A strange attractor, with all its mixed-upness, is still a highly stable, robust and structured dynamical object. It is virtually an infinite reservoir of resonance frequencies, and is tunable by controlled feedback. It has an organization. It generates 'chance' out of the 'necessity' of deterministic laws of motion. But there is also a simplicity at the far side of its complexity.

Appendix A

Lyapunov exponent

Lyapunov exponent, named after the Soviet mathematician A.M. Lyapunov (1857–1918), is one of the most important dynamical invariants of an attractor that quantifies its sensitivity to initial conditions (SIC). It measures the average rate of divergence (or separation) of neighbouring trajectories in phase space — the SIC-ness of the system — averaged over initial conditions spread over the trajectory. In a chaotic attractor this divergence increases exponentially. For example, consider a one-dimensional map $x_{n+1} = f(x_n)$. The two trajectories starting at the neighbouring points x_0 and $x_0 + \epsilon$ with $\epsilon \ll 1$ may diverge out after n iterations as $|f^n(x_0 + \epsilon) - f^n(x_0)| \sim \epsilon e^{n\lambda}$, $n \gg 1$. Here $f^n(x_0)$ stands for the nth iterate of x_0. Thus $f^2(x) \equiv f(f(x), f^3(x)) \equiv f(f(f(x)))$, and so on. We define the Lyapunov exponent λ as

$$\lambda = \lim_{n\to\infty} \frac{1}{n} \ln \left| \frac{\partial f^n(x_0)}{\partial x_0} \right| \tag{A.1}$$

Using the chain-rule for the derivative of the n^{th} iterate, we can write

$$\lambda = \lim_{n\to\infty} \frac{1}{n} \sum_{i=0}^{n-1} \ln \left| \frac{df(x_i)}{dx_i} \right| \tag{A.2}$$

where x_i is the i^{th} iterate of x_0. In the limit $n \to \infty$, the value of λ may be expected to be independent of the initial value x_0. Thus, for example, for the logistic map $x_{n+1} = \mu x_n(1 - x_n)$ with $\mu = 4$, one can readily show that $\lambda = \ln 2 > 0$.

The above definition can be generalized to higher-dimensional state spaces, maps or flows as

$$\lambda = \lim_{t\to\infty} \frac{1}{t} \ln \left| \frac{\epsilon(t)}{\epsilon(0)} \right|$$

$$\epsilon(o) \to 0 \tag{A.3}$$

where $\epsilon(t)$ is the distance between the points $x(t)$ and $x(t) + \epsilon(t)$, initially on the neighbouring trajectories (see Fig.A.1). The distance could be computed using any metric for the phase space and λ does not depend on it. Of course, the stretching and the contraction will depend on the direction, i.e. $\epsilon(t)$ is a d-dimensional vector for the d-dimensional phase-space and one must define 'd' Lyapunov exponents in general. All one has to do is to linearize the evolution equation at each point of the trajectory and look at the eigenvalues and eigenvectors of the d x d stability matrix that give the local exponential growth/decay of separation along the eigenvectors (tangent directions). Thus we have d exponents $\lambda_0 \geq \lambda_1 \geq \lambda_2 \ldots \geq \lambda_{d-1}$.

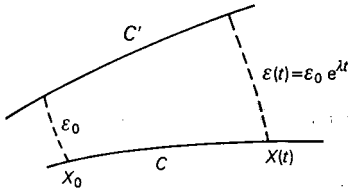

Fig.A.1 Lyapunov exponent λ. Points on neighbouring trajectories C and C' separate out exponentially.

It is clear that for chaos to occur, at least one of the λ's must have a positive real part. Also, for dissipative dynamics the sum of the λ's must be negative. Indeed, one can show that the phase-space volume element grows as

$$\Gamma(t) = \Gamma(0)\, e^{t\left(\sum_{i=0}^{d-1}\right)\lambda_i}$$

Also, for an autonomous system with $X_i = f_i(X)$, we have

$$\nabla \cdot f = \sum_i \lambda_i.$$

The positive Lyapunov exponents signifying the expansion of the initial phase-space volume elements and, therefore, enhancing the uncertainty of localizing the phase point in the phase space, are directly related to the average rate of increase of the so-called Kolmogorov entropy K. It is easily shown that $K \leq$ sum of all positive Lyapunov exponents. In particular, $K = 0$ for a regular motion (e.g. periodic), $K > 0$ for a chaotic motion, and $K = \infty$ for a truly stochastic (random) motion. The Kolmogorov entropy is an important calculable and measurable quantity whose reciprocal determines the time-scale for short-range prediction.

Appendix B

Randomness of deterministic sequences: Bernoulli shift, Baker transformation and the Smale horseshoe

Can a *given* sequence of numbers, or symbols, be random? This seems to be a contradiction in terms or, at the very least, as paradoxical as deterministic chaos. Yet a given sequence, generated through a deterministic algorithm, can be as random as the outcomes of tossing a coin in a very well-defined sense. We will illustrate this through what is known as the *Bernoulli shift*.

Consider the one-dimensional non-invertible map

$$x_{n+1} = 2\ x_n \ (\text{mod } 1) \tag{B.1}$$

that maps the unit interval [0,1] to itself. Thus, starting with a seed x_0, we can generate a well-defined sequence $(x_0, x_1, x_2, \ldots)$. As we have noted in the text the mod (1) is a highly non-linear feedback operation that causes folding-back, while multiplication by two causes the stretching-out. Together they produce the sensitivity to initial conditions which is essential to chaos. Let us now see the precise operational sense in which the sequence $(x_0, x_1, x_2, \ldots)$ generated by this deterministic algorithm is random.

Start with the seed x_0 written in the binary notation for convenience. All this means is to divide the unit interval $0 \leq x \leq 1$ in two equal halves and record 0 or 1 according as x_0 lies in the left half or the right half. Suppose it is in the left half, then subdivide the left half further in two equal halves and repeat the above procedure and so on and on. It is like zeroing in on the destination by travelling half way past to half way past to half ... This generates a string of zeros and ones that represents x_0 in the binary representation, i.e. symbolically $x_0 \equiv .a_0\ a_{-1}\ a_{-2} \ldots a_{-n} \ldots$ with a's 0 or 1. The longer the string, the greater the precision of specifying x_0 in the unit interval [0,1]. Written in this digitized binary base 2, we have

$$x_0 = \sum_{-\infty}^{0} \frac{a_n}{2^{-n+1}} \equiv .a_0\ a_{-1}\ a_{-2} \ldots \tag{B.2}$$

Now, our map gives the first iterate of x_0 as

$$x_1 = \sum_{-\infty}^{-1} \frac{a_n}{2^{-n+1}} \equiv .a_{-1}\, a_{-2} \ldots \tag{B.3}$$

because the first term $a_0/2$ in the sum drops out when we multiply it by two and perform the(mod 1) operation. Thus, the rule of this iterative game (or map) is just to shift the 'decimal point' one digit or bit to the right and drop whatever appears on its left. We have here a shift register so to say. This is the famous Bernoulli shift. Now, the point is that the initial seed x_0 is an input and as such the entries a_0, a_{-1}, a_{-2}, etc., are entirely unpredictable by definition. Thus, e.g., giving a_0 does not specify a_{-1}, a_{-2}, ..., etc. Thus, they may well be generated by the tossing of a coin with heads $\equiv$ 1 and tails $\equiv$ 0, say. But our map generates an output which is nothing but the input shifted and rounded off and is, therefore, just as unpredictable. After all, you cannot predict the entries of an input data tape. In computer parlance, to print out the output you have to have a program to print out the entire input string — the program length will be proportional to the bit length of the input. No short cut is possible. This is essentially what we mean by algorithmic complexity (a kind of computational complexity) of the given sequence.

There is yet another aspect to this randomness of a given sequence. The later entries in the binary representation of x_0 give higher numerical definition of x_0 with a_{-n} corresponding to an error of less than $1/2^{n+1}$. Now, given that all quantitative determinations have a finite accuracy (i.e. are known to a finite number of significant figures) we will have a rounding off error, $\sim 1/2^N$ say, that makes all a_{-n} for sufficiently large $n(> N)$ totally random, and just after N iterations these late error-laden entries will have been shifted left to the dominant place! This is a rather physically-motivated sense in which a given sequence may behave randomly.

We end this discussion with a few general number theoretic remarks. We have taken the sequence a_0, a_{-1}, a_{-2}, ... to be infinite. Why? Well, we know that there are countably infinitely many rational and uncountably infinitely many irrational numbers in the unit interval, but with the irrationals almost exhausting the measure (length) of the interval. Thus, any number drawn from the unit interval will almost always be irrational, and for irrational numbers the binary string (sequence) does not terminate. For rational numbers the sequence terminates — it is finite. Indeed, such an exceptional finite sequence corresponding to a rational seed will show recurrence (the celebrated *Poincaré recurrence*), i.e. it will be

repeated after a given number of iterations and will,therefore, yield a periodic orbit in the phase space, and hence is fully predictable. An irrational number too, almost always, contains any finite subsequence infinitely often. On iteration (*Bernoulli shift register*) these finite subsequences will also successively move left to a significant place and the corresponding phase trajectory will be quasi-periodic — the initial x_0 will get mapped arbitrarily close to any value x (including x_0) infinitely often. All this forms a fascinating subject of number-theoretic and symbolic dynamics for what might be called synthetic chaos.

B.1 Baker transformation

This is just a two-dimensional, invertible, two-sided generalization of the previous example of the one-dimensional, non-invertible, one-sided Bernoulli shift discussed above. The *baker transformation* is

$$\begin{aligned} X_{n+1} &= 2X_n,\ Y_{n+1} = Y_n/2\ ,0 \leq X_n < 1/2 \\ X_{n+1} &= 2X_n - 1,\ Y_{n+1} = (Y_n + 1)/2,\ 1/2 \leq X_n \leq 1 \end{aligned} \tag{B.4}$$

or its inverse

$$\begin{aligned} X_n &= X_{n+1}/2,\ Y_n = 2Y_{n+1},\ 0 \leq Y_n < 1/2 \\ X_n &= (X_{n+1} + 1)/2, Y_n = 2Y_{n+1} - 1,\ 1/2 \leq Y_n \leq 1 \end{aligned} \tag{B.5}$$

It obviously reminds one of the stretching-out and the folding-back operations of a baker working the dough.

As shown in the above figure (Fig.B.1), it leads to an intricately mixed and layered fine-structure that exhibits sensitivity to initial conditions (SIC-ness). The map is conservative (area preserving) as

$$| \partial(Y_{n+1},\ X_{n+1})/\ \partial(X_n, Y_n)\ | = 1,$$

and the Lyapunov exponents are $\pm$ ln 2. This contrasts with the earlier case of $X_{n+1} = 2\ X_n(\text{mod}1)$ which is non-conservative with the Lyapunov exponent = ln 2. We just note that it is again possible to represent the point (X, Y) as a binary sequence $\ldots\ a_3\ a_2\ a_1.\ a_0\ a_{-1}\ a_{-2}\ a_{-3}\ \ldots$ and then the map corresponds to a two-sided Bernoulli Shift where the 'decimal' point separating X and Y digits moves one digit to the right, i.e., $\ldots\ a_3\ a_2\ a_1.\ a_0\ a_{-1}\ a_{-2}\ a_{-3}\ \ldots \rightarrow \ldots\ a_3\ a_2\ a_1\ a_0.\ a_{-1}\ a_{-2}\ a_{-3}\ \ldots$ This is again a number theoretic model of mixing and SIC-ness.

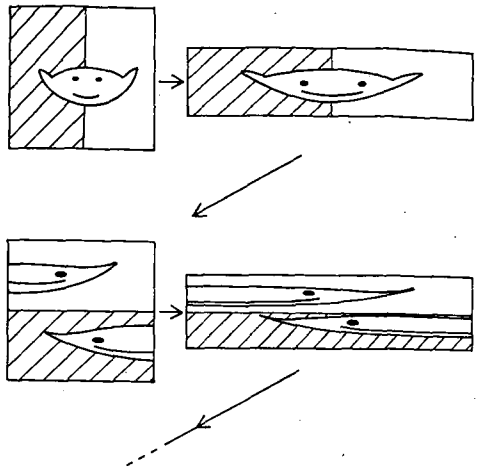

Fig.B.1 Baker's transformation. Notice the mixed-upness of "Arnold's Cat".

B.2 Smale horseshoe

This is a famous but rather abstract example of the chaotic behaviour of a dissipative or a conservative dynamical system invented by the American topologist Stephen Smale. It is a topological transformation involving stretching-out in one direction, and squeezing in another, followed by folding so as to stay within bounds. The resulting map demonstrates clearly the sensitive dependence on initial conditions — the instability which is at the heart of deterministic chaos. The transformation is shown schematically in Fig.B.2 for a dissipative system. Take a square S_0; squeeze it top and bottom into a horizontal bar S; bend the bar around into a horseshoe shape, with the arc and the two ends projecting outside the boundary of the original square. Thus, we have a contraction (dissipative) mapping of the original square S_0 into the straight legs R_1 and L_1 of the horseshoe S_1. It is readily seen that these two horizontal legs R_1 and L_1 are generated by the two vertical legs R_0 and L_0 shown in dotted lines on the original square S_0. The intersection squares s_1, s_2, s_3, s_4 thus contain subsets which are invariant under the transformation. We call these recurrent point sets. Now reiterate the above transformation on the horseshoe. The recurrent point set

will consist of 4^2 smaller squares, four in each of the earlier four squares. After n iterations we will have 4^n squares. Continued ad infinitum, this would lead to an uncountably infinite set of points covering zero measure (area). It will be a fractal. The dynamics on this set induced by our mapping involves stretching, squeezing and folding-back. Thus, each point is a saddle point by construction and signals instability. The horseshoe map is regarded as an archetype of chaotic dynamics.

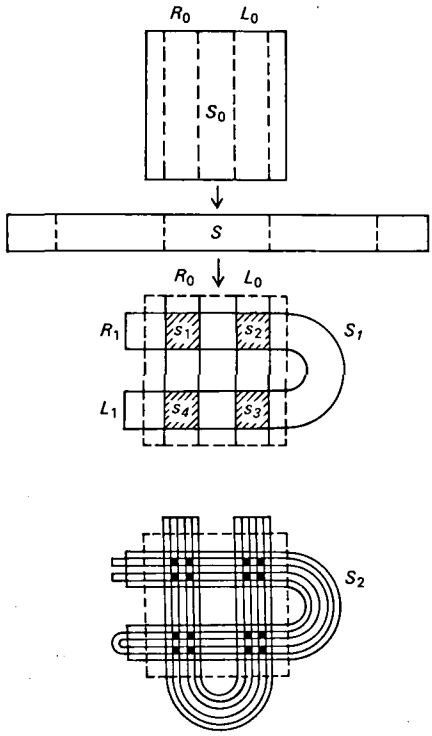

Fig.B.2 Smale horseshoe map obtained by stretching horizontally and compressing vertically by a factor of at least two recursively. Notice the invariant squares shown hatched (schematic).

Appendix C

Linear stability analysis

Linear stability of the state of a nonlinear dynamical system refers to the response of the system in that state to a small (infinitesimal) perturbation of the state. The state may be a stable/unstable fixed point (equilibrium) or a limit cycle or some reference trajectory in general, for a flow or map. If the perturbation grows exponentially with time, the state is said to be unstable; otherwise it is stable. In order to test this all one has to do is to linearize the nonlinear dynamical equations about that reference state in the phase space.

To fix ideas, consider the dynamical evolution equations $\dot{X}_i = f_i(X_1, \ldots, X_N)$, $i = 1, \ldots, N$ and let $(X_1^0, \ldots, X_N^0)$ be a fixed point, i.e., $f_i(X_1^0, \ldots, X_N^0) = 0$.

Let us slightly perturb this equilibrium state and set $X_i = X_i^0 + \delta x_i$, and write down the time-evolution for the perturbation δx_i by linearizing the nonlinear equation about the fixed point. We have the tangent map

$$\delta \dot{x}_i = \sum_j \left(\frac{\partial f_i}{\partial x_j} \right)_0 \delta x_j$$

where the matrix $(J_{ij} \equiv (\partial f_i / \partial x_j)_0$ is the stability matrix (a.k.a. the Jacobian or the plant matrix). The eigenvalues and eigenfunctions of this matrix now decide the linear stability/instability of the fixed point and the corresponding domain, or manifold, as follows (see Fig.C.1):

a) A real negative eigenvalue corresponds to the exponentially damped return to the fixed point. It implies stability and contraction along the corresponding eigenvector. Thus, if all eigenvalues are real and negative, then the fixed point is stable. In fact it is a stable node inasmuch as it is approached radially.
b) Real positive eigenvalues imply exponential divergence away from the fixed point. This implies stretching and instability along the corresponding eigenvectors. Thus, even a single positive real eigenvalue makes it an unstable fixed point (a repeller), or specifically an unstable node.

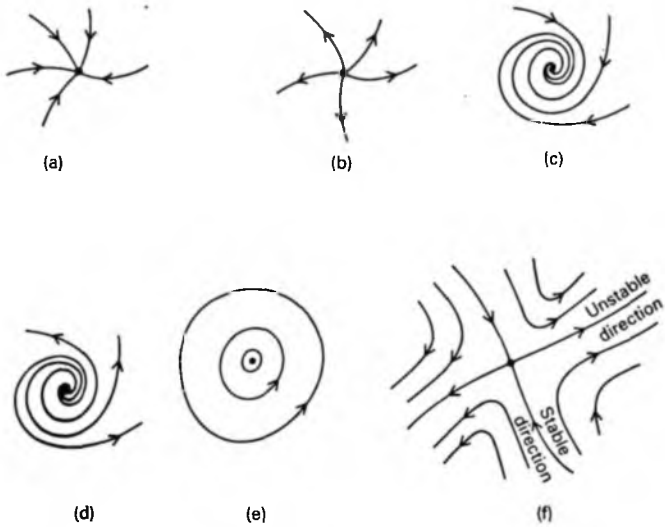

Fig.C.1 Fixed Points: **(a)** Stable fixed point (attractor node); **(b)** unstable fixed point (repeller node); **(c)** stable fixed point (attractor focus); **(d)** unstable fixed point (repeller focus); (e) centre (elliptic point); **(f)** saddle point (hyperbolic point).

c) Complex eigenvalues come necessarily in pairs and give a spiral motion falling into (stable focus) or away (unstable focus) from the fixed point according as their real parts are negative or positive. The spiral motion is in the plane defined by the two complex conjugate eigenvectors.

d) For a second-order system (i.e., two-dimensional phase space) a pair of purely imaginary eigenvalues give an elliptic point (i.e. a centre).

e) For a second-order system, two real eigenvalues of opposite signs give a saddle point (a.k.a. hyperbolic point). It implies stretching-out along the unstable direction and folding-back along the stable direction. Hyperbolic points are essential for SIC-ness and chaos.

f) An extremely interesting situation can arise in a third-order system (three-dimensional phase space) as in the Lorenz model where there is a positive real eigenvalue (unstable direction) and a pair of complex eigenvalues with negative real parts (a pair of

nodes). This can lead to a complex, irregular motion characteristic of the Lorenz strange attractor.

The above observations hold both for a continuous flow as well as a discrete map $X_i(n+1) = f_i(\{X_j(n)\})$. In the latter case, the Jacobian matrix is $(\partial f_i/\partial X_j)$.

An important idea when talking of stability is that of asymptotic stability as distinct from the orbital stability. Thus a limit cycle is asymptotically stable in the sense that neighbouring trajectories converge to it and points on those orbits get arbitrarily close as $t \to \infty$. This can happen only for a dissipative system. The centre, on the other hand is only orbitally stable — neighbouring periodic orbits stay neighbouring periodic orbits but do not converge to any limiting orbit, and points closest by on neighbouring orbits need not stay closest. Here a perturbation can lead to jittering. Centre is possible only for non-dissipative (conservative) systems.

Finally, each limit set (i.e. a fixed point, a limit cycle, etc.) has its domain or basin of attraction, or more generally its stable or unstable manifolds. These are generated by the iteration (evolution) of the full nonlinearized maps (flows) towards or away from the limit set. These domains (manifolds) are separated by separatrices.

Appendix D

The Saddle point and homoclinic point: Generator of disorder (GOD)

A saddle point is a hyperbolic fixed point in phase space with both the stable and the unstable eigendirections along which we have, respectively, folding-in and stretching-out of the trajectories (in mechanics, it represents a point on the potential surface shaped like a mountain pass. Geometrically, the surface has a negative Gaussian curvature there). The stable/unstable directions are determined by the Jacobian matrix J of the map $x_i(t+1) = f_i(x(t))$, or the flow $(dx_i(t)/dt) = f_i(x(t))$, linearized about the fixed point with $J_{ij} = (\partial f_i/\partial x_j)$. Thus, the unstable manifold is the subspace generated by the infinity of full nonlinearized iterations of the points lying within an elemental volume defined by the eigenvectors of the Jacobian matrix at the saddle point corresponding to the real eigenvalues of absolute magnitude greater than unity. Similarly, for the stable and the centre manifolds. To these manifolds, of course, correspond tangent spaces generated by the corresponding eigenvectors. The full nonlinearized iterations of the unstable eigenvector at the saddle point can give an infinitely folded curve. In conservative systems, this type of exceptional subspace of unstable manifold is called a *separatrix* (more generally, a separatrix separates basins of attraction of different attractors in the phase-portrait).

We will now briefly illustrate how saddle points can generate chaotic trajectories. This requires a proper understanding of the role of a separatrix and what is known as a *homoclinic point* [at which the stable (S) and the unstable (U) manifolds (separatrices) intersect]. Consider first the unstable (U_1) and the stable (S_1) separatrices associated with a hyperbolic point H_1. These two can terminate in one of the following ways (Fig.D.1). They can terminate in another co-existing hyperbolic point H_2 such that U_1 becomes S_2 and U_2 becomes S_1. Thus we get a heteroclinic orbit. Or, they may bootstrap so that U_1 closes on H_1 as S_1, giving a homoclinic orbit, or they can simply wander off to or in from infinity, respectively.

The existence of the homoclinic orbit does imply, however, that a certain trajectory initially in the unstable manifold may enter the

stable manifold and after an *infinite* time hit the fixed point (get reinjected) from which it had once begun (Fig.D.2). The existence

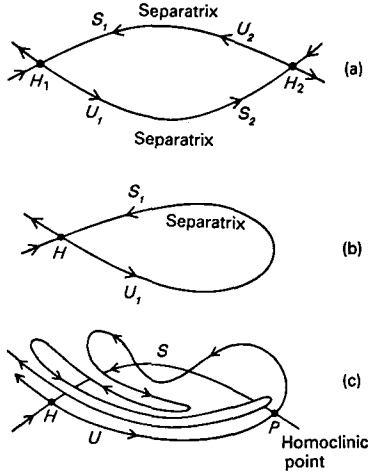

Fig.D.1 (a) Heteroclinic orbit joining two saddle points H_1 and H_2; (b) bootstrapping of separatrix at H; (c) Homoclinic point P and chaotic behaviour near H.

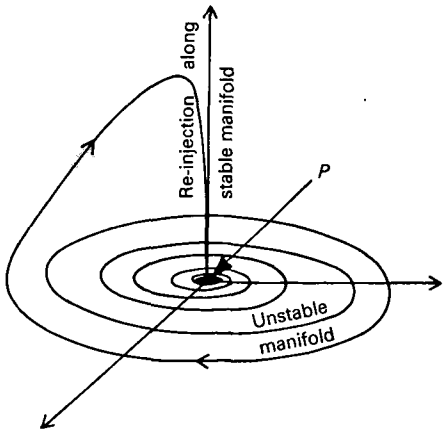

Fig.D.2 Homoclinic orbit to a focal fixed point possible for 3-dimensional phase space with a 2-dimensional stable and 1-dimensional unstable manifolds.

of P demands tuning of the parameter value. A small deviation from this parameter value produces time-periodic orbits near the homoclinic orbit (see Fig.D.2). The corresponding case for the heteroclinic orbit is, for example, as shown in Fig.4.2(a) for the Lorenz attractor.

But the most interesting case is when U_1 intersects S_1 at a point P (not a fixed point) called the homoclinic point. We must note that we are now really talking about the intersections of the separatrices with the Poincaré surface of section and hence the existence of P does not violate the non-self-intersection property of phase trajectories. It is clear then that the unstable and the stable separatrices must intersect infinitely often as shown in (Fig.D.1). This follows from the fact that, inasmuch as P lies on the stable separatrix S, it must get mapped on S and converge to the hyperbolic fixed point H as a limit along the stable separatrix S. But, since P also lies on U, its pre-images must be traceable back to H along U. Further, as the map is conservative, for a Hamiltonian system say, it can be shown that the loops created by the repeated intersections of U and S must have equal areas. It follows, therefore, that as the points of intersection along the stable separatrix S become closer and closer on approaching the limit point H, the loops must become more and more elongated and entangled in the transverse direction. This combination of large transverse excursions and folding-back (re-injection) leads to irregular, chaotic motion.

Suggested further reading

Books

1. Robert C. Hilborn, *Chaos and Nonlinear Dynamics: An Introduction for Scientists and Engineers* (Oxford University Press, Oxford, 1994)
2. G.L. Baker and J.P. Gollub, *Chaotic Dynamics: An Introduction* (Cambridge University Press, New York, 1990).
3. P. Bergé, Y. Pomeau and C. Vidal, *Order Within Chaos* (Wiley, New York, 1986).
4. P. Collet and J.P. Eckmann, *Iterated Maps on the Interval as Dynamics* (Birkhauser, Cambridge (MA), 1980).
5. R.L. Devaney, *An Introduction to Chaotic Dynamical Systems* (Benjamin-Cummings, Menlo Park (CA), 1986).
6. R.L. Devaney, *A First Course in Chaotic Dynamical Systems* (Addison-Wesley, Reading (MA), 1992).
7. R.L. Devaney, *Chaos, Fractals and Dynamics: Computer Experiments in Mathematics* (Addison-Wesley, Reading (MA), 1990).
8. B.B. Mandelbrot, *The Fractal Geometry of Nature* (W.H.Freeman, San Francisco, 1982).
9. Francis C. Moon, *Chaotic and Fractal Dynamics: An Introduction for Applied Scientists and Engineers* (Wiley, New York, 1992).
10. G. Nicolis and I. Prigogine, *Exploring Complexity* (W.H.Freeman, San Francisco, 1989).
11. R.H. Abraham and C.D.Shaw, *Dynamics: The Geometry of Behaviour* (Addison-Wesley, Reading (MA), 1992).
12. H.G. Schuster, *Deterministic Chaos: An Introduction*, Second revised edition (VCH, New York, 1988).

Semi-popular Articles

1. J.P. Crutchfield, J.D.Farmer, N.H.Packard and R.S.Shaw, 'Chaos', *Scientific American*, **255**, 38 (December, 1986).

2. Joseph Ford, 'How random is a coin toss', *Physics Today*, **36**, 40 (April, 1983).

3. H. Jurgens, H.-O.Petigen and D.Saupe, 'The Language of Fractals', *Scientific American*, **263**, 40 (August, 1990).

4. G.B. Lubkin, 'Period-Doubling Route to Chaos Shows Universality', *Physics Today*, **34**, 17 (March, 1981).

5. D.R. Hofstadter, 'Metamagical Themas', *Scientific American*, **245**, 16 (November, 1981).

6. J.M. Ottino, 'The Mixing of Fluids', *Scientific American*, **260**, 40 (January, 1989).

7. E. Ott and Mark Spano, 'Controlling Chaos', *Physics Today*, **48**, 34 (May, 1995).

8. T. Shinbrot, C. Grebogi, E. Ott and J.A. Yorke, 'Using Small Perturbations to Control Chaos', *Nature*, **363**, 411 (1993).

Index

Arnold's cat, 85
attractors, 18
  asymptotically stable, 18, 19
  basins of attraction, 21
  biperiodic torus, 20
  fixed point, 18
  Hénon, 22
  limit cycle, 19
  phase portrait, 21
  quasi-periodic motion, 20
  Robinsonization, 19
  strange, 21, 41

baker's transformation, 7, 84
  algorithmic complexity, 7
  folding-back, 7
  stretching-out, 7
Bernoulli shift, 6, 7, 82

capacity dimension, 64, 65
chaos, 1
  algorithmic complexity, 7
  attractors, 18
  controlling, 77
  Hamiltonian, 47
  models of, 25
  phase space, 16
  soft, 59
circle map, 33
  Arnold's tongues or horns, 36
  Daedalus, 36
  Krebs cycle, 36
  Pace Maker, 36
  phase locking, 33
  quasi-periodicity, 33
correlation dimension, 68

deterministic chaos, 1
  Belousov–Zhabotinski reaction, 14
  Brownian motion, 1
  circadian rhythms, 15
  leaking faucet, 9
  pseudo-random numbers, 2
  Rayleigh–Bénard convection, 12
  turbulence in pipe flow, 10

fractals, 64
  Cantor set, 66
  dimension, 65
  Koch snow flake, 67
  self-similarity, 64
frequency dimension, 68
frequency entrainment, 9

Hamiltonian chaos, 47
  action(J)–angle(θ) variables, 52
  Arnold diffusion, 60
  Cassini divisions, 48
  elliptic points, 48
  Ergodicity problem, 63
  first integral, 51
  golden ratio, 59
  hyperbolic point, 48
  KAM gaps, 48
  KAM theorem, 48, 55
  Kirkwood gaps, 48
  integrable system, 52
  invariant tori, 53
  Mark Twain boils, 62
  mixing, 50
  nonintegrable system, 48
  soft chaos, 59
  Sinai billiard-ball models, 62
  Sinai stadium, 63
  soft chaos, 59
  standard map, 60
  structural stability of governing equations, 62
  twist map, 56
heteroclinic point, 92
homoclinic point, 90, 92

KAM theorem, 48, 55, 56
  KAM surfaces, 55
  KAM tori, 56
Kolmogorov entropy, 81
information dimension, 68
invariant tori, 53
  rational tori, 55
  resonant tori, 55
  irrational or non-resonant tori, 55

Legendre transformation, 70
logistic map, 25
  boom and bust parameter, 25
  intermittency, 28, 33
  period-doubling bifurcation, 28, 31
  pitchfork bifurcations, 28
  tangent bifurcation, 31
  universality, 29
Lorenz, Edward, 43
  attractor, 43
  model, 46
Lyapunov exponent, 4, 80

Mandelbrot, Benoît, 64
models of chaos, 25
  circle map, 33
  logistic map, 25
multifractals, 69

nonlinearity, 5
  baker's transformation, 7
  Bernoulli shift, 6, 7
  Sisyphean bank account, 6

Poincaré Henri, 16
  recurrence, 83
  section, 21
phase space, 16
  phase portrait, 21
  state space, 16
Poincaré section, 21
  first return map, 22
  Hénon attractor, 22
  quasi-continuous curve, 22
  surface of section, 22

Rayleigh number, 14
Robinsonization, 19
routes to deterministic chaos, 39
  Couette–Taylor flow, 39
  Hopf bifurcation, 39
  intermittency, 39
Ruelle, David, 41

sensitive dependence on initial conditions, 3
  butterfly effect, 4
  clinamen, 4
  Lyapunov exponent, 4
separatrix, 90
Smale, Stephen, 85
  horseshoe, 85
soft chaos, 59
  intermittency, 62
strange attractors, 41
  embedding dimensionality, 72
  embedding theorem, 72, 74
  ECG, 74
  EEG, 74
  Lorenz attractor, 43
  Rössler attractor, 42
  Ruelle, David 41

Takens, Floris, 72
  embedding theorem, 72, 74
topological dimension, 64
turbulence in pipe flow, 10
  Navier–Stokes equation, 12
  Reynold's number, 11

universality, 29
  Feigenbaum number, 29
  Mandelbrot set, 31
  metric, 29
  structural, 29

The book

Deterministic Chaos addresses the newly emerged paradigm of complexity of change. It describes how a simple system ruled by a deterministic law can evolve in a manner too complex to predict in the long run, even in principle, in an operationally qualitative, well-defined sense. With brevity and without oversimplification, it presents the concepts of Deterministic Chaos and powerful qualitative techniques to explore it. The book is within the grasp of any curious reader with a science background.

The author

Dr N Kumar is the Director of the Raman Research Institute, Bangalore. In a career spanning over thirty years, he has been Fellow of a number of prestigious institutions including the Indian Academy of Sciences, the Indian National Science Academy, the American Physical Society and the Third World Academy of Sciences (TWAS), to name a few. He has received a number of awards including the S S Bhatnagar Award in 1985 and the TWAS-Award in Physics in 1992.

Dr Kumar is an accomplished author and has a number of research papers, articles and books to his credit.

New and forthcoming books

J V Narlikar : *Elements of Cosmology*

K S Valdiya : *Dynamic Himalaya*

R Gadagkar : *Cooperation and Conflict in Animal Societies*

S B Gadre : *Electrostatics of Atoms and Molecules*

Cover A schematic representation of the butterfly effect.

The Educational Monographs published by Universities Press in collaboration with JNCASR address the needs of students and the teaching and research community.

Universities Press

N Kumar : *Deterministic Chaos: Complex Chance Out of Simple Necessity*

ISBN 81 7371 042 2

Rs 70.00

Cover design by GSDATA